

Title: The Genetic Legacy of African Americans from Catocin Furnace

Authors: Éadaoin Harney ^{1,2*}, Steven Micheletti ¹, Karin S. Bruwelheide ³, William A. Freyman ¹, Katarzyna Bryc ¹, Ali Akbari ^{2,4}, Ethan Jewett ¹, Elizabeth Comer ⁵, Henry Louis Gates Jr. ⁶, Linda Heywood ⁷, John Thornton ⁷, Roslyn Curry ^{1,2}, Samantha Ancona Esselmann ¹, Kathryn G. Barca ³, Jakob Sedig ^{2,4}, Kendra Sirak ^{2,4}, Iñigo Olalde ^{2,8,9}, Nicole Adamski ^{4,10}, Rebecca Bernardos ^{4,10}, Nasreen Broomandkhoshbacht ^{4,10}, Matthew Ferry ^{4,10}, Lijun Qiu ^{4,10}, Kristin Stewardson ^{4,10}, J. Noah Workman ^{4,10}, Fatma Zalzala ^{4,10}, Shop Mallick ^{4,10,11}, Adam Micco ^{4,11}, Matthew Mah ^{4,10,11}, Zhao Zhang ⁴, 23andMe Research Team ¹, Nadin Rohland ⁴, Joanna L. Mountain ^{1,*†}, Douglas W. Owsley ^{3,*†}, David Reich ^{2,4,10,11,*†}

10 Affiliations:

¹ 23andMe, Inc.; Sunnyvale, CA 94043, USA.

² Department of Human Evolutionary Biology, Harvard University; Cambridge, MA, 02138, USA.

15 ³ Department of Anthropology, National Museum of Natural History, Smithsonian Institution; Washington DC 20560, USA.

⁴ Department of Genetics, Harvard Medical School; Boston, MA, 02115, USA.

⁵ Catocin Furnace Historical Society; Thurmont, MD, 21788, USA.

⁶ Hutchins Center for African and African American Research, Harvard University; Cambridge, MA 02138, USA.

20 ⁷ Department of History/African American Studies, Boston University; Brookline, MA 02446, USA.

⁸ BIOMICs Research Group, Department of Zoology and Animal Cell Biology, University of the Basque Country UPV/EHU, Vitoria-Gasteiz, Spain

⁹ Ikerbasque—Basque Foundation of Science, Bilbao, Spain.

25 ¹⁰ Howard Hughes Medical Institute, Harvard Medical School; Boston, MA, 02115, USA.

¹¹ Broad Institute of MIT and Harvard; Cambridge, MA, 02142, USA.

†These authors jointly supervised this work: Joanna Mountain, Douglas Owsley, David Reich.

*Corresponding authors. Email: eadaoinh@23andme.com (E.H.); jlmountain@gmail.com (J.M.); owsleyd@si.edu (D.W.O.); reich@genetics.med.harvard.edu (D.R).

30

35

One Page Summary:

Introduction:

Genetic analysis of historical individuals has the potential to help restore knowledge of people whose stories were omitted from written records. During the late 18th and early 19th centuries, Catoctin Furnace in Maryland relied on a workforce of enslaved individuals to operate the iron furnace and carry out domestic and agricultural tasks. Despite the role that Catoctin Furnace played in early United States history (including supplying munitions to combatants during the Revolutionary War), relatively little is known about the African Americans who labored there or their descendants compared to the furnace's later predominantly white workforce.

Rationale:

We produced whole-genome data for 27 individuals buried in the Catoctin Furnace African American cemetery and compared them to approximately 9.3 million consenting research participants genotyped by 23andMe, Inc. to address the following questions: (i) How were the Catoctin individuals related to each other? (ii) What were the sources of their African and European ancestry? (iii) Where in the United States do their genetic relatives live today, including their direct descendants? (iv) What can their genomes reveal about their health?

Results:

We identified five genetic families, consisting of biological mothers, children, and siblings, among the Catoctin individuals. In most cases, biological family members were buried in close proximity. All but one of the Catoctin individuals had primarily African ancestry, with variable amounts of European ancestry. To learn more about their ancestry we developed a new approach to detect identical-by-descent segments of the genome shared between the Catoctin individuals and 23andMe research participants. Identical-by-descent segments of DNA are shared by two or more

people because they have been inherited from a recent common ancestor. We identified 41,799 close and distant relatives of the Catoctin individuals among 23andMe research participants. Within Africa, we found the highest rates of genetic sharing between Catoctin individuals and research participants who self-identified as belonging to the Wolof or Kongo ethnolinguistic groups. Within Europe, we observed the highest rates of genetic sharing with research participants that have ties to Great Britain and Ireland.

Within the United States, we observed elevated rates of sharing with participants from the South, largely reflecting distant connections to 23andMe research participants with Sub-Saharan African ancestry (possibly tracing back to shared common ancestors in Africa). When we considered genetic relatives who share the most identical DNA with the Catoctin individuals, we observed the highest rates of sharing in Maryland, suggesting that at least some descendants stayed in the region following the furnace's transition away from enslaved and paid African American labor.

Finally, we found that some of the Catoctin individuals carried risk factors for sickle cell anemia and G6PD deficiency, genetic diseases that are common in African Americans today.

15 **Conclusion:**

These results demonstrate the power of joint analysis of DNA from historical individuals and the extremely large datasets generated through direct-to-consumer ancestry testing, and serve as a model for obtaining direct insights into the genome-wide genetic ancestry of enslaved people in the historical United States.

20

Abstract

Few African Americans have been able to trace family lineages back to ancestors who died before the 1870 United States Census, the first in which all Black people were listed by name. We analyze 27 individuals from Maryland's Catoctin Furnace African American Cemetery (1774-1850), identifying 41,799 genetic relatives among consenting research participants in 23andMe, Inc.'s genetic database. One of the highest concentrations of close relatives is in Maryland, suggesting that descendants of the Catoctin individuals remain in the area. We find that many of the Catoctin individuals derived African ancestry from the Wolof and Kongo groups and European ancestry from Great Britain and Ireland. This study demonstrates the power of joint analysis of historical DNA and large datasets generated through direct-to-consumer ancestry testing.

One Sentence Summary

Identifying genetic connections between historical African Americans from Catoctin Furnace and present-day people.

20

25

30

Main Text:

The vast majority of the ~45 million self-identified Black and/or African American individuals living in the United States (US) descend from approximately 456,600 enslaved Africans who were forcibly transported to the US from Africa during the transatlantic slave trade between 1501 and 5 1867 (1, 2). However, African Americans often have little information about these ancestors or their African origins due to a history of inhumane treatment of the enslaved and their descendants, which included marginalization and the obfuscation of family histories (3). In this study, we demonstrate that when combined with genome-wide data from a sufficiently large and diverse genetic database, DNA from historical individuals provides a means for restoring knowledge of 10 familial connections between contemporary peoples and their historical relatives. Specifically, we report on the DNA of enslaved and free African Americans from Catoctin Furnace, Maryland, who lived, worked, died, and were buried there in the late 18th and early 19th centuries.

As early as December 1768, a tract of land was acquired in order to build an iron works at the foot 15 of Catoctin Mountain near present-day Thurmont, Maryland (4). The furnace was in blast by 1776, producing pig iron, tools, household items, and munitions used during the Revolutionary War. At least 271 enslaved and an unknown number of free African Americans worked at Catoctin within and outside the furnace, as ore miners, colliers, forgers, fillers, teamsters, and woodcutters, as well as in domestic and agrarian roles in the furnace owners' households and plantations (5). In 20 the second quarter of the 19th century, the furnace's labor force switched primarily to wage labor and a primarily white workforce (6). Gradually, the contribution of African Americans in this early industrial complex was largely forgotten. The Catoctin Furnace African American cemetery, near an old ore pit, was excavated in 1979–1980 in advance of highway construction (Fig. 1A) (7–10).

The Maryland State Highway Administration transferred stewardship of the recovered remains of deceased humans to the Smithsonian Institution, where curator Dr. J. Lawrence Angel conducted preliminary forensic anthropological investigations (11).

5 The Catoctin Furnace Historical Society, Inc. (CFHS) was initially founded to save the Catoctin Furnace village and its archaeological and architectural heritage from this highway construction (4). In recent years, its mission expanded to include restorative justice, highlighting the critical role that enslaved and free African Americans played in the furnace's history and in the growth of industrial wealth and power in the young US. In 2015, a grant from the Maryland Heritage Areas Authority supported further scientific analysis of individuals buried in the cemetery. The first 10 phase of the project involved historical documentary research and osteological re-analysis that refined previous assessments of demography and bone and dental pathology, with testing for stable carbon and nitrogen isotopes, and trace elements to shed light on the life histories of the individuals (12). The project's second phase used DNA to explore their biogeographic ancestries and 15 relationships to one another, details of which were summarized in a technical note (13) and are expanded upon here. These data address a critical component of CFHS's mission, pursued jointly with the African American Resources Cultural and Heritage Society (AARCH) of Frederick County, to return knowledge to the African American community and identify descendants of Catoctin's enslaved and free workers.

20

Advances in ancient DNA (aDNA) technology have made it possible to use genetic data as a tool for restoring knowledge of enslaved and historically marginalized peoples whose stories were often omitted from or disregarded in written records. Studies of the New York African Burial

Ground (14, 15), the Anson Street ancestors (16, 17) and others (18, 19) used a combination of anthropological and biomolecular tools to provide insight into the identity and life history of enslaved individuals through the study of their remains. However, their ability to localize the African origins of these individuals was limited by the exclusive use of mitochondrial (mt) DNA (20) and/or reliance on comparisons with data from publicly available reference datasets (21, 22). This study shows how deeper insights into the precise ancestral origins and genetic legacy of enslaved and free African Americans, such as those buried at Catoctin Furnace, can be obtained from genome-wide aDNA data when compared to a reference database containing genetic data from millions of living people, like the one maintained by 23andMe, Inc.

10

We recovered genome-wide aDNA from all 27 of the Catoctin individuals who were selected for sampling, targeting ~1.2 million single nucleotide polymorphisms (SNPs) using a capture-based approach (23–26), which we combined with imputation to further increase the amount of available genetic information (Table S1). By comparing the DNA of the Catoctin individuals with genotype data from 9,255,493 participants in the 23andMe cohort, all of whom consented to participate in research, we were able to learn about their biogeographic ancestries, genetic relationships with one another, and to provide insight into their genetic legacy by identifying identical-by-descent (IBD) connections with living relatives.

20 **Community Engagement and Ethical Considerations**

This research analyzed data from deceased individuals who were unable to directly consent to participate in this study, as well as from millions of research participants (including those genotyped by 23andMe) who actively consented to participate in research. The ties between

present-day African Americans, their ancestors within the US, and their ancestors in Africa were forcibly severed by the transatlantic slave trade, the centuries-long institution of slavery, and generational systemic racist practices that have endured after the abolition of race-based slavery (27), as illustrated by Frederick Douglas' famous words: "Genealogical trees do not flourish among slaves" (28). Our objective is to contribute to the restoration of memories of a past community whose legacy was intentionally obscured and to create an avenue for living people to learn about their ancestors. We followed guidelines for the ethical analysis of the DNA of historical and living people (29, 30), including consultation with stakeholder groups, as emphasized in recent discussions on the future of studies involving the remains of African Americans (31–35). Based on interactions with stakeholders, we believe there is interest among African Americans and the public to harness aDNA to learn about historical connections to people who lived in the past, and to leverage this technology to develop accurate methods to identify genetic relationships, many of which were previously unknown. Equally important is the need to communicate the results of these analyses with descendants and others in a sensitive and accurate manner.

In the case of Catoctin Furnace, the goals of CFHS, developed in partnership with AARCH, include identifying descendants and widening the community of stakeholders. To date, researchers at CFHS have traced the lineages of two African Americans (one enslaved and one free) who labored at Catoctin Furnace to their living descendants by utilizing historical documents and genealogical data. Members of CFHS, AARCH, and the recently discovered descendants all expressed support for the use of genetic approaches that could identify a larger descendant community. Based on conversations with these stakeholders about their research interests, we sought not only to identify living genetic relatives of the Catoctin individuals, but also to conduct analyses to shed light on their life stories, such as identifying family relationships shared between

the Catoctin individuals, exploring their African and European origins, and identifying biologically significant variants. In collaboration with CFHS and AARCH we also held a series of public events to directly return research results at various phases of the project (36). One of the ways in which stakeholders chose to honor the legacy of enslaved individuals at Catoctin during these events was through the act of reading the names of individuals that could be abstracted from a variety of sources, including land records, probate inventories, church records, diaries, and freedom-seeker ads (although not associated with specific burials) (5). We include these names in the supplementary text (36). Establishing family connections to living people through genetics contributes to remembering and honoring those buried at Catoctin.

10

In this study, we show that the joint analysis of DNA extracted from the remains of deceased humans and millions of living people in a re-contactable research cohort (i.e., a cohort in which participants can be asked follow-up questions or receive results), like the one maintained by 23andMe, makes it possible to recover previously unknown connections between present-day people and historical individuals from sites like Catoctin Furnace. Not all members of the Catoctin stakeholder community have a known genetic connection to Catoctin. While this study is responsive to community requests to use genetic approaches to identify descendants, future studies applying these methods should be cautious about the danger of contributing to the biologization of notions of identity, as genetic connections represent one of many ways in which people may feel connected to historical individuals. A full ethics statement is provided in (36). Additional ethical considerations involving the co-analysis of aDNA and data from private genetic databases are discussed in (37).

20

Multiple families buried at Catoctin Furnace

Among the 27 Catoctin individuals, we identified five distinct genetic families (labeled A–E) that are primarily composed of mothers, children, and siblings; in this study, the term "genetic family" refers to a group of people who are closely related biologically. Similarly, specific relationship terms (e.g., mother, son, or daughter) are used in a biological sense and based on genetic sex as inferred by the presence or absence of sex chromosomes; thus, they may not reflect the actual kin-based relationships, biological presentation, or gender identities recognized by the Catoctin individuals. Fifteen Catoctin individuals could be assigned to one of the five genetic families, while the remaining 12 individuals appear genetically unrelated, except for the individual from Burial 28, whose coverage was insufficient to confidently assign to Family B. Some unrelated individuals share mt or Y-chromosome haplogroups, which may indicate more distant relationships that fall outside the limits of our resolution. We used information about genetic sex and mt and Y haplogroups to further resolve these family groupings (Fig. 1B). Close genetic relatives tended to be buried near one another (Fig. 1A), while individuals who were buried separately from their genetic families were typically more distantly related. For instance, Family A consists of a mother (Burial 3) and two sons (Burials 1 and 2), interred side-by-side, in addition to a 2nd–3rd-degree relative (Burial 24) who was buried separately and whose exact relationship to the other individuals is unresolved. While genetic relatedness had a role in burial patterning, other factors, such as temporal context and cultural and religious practices likely contributed as well.

20

Sex-biased reproduction

The European ancestry of enslaved African Americans originated largely through a process whereby white men reproduced with Black women through rape. This gender-based sexual violence contributed to the brutal systematic enslavement of African Americans and frequently

produced children born into slavery (22, 38). This pattern of behavior, a form of sex-biased admixture, is reflected in the distribution of the mt and Y haplogroups observed among the Catoctin individuals. Three of the 16 Catoctin males have Y haplogroups that are broadly associated with West Eurasian ancestry (Fig. S1). These include subclades of the R1a and R1b haplogroups which are common throughout Europe, indicating that their paternal lineages likely trace back to a fully European ancestor. In contrast, only one individual (Burial 32) has a European-associated mt haplogroup (J1b1a1a) (Fig. S2). This individual is an outlier with respect to ancestry as they also have a European-associated Y haplogroup (R1a1a1b1a3b) and over 50% European ancestry. Among other possible causes, their spatially separated grave, located in the northwestern edge of the burial ground, may reflect their distinct ancestral origins or lack of relatedness within the community represented in the cemetery.

Variable proportions of African, European, and Indigenous American-related ancestry in Catoctin individuals

All individuals (except the individual from Burial 32) were assigned a majority of African ancestry by qpAdm, using a model designed to estimate each individual's African, European, and Indigenous American ancestry proportions (Fig. 1C, Table S2-3). Over one quarter of individuals (n=7) could be modeled as having no detectable European admixture (i.e., the amount of ancestry assigned to the European source population is within a single standard error of zero). This is in sharp contrast to nearly all present-day self-identifying African Americans who typically have at least some European-derived ancestry (e.g., there is an average of 24% European ancestry among 23andMe research participants who self-identify as African American (39)). Several individuals could be modeled as having Indigenous American ancestry, but in all cases, estimates were within

three standard errors of zero. It is therefore uncertain based on these analyses alone whether these estimates represent true Indigenous American ancestry.

We next imputed genotypes across the whole genome for each Catoctin individual using the software GLIMPSE (40) with an approach optimized for low-coverage, capture-based aDNA data. To ensure that the imputation process would not bias results, we tested the performance of the Templated Positional Burrows–Wheeler Transform (41) (TPBWT) IBD detection tool and 23andMe’s Ancestry Composition (42) tool on a dataset composed of 48 high-coverage ancient individuals who were downsampled to varying degrees (36). Further, we compared the results of ADMIXTURE (Fig. S3), PCA (Fig. S4), and qpAdm (Fig. S5) analyses using the imputed and non-imputed datasets to ensure that the imputation process did not substantially bias ancestry estimates. We observed a bias towards estimating excess European-related ancestry in the lowest coverage individuals when using the imputed dataset relative to the non-imputed dataset; however, this did not appear to substantially impact individuals with >0.5x coverage, which is the group we focused on for subsequent analyses.

Using the imputed dataset, we applied 23andMe’s Ancestry Composition tool (42) to infer local ancestry along the chromosomes of the Catoctin individuals. Each region of their genomes was assigned to one of six previously determined broad ancestry categories: Sub-Saharan African, European, East Asian & Indigenous American, Western Asian & North African, Melanesian, and Central & South Indian (Fig. S6, Table S4). These assignments are correlated with qpAdm estimates (Fig. S7) and provide support for the identification of Indigenous American ancestry in several Catoctin individuals. For instance, we inferred low levels of Indigenous American ancestry

in two brothers (Burials 1 and 2) from Family A, but not in their mother (Burial 3) (Fig. 2), suggesting that their un-sampled father had some Indigenous American ancestry.

Identity-by-Descent (IBD)

5 To learn more about the biogeographic ancestry and genetic legacy of the Catoctin individuals, we searched for identical-by-descent (IBD) segments of the genome—that is, long segments of DNA that are identical in two or more people because they have been inherited from a recent common ancestor. We searched for IBD shared between each of the Catoctin individuals and ~9.3 million 23andMe research participants. We identified 55,342 IBD segments shared between the historical
10 Catoctin individuals and 41,799 research participants, ranging up to 60 cM in length (Table 1, Figs. S8–9, Tables S5-6). We calculated the total IBD shared between each pair of individuals to estimate their most likely genetic relationship; however, we caution that we are likely underestimating the true amount of DNA shared between these individuals, particularly among close relatives (36). In Box 1, we discuss how the relationships between Catoctin individuals and
15 research participants with whom they share DNA can be interpreted (Table S7), noting that not all present-day individuals who share DNA with Catoctin individuals are direct descendants. In fact, most connections are likely between collateral relatives—relatives who are neither direct ancestors nor descendants of one another, but instead both descend from a common ancestor who lived generations before the Catoctin individuals. Further, many of the most distant relatives that we
20 identified may not share a common ancestor who lived in the Americas. Instead, their connection may trace back to an individual who lived in Africa or Europe prior to their descendants' arrival in the Americas, either willingly or as part of the transatlantic slave trade.

Genetic connections to present-day Africans

We examined IBD segments shared between Catoctin individuals and members of the African cohort (i.e., 23andMe research participants with $\geq 95\%$ Sub-Saharan African ancestry who indicated that either they or all four of their grandparents were born in Africa) to identify the geographical regions in Africa with which these present-day people are associated. We observed the highest rates of IBD sharing between the Catoctin individuals and participants linked to Senegal, Gambia, Angola, and Democratic Republic of the Congo (DRC) (Fig. 3A, Fig. S10, and Table S8), confirming via randomization testing that we would be unlikely to detect the same number of IBD connections ($n=10$) with an identically sized sample ($n=166$) of randomly selected individuals from the Atlantic African cohort (i.e., research participants in the African cohort with ties to specific Atlantic African countries, defined in (36)) ($p\text{-value} < 0.001$) (Table S9).

Many African ethnolinguistic groups occupy wide geographic ranges that cross present-day national borders. We therefore also determined the amount of IBD each Catoctin individual shared with genetic clusters in Atlantic Africa that correspond to the self-identified ethnolinguistic groups of research participants (Fig. 3B, Table S10). Of the 15 Catoctin individuals with detectable IBD connections to Africa, seven share a connection with only a single cluster. Six of these individuals have high proportions of Sub-Saharan African ancestry ($>90\%$). In contrast, it is less common for present-day research participants with four grandparents born in the US and $\geq 50\%$ Sub-Saharan African ancestry to have a connection to only a single cluster (36). Among the Catoctin individuals with connections to Atlantic Africans, the most commonly observed connections are to genetic groups associated with the Wolof, Mandinka, and Kongo (whose present-day geographic distribution is described in Table S11). Overall, the Catoctin individuals share relatively more connections with Senegambian groups, like Wolof and Mandinka, than do research participants

with four grandparents born in the US and $\geq 50\%$ Sub-Saharan African ancestry (Fig. 3, Supplementary Text S5).

Genetic connections to present-day Europeans

5 Next, we explored the rate of IBD sharing with members of the European cohort (i.e., 23andMe research participants with $\geq 99\%$ European ancestry who indicated that either they or all four of their grandparents were born in Europe) to learn about the origins of the European-related ancestry that we observed in over half of the Catoctin individuals. We detect the highest rates of IBD among participants associated with Great Britain and Ireland (Fig. 4A, Table S12). Randomization testing
10 confirms that we would be unlikely to detect the same number of IBD connections ($n=467$) with an identically sized sample ($n=101,262$) of randomly selected individuals from the European cohort ($p\text{-value} < 0.001$) (Table S9). Much of the Irish-related signal is driven by connections to the individual from Burial 15, an adolescent male belonging to Family C, who, when projected onto a graph network of clusters that correspond to European geography again shares the most IBD with
15 clusters of participants associated with the northern, western, and southeastern regions of the island of Ireland (Fig. 4B). Multiple other Catoctin individuals (in particular, those from Burials 2, 10, and 34) share broader connections with participants from Great Britain and Ireland (Fig. 4B, Fig. S11, Table S13).

20 ***Distant and close relatives in the United States***

When we considered IBD sharing between research participants in the US cohort (i.e., research participants who indicated that either they or all four of their grandparents were born in the US) and each of the Catoctin individuals separately, each historical individual exhibited a unique

pattern of IBD sharing with respect to geography. However, when we considered the Catoctin individuals together, we observed the highest rates of sharing between Catoctin and research participants from the southern US (Fig. 5A, Fig. S12, Table S14). This signal resembles the geographic distribution of 23andMe research participants with Sub-Saharan African ancestry in the US (Fig. S13) and is therefore plausibly driven by a higher rate of IBD sharing in genomic regions with Sub-Saharan African ancestry. To address this source of bias, we restricted our analysis to research participants in the US cohort with $\geq 5\%$ Sub-Saharan African ancestry (Fig. 5B, Table S15). This filtering strategy increases the rate of IBD sharing from 0.45% of all US participants to 4.25% (Table 1).

10

For participants included in this filtered dataset, we continued to observe elevated rates of IBD sharing with Catoctin in the southern US (including Maryland) (Fig. 5B). We confirmed via randomization test that we would be unlikely to detect the same number of IBD connections ($n=2,034$) with an identically sized sample ($n=42,132$) of randomly sampled individuals from the US cohort with $\geq 5\%$ Sub-Saharan African ancestry (p -value < 0.001) (Table S9). In contrast, when we filtered to include only participants in the US cohort with $\geq 99\%$ European ancestry to focus on the genetic legacy of the admixed Catoctin individuals' European ancestors along lineages with little to no African admixture, we did not detect any clear geographic patterns (Fig. 5C, Table S12).

15

20

When we focused on “close relatives” (referred to here as pairs of individuals who share at least 30 cM of IBD with a Catoctin individual, reflecting a relationship that is predicted to be 9th-degree or closer), we observed particularly pronounced connections to Maryland, identifying a total of 30 close relatives in the state (Table S16). A randomization test confirmed that we would be unlikely

to identify 30 or more close relatives among an identically sized sample (n=19,972) of randomly selected individuals (p-value<0.001) (Table S17). These results suggest that at least some descendants of the Catoctin individuals or their family members remain in the Maryland area.

5 Next, we considered population substructure among the close relatives of the Catoctin individuals in the US using an IBD network approach. We analyzed 443 close relatives of the Catoctin individuals (≥ 30 cM of IBD) along with 4,385 of those participants' closest relatives who share ≥ 100 cM of IBD—many of whom we hypothesize could be genetically related to the Catoctin individuals, even if we did not detect IBD sharing between them due to the high false negative rate
10 of our approach—and identified 123 familial groups (Fig. 5D, Table S18). The positions of these familial clusters within the IBD network appear to be primarily correlated with the relative proportions of European and Sub-Saharan African ancestry detected among each cluster's members, likely reflecting the ancestry of the individual IBD segments shared with the Catoctin individuals. In most cases, the familial groups do not appear to be correlated with geography.
15 However, notably, all members of familial group 36 who provided location information have ties to Maryland, providing further evidence that Catoctin descendants and close relatives remained in or returned to Maryland after emancipation.

While elevated rates of IBD sharing are particularly evident in the Maryland region, we also
20 identified other regions of the US with an enrichment of Catoctin close relatives. For example, the maximum amount of IBD (280 cM) is observed among a set of individuals from Southern California. This amount of sharing (corresponding to ~4% of the autosomal genome) is consistent with a 5th-degree relationship to the individual from Burial 35 based on maximum likelihood predictions (although the actual relationship may differ by a few degrees in either direction).

Individuals with this amount of IBD sharing are likely either direct descendants of those buried at Catoctin or direct descendants of very close relatives of the Catoctin individuals (given that the Catoctin individuals likely lived at least five generations before most of the research participants included in this study) (Box 1, Table S7).

5

To reconstruct pedigrees describing the connections shared between the Catoctin individuals and their closest genetic relatives in the 23andMe cohort, we used a modified version of the tool Bonsai (36, 43). The informed consent process for participation in 23andMe research requires strict protection of research participant anonymity, which means full pedigrees cannot be published.

10 Instead, we highlight the ways in which 8,721 independent pedigrees (636 of which contain more than one research participant) are connected to Catoctin Family A (Fig. 6, Table S19). We found no cases where the most likely connection was via a direct descendant of individuals from Burials 1, 2, or 24, consistent with our expectations since these individuals died during childhood. The most probable path for most (83%) of the pedigrees we considered connects through an ancestor
15 of the unsampled father of individuals from Burials 1 and 2 (referred to as un-genoyped individual *f* in Fig. 6). We find that pedigrees that include research participants who have at least twice as much Indigenous American ancestry as Sub-Saharan African ancestry were significantly more likely to connect through this unsampled individual than through other Catoctin individuals ($p < 10^{-6}$; calculated via a permutation test with 10^6 replicates) (Supplementary Text S6), consistent
20 with our earlier prediction that this unsampled individual had some Indigenous American ancestry.

Most inferred connections extend upward in pedigrees generated for Families A, C and D (meaning that they connect through an ancestor of one or more members of the family, and therefore do not

involve a direct descent relationship) (Figs. 6 and S14, Table S19). This is consistent with expectations, as individuals who lived in the last few hundred years are expected to have far more living collateral relatives than direct descendants. Notably, lineages that extend upwards from the Catoctin pedigrees tend to involve research participants who have more European ancestry than those lineages that extend downward. This suggests that a relatively large fraction of the connections that we identified involve ancestors of members of Family A with European ancestry, which in part may reflect biases in the 23andMe cohort where European ancestry is overrepresented.

These results demonstrate the power of our IBD-based approach to identify connections between historical and present-day individuals. In the future, by obtaining additional informed consent from research participants it may be possible to present more complex pedigrees that include direct descendants of historical individuals using this approach.

15 **Biologically significant variants**

We considered sites in the Catoctin individuals' genomes that might shed light on their physical traits and health (Table S20, Fig. S15). However, we caution that these results are based on low coverage data, and further work is required to conclusively infer genotypes at these positions.

For three Catoctin individuals, we identified copies of only the causal A allele at the genetic position (*rs334/i3003137*) which is associated with protection against malaria in the heterozygous form and sickle cell disease—a red blood cell disorder that causes pain and increased susceptibility to infection and early mortality (44)—in individuals with two copies of the allele. Although we

only have limited coverage at this position for each of these three individuals (range: 1–5x coverage), making it impossible to confidently determine their genotypes, we note that two individuals (Burials 17 and 19) are siblings who died during early childhood. If they had sickle cell disease, this may have contributed to their early mortality.

5

We also observed four individuals with at least one copy of the causal T allele at another genetic position (*rs1050828*) that provides protection against malaria in genetically female individuals who carry one copy of this allele on only one of their X chromosomes. In genetic males, who are hemizygous, and in genetic females who are homozygous for the T allele at this position, it is associated with G6PD deficiency (45). Both variants occur at elevated rates in populations with ancestry from Sub-Saharan Africa where malaria has historically been endemic (46). Understanding how the frequency of these alleles may have changed in African American populations over time is a question of great interest (47, 48), which may be informed by ancient DNA data as more historical African Americans are sequenced.

15

Discussion

This study demonstrates the power of genetic analyses to uncover previously unknown information about the family structure and ancestry of historical individuals, and to connect them with living relatives. For Catoctin Furnace, this research is a critical step toward identifying a larger descendant community, one of the main goals expressed by stakeholders from CFHS, AARCH, and the two Catoctin descendant families recently identified using historical documents and genealogical data. By developing an approach to identify genetic connections between historical

individuals and their present-day relatives, DNA can be a significant means through which these relationships can be re-constructed.

At least 15 of the Catoctin individuals can be clustered into five genetic families, providing insight into the social structure of African Americans at this early industrial site. Historical records suggest that iron works enslavers often kept families together to benefit from a sustained knowledge transfer between generations. It was also believed that this practice minimized the likelihood of revolt or escape caused by family separation (49–51). The majority of the genetic connections we identified were between first-degree relatives, usually mothers and children. No fathers were identified, nor did we find families with representation of three or more generations. There were at least 11 individuals who appeared unrelated to others buried in the cemetery. These results may therefore indicate that, in practice, families did not remain together at this iron works. One possible explanation is that partners may have been sought outside of the Catoctin village. However, additional consideration must be given to how the types of genetic relationships we observed may be biased by incomplete excavation combined with burial patterning at the site, which was likely influenced by personal choice and/or imposed religious practices. For instance, from first-hand accounts recorded in journals and diaries, we know that some African American funerals at Catoctin were conducted by Moravian ministers (52, 53). The Moravians prescribed burial protocols in which families were not interred together, instead, they were buried in “choirs,” separated by marital status, age, and gender (54). This tradition introduces the possibility that married men were buried elsewhere in the cemetery, and therefore not sampled as part of this study (54). It was only through the co-analysis of aDNA and archival Moravian diaries that this unique aspect of burial and demography at Catoctin could be considered.

The genetically inherited conditions identified in this study (sickle cell anemia and G6PD deficiency) provide additional insight into the health and well-being of the Catoctin African Americans. Although these results are tentative and require more refined analyses, they offer
5 insight and potential future avenues by which to explore the remains of deceased humans recovered from archaeological contexts.

At the population level, the Catoctin individuals have diverse ancestry, with clear genetic links to Africa, Europe, and the Americas. Most individuals have primarily Sub-Saharan African ancestry,
10 with the strongest ties to present-day peoples in Senegambia and West Central Africa, a region that primarily encompasses present-day Angola and the Democratic Republic of the Congo. These findings correlate with historical records that show that slave ships originating from Senegambia (particularly before the end of the 18th century) and West Central Africa accounted for the highest disembarkation rates in Maryland over the course of the transatlantic slave trade, while lower
15 disembarkation rates were recorded from intervening coastal regions and the Caribbean (Table S21) (55). However, records of the intra-American slave trade, which was responsible for the arrival of many enslaved African Americans to Maryland, are more limited, making it challenging to infer what the most likely major sources of African ancestry in Maryland might have been based on historical records alone. According to the transatlantic slave trade database, ships departing
20 from Senegambia and West Central Africa account for 15.8% and 20.8% of overall disembarkations in North America (55). Notably, the most common sources of African ancestry among the Catoctin individuals do not align with larger trends in the greater Chesapeake region,

where the highest rate of disembarkation was from the Bight of Biafra—home to people of Igbo and Yoruba ancestry (55).

The Catoctin individuals were less likely to have genetic connections to multiple distinct African ethnolinguistic groups than research participants with substantial ($\geq 50\%$) Sub-Saharan African ancestry and longstanding ties to the US (i.e., four grandparents born in the US), likely reflecting admixing between individuals with diverse African ancestries that occurred among enslaved African Americans and their descendants over time, following forced migration to the Americas (22, 56).

10

Due to the overrepresentation of research participants with European (particularly British and Irish) ancestry in the 23andMe cohort, we have even more power to localize the European ancestry of the Catoctin individuals. Eight individuals exhibit connections to Great Britain and/or Ireland. Differing frequencies of European associated maternal and paternal haplogroups observed at Catoctin indicate that their European ancestry was likely introduced through a sex-biased process almost certainly driven by rape of enslaved women as part of the gender-based sexual violence inherent in the US's system of chattel slavery (38). We also observed a single European-associated mt haplogroup (in an individual who we estimate to have over 50% European ancestry). This may be one of numerous examples present in the historical record of enslaved or free Black men having children with white women (often indentured servants) (57).

20

Another objective of this study was to explore the possibility of identifying direct descendants using DNA. We identified 41,799 research participants with genetic connections to the Catoctin

individuals. In many cases, it was possible to construct detailed genetic pedigrees that directly link 23andMe research participants to the historical individuals from Catoctin, either as direct descendants or, most commonly, as collateral relatives with a shared common ancestor. While most of these connections are very distant, we identified over 500 relatives who share ≥ 30 cM of 5 IBD, reflecting a maximum likelihood estimate of 9th-degree relationship or closer.

It has been suggested that Catoctin's enslaved workers were sold and transported to more southern states when the furnace transitioned to white wage labor (4). During the early 19th century large numbers of enslaved individuals were sold from Mid-Atlantic states and transported south (58). 10 While we observe strong connections to Maryland that suggest that this was unlikely to be the fate of Catoctin's entire enslaved population, we do observe small clusters of close relatives throughout the US, including in the South.

The methodological approach we present in this study can be applied to the remains of deceased 15 humans from other sites and contexts, offering a new scientific tool for individuals and descendant communities seeking greater knowledge of their ancestors, as well as archaeologists, bioarchaeologists, historians, genealogists. Museums and universities that steward the remains of deceased humans now have an additional means by which to identify past individuals and potentially link them to biological descendants. This work can currently only be done in 20 partnership with organizations with access to massive, genetically diverse, re-contactable research cohorts, such as those maintained by genetic-ancestry companies. These partnerships will require conversations on the ethical implications and consequences of this work, particularly how to avoid reinforcing the biologization of identity (37). For researchers, this study represents advances in

scientific methodology, but the impact may be even greater for those seeking connections to their past.

Materials and Methods Summary

We sampled aDNA from the temporal bones of 27 Catocin individuals, using a minimally
5 destructive cranial based drilling approach when sampling from intact skulls (59). We generated
double stranded, partially uracil-DNA glycosylase (UDG) treated DNA libraries (60–64). Before
sequencing, we enriched the libraries for DNA aligning to the mitochondrial genome and 1.2
million positions in the nuclear genome using a capture-based approach (23–26). Following
bioinformatic processing, all 27 DNA samples were deemed suitable for analysis, although the
10 data for two individuals was subjected to damage restriction based on slightly elevated MT (26)
or X-chromosome (65) contamination rates. For each individual, we inferred genetic sex (66)
and uniparental haplogroups (67) and estimated the proportion of African, European and
Indigenous American-related ancestry by comparing to publicly available datasets (68–71).
Diploid genotypes were imputed using GLIMPSE (72) with the 1000 Genomes project phase 3
15 dataset (68) as a reference panel. After filtering and rephasing the data (73), we searched for IBD
(41) between the imputed Catocin individuals and 9,255,493 participants (elsewhere referred to
as the “23andMe cohort”) who had been genotyped by 23andMe, Inc., a consumer personal
genetics company, and provided informed consent to participate in research by July 28th, 2020.
Summary statistics were generated describing these IBD connections for cohorts of research
20 participants that were created based on each research participant’s genetic ancestry (as
determined by the tool Ancestry Composition) and answers to 23andMe survey questions about
their birth and grandparent birth locations. Genetic pedigrees were reconstructed using a

This is the author's version of the work. It is posted here by permission of the AAAS for personal use, not for redistribution. The definitive version was published in Science on August 4th, 2023, DOI: [10.1126/science.ade4995](https://doi.org/10.1126/science.ade4995).

modified version of the Bonsai pedigree inference algorithm (43). Finally, we counted the number of unique DNA sequences that overlap biologically significant positions in the genome for each Catoctin individual.

References

1. D. Eltis, D. Richardson, *Atlas of the Transatlantic Slave Trade* (Yale University Press, 2010).
- 5 2. U.S. Census Bureau QuickFacts: United States, (available at <https://www.census.gov/quickfacts/fact/table/US/RHI225219#RHI225219>).
3. H. A. Williams, *Help me to find my people: The African American search for family lost in slavery* (Univ of North Carolina Press, 2012).
4. E. Y. Anderson, *Catoctin Furnace: Portrait of an Iron Making Village* (Arcadia Publishing, 10 2013).
5. Catoctin Furnace Historical Society, Compiled by donated labor for the Catoctin Furnace Historical Society. Primary manager, Elizabeth Anderson Comer., Access database of confirmed and potential members of the Catoctin Furnace community. (2015).
6. Frederick County Account of Sales Liber GME 9, Folio 353-361. List of names appears on 15 page 355.
7. R. A. Thomas, G. S. Mellin, T. Payne, S. Burnston, J. P. McCarthy, "Archaeological Investigations at Catoctin Furnace, Frederick County, Maryland" (Mid-Atlantic Archaeological Research, Inc., 1980).
8. A. Townsend, R. Thomas, K. Orr, "Specifications and Research Designs. The Catoctin 20 Furnace Archaeological Mitigation Project. U.S. Route 15 from Putman Road to Route 77." (Prepared for the State Highway Administration, Baltimore, Md., Thurmont, MD, 1979).
9. K. Orr, R. Orr, "Interim Report of the Catoctin Furnace Archaeological Mitigation Project Contract F522-152-770" (Prepared for the Maryland State Highway Administration, Baltimore, 1980).
- 25 10. S. Burnston, R. A. Thomas, "Archaeology Data Recovery at Catoctin Furnace Cemetery" (Prepared for Orr and Son, Consulting Archaeologists, 1981).
11. A. Kelley, J.O. J. L., The workers of Catoctin furnace. *Maryland Archeology*. **19**, 2–17 (1983).
12. K. S. Bruwelheide, D. W. Owsley, K. G. Barca, C. A. M. France, N. Little, E. A. Comer, 30 Restoring Identity to People and Place: Reanalysis of Human Skeletal Remains from a Cemetery at Catoctin Furnace, Maryland. *Hist Arch*. **54**, 110–137 (2020).
13. É. Harney, I. Olalde, K. Bruwelheide, K. G. Barca, R. Curry, E. Comer, N. Rohland, D. Owsley, D. E. Reich, Technical Report on Ancient DNA analysis of 27 African Americans from Catoctin Furnace, Maryland. *bioRxiv* (2022), p. 2022.06.12.495320, , 35 doi:10.1101/2022.06.12.495320.
14. M. L. Blakey, L. M. Rankin-Hill, Howard University, United States, General Services Administration, *The skeletal biology of the New York African Burial Ground* (Howard University Press : in association with the U.S. General Services Administration, Washington, D.C., 2009).
- 40 15. C. K. Clinton, F. L. C. Jackson, Historical overview, current research, and emerging bioethical guidelines in researching the New York African burial ground. *American Journal of Physical Anthropology* (2021), doi:<https://doi.org/10.1002/ajpa.24171>.
16. R. E. Fleskes, A. A. Ofunniyin, J. K. Gilmore, E. Poplin, S. M. Abel, W. D. Bueschgen, C. Juarez, N. Butler, G. Mishoe, G. S. Cabana, Ancestry, health, and lived experiences of 45 enslaved Africans in 18th century Charleston: An osteobiographical analysis. *American Journal of Physical Anthropology* (2021).

17. R. E. Fleskes, G. S. Cabana, J. K. Gilmore, C. Juarez, E. Karcher, L. Oubré, G. Mishoe, A. A. Ofunniyin, T. G. Schurr, Community-engaged ancient DNA project reveals diverse origins of 18th-century African descendants in Charleston, South Carolina. *Proceedings of the National Academy of Sciences*. **120**, e2201620120 (2023).
- 5 18. R. Barquera, T. C. Lamnidis, A. K. Lankapalli, A. Kocher, D. I. Hernández-Zaragoza, E. A. Nelson, A. C. Zamora-Herrera, P. Ramallo, N. Bernal-Felipe, A. Immel, K. Bos, V. Acuña-Alonzo, C. Barbieri, P. Roberts, A. Herbig, D. Kühnert, L. Márquez-Morfin, J. Krause, Origin and Health Status of First-Generation Africans from Early Colonial Mexico. *Current Biology*. **30**, 2078-2091.e11 (2020).
- 10 19. R. E. Fleskes, K. S. Bruwelheide, F. L. West, D. W. Owsley, D. R. Griffith, K. G. Barca, G. S. Cabana, T. G. Schurr, Ancient DNA and bioarchaeological perspectives on European and African diversity and relationships on the colonial Delaware frontier. *American Journal of Physical Anthropology*. **170**, 232–245 (2019).
- 15 20. A. Salas, M. Richards, M.-V. Lareu, R. Scozzari, A. Coppa, A. Torroni, V. Macaulay, Á. Carracedo, The African Diaspora: Mitochondrial DNA and the Atlantic Slave Trade. *The American Journal of Human Genetics*. **74**, 454–465 (2004).
21. A. R. Bentley, S. Callier, C. N. Rotimi, Diversity and inclusion in genomic research: why the uneven progress? *J Community Genet*. **8**, 255–266 (2017).
- 20 22. S. J. Micheletti, K. Bryc, S. G. Ancona Esselmann, W. A. Freyman, M. E. Moreno, G. D. Poznik, A. J. Shastri, S. Beleza, J. L. Mountain, M. Agee, S. Aslibekyan, A. Auton, R. Bell, S. Clark, S. Das, S. Elson, K. Fletez-Brant, P. Fontanillas, P. Gandhi, K. Heilbron, B. Hicks, D. Hinds, K. Huber, E. Jewett, Y. Jiang, A. Kleinman, K. Lin, N. Litterman, J. McCreight, M. McIntyre, K. McManus, S. Mozaffari, P. Nandakumar, L. Noblin, C. Northover, J. O'Connell, A. Petrakovitz, S. Pitts, J. Shelton, S. Shringarpure, C. Tian, J. Tung, R. Tunney, V. Vacic, X. Wang, A. Zare, Genetic Consequences of the Transatlantic Slave Trade in the Americas. *The American Journal of Human Genetics*. **107**, 265–277 (2020).
- 25 23. I. Mathieson, I. Lazaridis, N. Rohland, S. Mallick, N. Patterson, S. A. Roodenberg, E. Harney, K. Stewardson, D. Fernandes, M. Novak, Genome-wide patterns of selection in 230 ancient Eurasians. *Nature*. **528**, 499–503 (2015).
- 30 24. W. Haak, I. Lazaridis, N. Patterson, N. Rohland, S. Mallick, B. Llamas, G. Brandt, S. Nordenfelt, E. Harney, K. Stewardson, Massive migration from the steppe was a source for Indo-European languages in Europe. *Nature*. **522**, 207–211 (2015).
- 35 25. Q. Fu, M. Hajdinjak, O. T. an, S. Constantin, S. Mallick, P. Skoglund, N. Patterson, N. Rohland, I. Lazaridis, B. Nickel, B. Viola, K. Prüfer, M. Meyer, J. Kelso, D. Reich, S. Pääbo, An early modern human from Romania with a recent Neanderthal ancestor. *Nature*. **524**, 216–219 (2015).
- 40 26. Q. Fu, A. Mittnik, P. L. F. Johnson, K. Bos, M. Lari, R. Bollongino, C. Sun, L. Giemsch, R. Schmitz, J. Burger, A. M. Ronchitelli, F. Martini, R. G. Cremonesi, J. Svoboda, P. Bauer, D. Caramelli, S. Castellano, D. Reich, S. Pääbo, J. Krause, A Revised Timescale for Human Evolution Based on Ancient Mitochondrial Genomes. *Current Biology*. **23**, 553–559 (2013).
27. H. L. Gates, *Life Upon These Shores: Looking at African American History, 1513-2008* (Alfred A. Knopf, 2011).
- 45 28. F. Douglass, *My Bondage and My Freedom* (Oxford University Press, 2019).
29. J. K. Wagner, C. Colwell, K. G. Claw, A. C. Stone, D. A. Bolnick, J. Hawks, K. B.

- Brothers, N. A. Garrison, Fostering Responsible Research on Ancient DNA. *The American Journal of Human Genetics*. **107**, 183–195 (2020).
30. S. Alpaslan-Roodenberg, D. Anthony, H. Babiker, E. Bánffy, T. Booth, P. Capone, A. Deshpande-Mukherjee, S. Eisenmann, L. Fehren-Schmitz, M. Frachetti, R. Fujita, C. J. Frieman, Q. Fu, V. Gibbon, W. Haak, M. Hajdinjak, K. P. Hofmann, B. Holguin, T. Inomata, H. Kanzawa-Kiriyama, W. Keegan, J. Kelso, J. Krause, G. Kumaresan, C. Kusimba, S. Kusimba, C. Lalueza-Fox, B. Llamas, S. MacEachern, S. Mallick, H. Matsumura, A. Y. Morales-Arce, G. M. Matuzeviciute, V. Mushrif-Tripathy, N. Nakatsuka, R. Nores, C. Ogola, M. Okumura, N. Patterson, R. Pinhasi, S. P. R. Prasad, M. E. Prendergast, J. L. Punzo, D. Reich, R. Sawafuji, E. Sawchuk, S. Schiffels, J. Sedig, S. Shnaider, K. Sirak, P. Skoglund, V. Slon, M. Snow, M. Soressi, M. Spriggs, P. W. Stockhammer, A. Szécsényi-Nagy, K. Thangaraj, V. Tiesler, R. Tobler, C.-C. Wang, C. Warinner, S. Yasawardene, M. Zahir, Ethics of DNA research on human remains: five globally applicable guidelines. *Nature* (2021), doi:10.1038/s41586-021-04008-x.
- 15 31. J. Dunnivant, D. Justinvil, C. Colwell, Craft an African American Graves Protection and Repatriation Act. *Nature*. **593**, 337–340 (2021).
32. F. Jackson, C. Clinton, J. Graves, Genomics of African American remains — limits must not compound inequity. *Nature*. **596**, 35–35 (2021).
33. J. Benn Torres, Anthropological perspectives on genomic data, genetic ancestry, and race. *American Journal of Physical Anthropology*. **171**, 74–86 (2020).
- 20 34. A. M. Lans, Decolonize this collection: Integrating black feminism and art to re-examine human skeletal remains in museums. *Feminist Anthropology*. **2**, 130–142 (2021).
35. R. M. Austin, M. Zuckerman, T. P. Honap, H. Lee, G. K. Ward, C. Warinner, K. Sankaranarayanan, C. A. Hofman, Remembering St. Louis Individual—structural violence and acute bacterial infections in a historical anatomical collection. *Commun Biol*. **5**, 1–10 (2022).
- 25 36. Detailed information is provided in the supplementary materials.
37. É. Harney, K. Sirak, J. Sedig, S. Micheletti, R. Curry, S. Ancona Esselmann, D. Reich, Ethical considerations when co-analyzing ancient DNA and data from private genetic databases. *AJHG* (2023).
- 30 38. E. E. Baptist, “Cuffy,” “fancy maids,” and “one-eyed men”: rape, commodification, and the domestic slave trade in the United States. *The American Historical Review*. **106**, 1619–1650 (2001).
39. K. Bryc, E. Y. Durand, J. M. Macpherson, D. Reich, J. L. Mountain, The Genetic Ancestry of African Americans, Latinos, and European Americans across the United States. *The American Journal of Human Genetics*. **96**, 37–53 (2015).
- 35 40. R. Hui, E. D’Atanasio, L. M. Cassidy, C. L. Scheib, T. Kivisild, Evaluating genotype imputation pipeline for ultra-low coverage ancient genomes. *Sci Rep*. **10**, 18542 (2020).
41. W. A. Freyman, K. F. McManus, S. S. Shringarpure, E. M. Jewett, K. Bryc, the 23andMe Research Team, A. Auton, Fast and robust identity-by-descent inference with the templated positional Burrows-Wheeler transform. *Molecular Biology and Evolution* (2020), doi:10.1093/molbev/msaa328.
- 40 42. E. Y. Durand, C. B. Do, P. R. Wilton, J. L. Mountain, A. Auton, G. D. Poznik, J. M. Macpherson, *bioRxiv*, doi:10.1101/2021.01.19.427308.
- 45 43. E. M. Jewett, K. F. McManus, W. A. Freyman, A. Auton, Bonsai: An efficient method for inferring large human pedigrees from genotype data. *The American Journal of Human*

- Genetics*. **108**, 2052–2070 (2021).
44. L. Pauling, H. A. Itano, S. J. Singer, I. C. Wells, Sickle Cell Anemia, a Molecular Disease. *Science*. **110**, 543–548 (1949).
45. E. Beutler, G6PD Deficiency. *Blood*. **84**, 3613–3636 (1994).
- 5 46. K. Esoh, A. Wonkam, Evolutionary history of sickle-cell mutation: implications for global genetic medicine. *Human Molecular Genetics*. **30**, R119–R128 (2021).
47. W. Jin, S. Xu, H. Wang, Y. Yu, Y. Shen, B. Wu, L. Jin, Genome-wide detection of natural selection in African Americans pre- and post-admixture. *Genome Res*. **22**, 519–527 (2012).
48. G. Bhatia, A. Tandon, N. Patterson, M. C. Aldrich, C. B. Ambrosone, C. Amos, E. V. Bandera, S. I. Berndt, L. Bernstein, W. J. Blot, C. H. Bock, N. Caporaso, G. Casey, S. L. Deming, W. R. Diver, S. M. Gapstur, E. M. Gillanders, C. C. Harris, B. E. Henderson, S. A. Ingles, W. Isaacs, P. L. De Jager, E. M. John, R. A. Kittles, E. Larkin, L. H. McNeill, R. C. Millikan, A. Murphy, C. Neslund-Dudas, S. Nyante, M. F. Press, J. L. Rodriguez-Gil, B. A. Rybicki, A. G. Schwartz, L. B. Signorello, M. Spitz, S. S. Strom, M. A. Tucker, J. K. Wiencke, J. S. Witte, X. Wu, Y. Yamamura, K. A. Zanetti, W. Zheng, R. G. Ziegler, S. J. Chanock, C. A. Haiman, D. Reich, A. L. Price, Genome-wide Scan of 29,141 African Americans Finds No Evidence of Directional Selection since Admixture. *The American Journal of Human Genetics*. **95**, 437–444 (2014).
49. C. B. Dew, David Ross and the Oxford Iron Works: A Study of Industrial Slavery in the Early Nineteenth-Century South. *The William and Mary Quarterly*. **31**, 189–224 (1974).
- 20 50. C. B. Dew, *Bond of Iron: Master and Slave at Buffalo Forge* (W. W. Norton & Company, 1995).
51. R. L. Lewis, *Coal, Iron, and Slaves: Industrial Slavery in Maryland and Virginia, 1715–1865*. (Greenwood Press, Westport, CT, 1979).
- 25 52. Moravian Missionary Letters – 1766-1787, Moravian Archives, Bethlehem, Pennsylvania. Translated by Edward Quinter, 2021-2022.
53. Diaries of Moravian clergy – 1798-1850, Moravian Archives, Bethlehem, Pennsylvania. Translated by Edward Quinter, 2021-2022.
54. S. P. Gordon, Fishing for a Few: Moravians on the Eighteenth-Century Pennsylvania Frontier. *Pennsylvania History: A Journal of Mid-Atlantic Studies*. **88**, 319–350 (2021).
- 30 55. D. Eltis, A brief overview of the Trans-Atlantic Slave Trade. Voyages: The trans-atlantic slave trade database: 1700-1810 (2007) (available at <https://slavevoyages.org/>).
56. J. K. Thornton, *A Cultural History of the Atlantic World, 1250-1820* (Cambridge University Press, 2012).
- 35 57. L. M. Heywood, J. K. Thornton, *Central Africans, Atlantic Creoles, and the Foundation of the Americas, 1585-1660* (Cambridge University Press, 2007).
58. *Maryland: A History of Its People* (JHU Press, 1986).
59. K. A. Sirak, D. M. Fernandes, O. Cheronet, M. Novak, B. Gamarra, T. Balassa, Z. Bernert, A. Cséki, J. Dani, J. Z. Gallina, G. Kocsis-Buruzs, I. Kővári, O. László, I. Pap, R. Patay, Z. Petkes, G. Szenthe, T. Szeniczey, T. Hajdu, R. Pinhasi, A minimally-invasive method for sampling human petrous bones from the cranial base for ancient DNA analysis. *BioTechniques*. **62**, 283–289 (2017).
- 40 60. J. Dabney, M. Knapp, I. Glocke, M.-T. Gansauge, A. Weihmann, B. Nickel, C. Valdiosera, N. García, S. Pääbo, J.-L. Arsuaga, M. Meyer, Complete mitochondrial genome sequence of a Middle Pleistocene cave bear reconstructed from ultrashort DNA fragments. *PNAS*. **110**, 15758–15763 (2013).
- 45

61. P. Korlević, T. Gerber, M.-T. Gansauge, M. Hajdinjak, S. Nagel, A. Aximu-Petri, M. Meyer, Reducing microbial and human contamination in DNA extractions from ancient bones and teeth. *BioTechniques*. **59**, 87–93 (2015).
- 5 62. N. Rohland, I. Glocke, A. Aximu-Petri, M. Meyer, Extraction of highly degraded DNA from ancient bones, teeth and sediments for high-throughput sequencing. *Nature Protocols*. **13**, 2447–2461 (2018).
63. N. Rohland, E. Harney, S. Mallick, S. Nordenfelt, D. Reich, Partial uracil–DNA–glycosylase treatment for screening of ancient DNA. *Philosophical Transactions of the Royal Society B: Biological Sciences*. **370**, 20130624 (2015).
- 10 64. M.-T. Gansauge, A. Aximu-Petri, S. Nagel, M. Meyer, Manual and automated preparation of single-stranded DNA libraries for the sequencing of DNA from ancient biological remains and other sources of highly degraded DNA. *Nature Protocols*. **15**, 2279–2300 (2020).
- 15 65. T. S. Korneliussen, A. Albrechtsen, R. Nielsen, ANGSD: analysis of next generation sequencing data. *BMC bioinformatics*. **15**, 1–13 (2014).
66. P. Skoglund, J. Storå, A. Götherström, M. Jakobsson, Accurate sex identification of ancient human remains using DNA shotgun sequencing. *Journal of Archaeological Science*. **40**, 4477–4482 (2013).
- 20 67. H. Weissensteiner, D. Pacher, A. Kloss-Brandstätter, L. Forer, G. Specht, H.-J. Bandelt, F. Kronenberg, A. Salas, S. Schönherr, HaploGrep 2: mitochondrial haplogroup classification in the era of high-throughput sequencing. *Nucleic acids research*. **44**, W58–W63 (2016).
- 25 68. A. Auton, G. R. Abecasis, D. M. Altshuler, R. M. Durbin, G. R. Abecasis, D. R. Bentley, A. Chakravarti, A. G. Clark, P. Donnelly, E. E. Eichler, P. Flicek, S. B. Gabriel, R. A. Gibbs, E. D. Green, M. E. Hurles, B. M. Knoppers, J. O. Korbel, E. S. Lander, C. Lee, H. Lehrach, E. R. Mardis, G. T. Marth, G. A. McVean, D. A. Nickerson, J. P. Schmidt, S. T. Sherry, J. Wang, R. K. Wilson, R. A. Gibbs, E. Boerwinkle, H. Doddapaneni, Y. Han, V. Korchina, C. Kovar, S. Lee, D. Muzny, J. G. Reid, Y. Zhu, J. Wang, Y. Chang, Q. Feng, X. Fang, X. Guo, M. Jian, H. Jiang, X. Jin, T. Lan, G. Li, J. Li, Y. Li, S. Liu, X. Liu, Y. Lu, X. Ma, M. Tang, B. Wang, G. Wang, H. Wu, R. Wu, X. Xu, Y. Yin, D. Zhang, W. Zhang, J. Zhao, M. Zhao, X. Zheng, E. S. Lander, D. M. Altshuler, S. B. Gabriel, N. Gupta, N. Gharani, L. H. Toji, N. P. Gerry, A. M. Resch, P. Flicek, J. Barker, L. Clarke, L. Gil, S. E. Hunt, G. Kelman, E. Kulesha, R. Leinonen, W. M. McLaren, R. Radhakrishnan, A. Roa, D. Smirnov, R. E. Smith, I. Streeter, A. Thormann, I. Toneva, B. Vaughan, X. Zheng-Bradley, D. R. Bentley, R. Grocock, S. Humphray, T. James, Z. Kingsbury, H. Lehrach, R. Sudbrak, M. W. Albrecht, V. S. Amstislavskiy, T. A. Borodina, M. Lienhard, F. Mertes, M. Sultan, B. Timmermann, M.-L. Yaspo, E. R. Mardis, R. K. Wilson, L. Fulton, R. Fulton, S. T. Sherry, V. Ananiev, Z. Belaia, D. Beloslyudtsev, N. Bouk, C. Chen, D. Church, R. Cohen, C. Cook, J. Garner, T. Hefferon, M. Kimelman, C. Liu, J. Lopez, P. Meric, C. O’Sullivan, Y. Ostapchuk, L. Phan, S. Ponomarov, V. Schneider, E. Shekhtman, K. Sirotkin, D. Slotta, H. Zhang, G. A. McVean, R. M. Durbin, S. Balasubramaniam, J. Burton, P. Danecek, T. M. Keane, A. Kolb-Kokocinski, S. McCarthy, J. Stalker, M. Quail, J. P. Schmidt, C. J. Davies, J. Gollub, T. Webster, B. Wong, Y. Zhan, A. Auton, C. L. Campbell, Y. Kong, A. Marcketta, R. A. Gibbs, F. Yu, L. Antunes, M. Bainbridge, D. Muzny, A. Sabo, Z. Huang, J. Wang, L. J. M. Coin, L. Fang, X. Guo, X. Jin, G. Li, Q. Li, Y. Li, Z. Li, H. Lin, B. Liu, R. Luo, H. Shao, Y. Xie, C. Ye, C. Yu, F. Zhang, H. Zheng, H. Zhu, C. Alkan, E. Dal, F. Kahveci, G. T. Marth, E. P. Garrison, D. Kural, W.-P. Lee, W. Fung Leong, M. Stromberg,
- 40 45

- A. N. Ward, J. Wu, M. Zhang, M. J. Daly, M. A. DePristo, R. E. Handsaker, D. M. Altshuler, E. Banks, G. Bhatia, G. del Angel, S. B. Gabriel, G. Genovese, N. Gupta, H. Li, S. Kashin, E. S. Lander, S. A. McCarroll, J. C. Nemesh, R. E. Poplin, S. C. Yoon, J. Lihm, V. Makarov, A. G. Clark, S. Gottipati, A. Keinan, J. L. Rodriguez-Flores, J. O. Korbel, T. Rausch, M. H. Fritz, A. M. Stütz, P. Flicek, K. Beal, L. Clarke, A. Datta, J. Herrero, W. M. McLaren, G. R. S. Ritchie, R. E. Smith, D. Zerbino, X. Zheng-Bradley, P. C. Sabeti, I. Shlyakhter, S. F. Schaffner, J. Vitti, D. N. Cooper, E. V. Ball, P. D. Stenson, D. R. Bentley, B. Barnes, M. Bauer, R. Keira Cheetham, A. Cox, M. Eberle, S. Humphray, S. Kahn, L. Murray, J. Peden, R. Shaw, E. E. Kenny, M. A. Batzer, M. K. Konkel, J. A. Walker, D. G. MacArthur, M. Lek, R. Sudbrak, V. S. Amstislavskiy, R. Herwig, E. R. Mardis, L. Ding, D. C. Koboldt, D. Larson, K. Ye, S. Gravel, The 1000 Genomes Project Consortium, Corresponding authors, Steering committee, Production group, Baylor College of Medicine, BGI-Shenzhen, Broad Institute of MIT and Harvard, Coriell Institute for Medical Research, E. B. I. European Molecular Biology Laboratory, Illumina, Max Planck Institute for Molecular Genetics, McDonnell Genome Institute at Washington University, US National Institutes of Health, University of Oxford, Wellcome Trust Sanger Institute, Analysis group, Affymetrix, Albert Einstein College of Medicine, Bilkent University, Boston College, Cold Spring Harbor Laboratory, Cornell University, European Molecular Biology Laboratory, Harvard University, Human Gene Mutation Database, Icahn School of Medicine at Mount Sinai, Louisiana State University, Massachusetts General Hospital, McGill University, N. National Eye Institute, A global reference for human genetic variation. *Nature*. **526**, 68–74 (2015).
69. A. Bergström, S. A. McCarthy, R. Hui, M. A. Almarri, Q. Ayub, P. Danecek, Y. Chen, S. Felkel, P. Hallast, J. Kamm, H. Blanché, J.-F. Deleuze, H. Cann, S. Mallick, D. Reich, M. S. Sandhu, P. Skoglund, A. Scally, Y. Xue, R. Durbin, C. Tyler-Smith, Insights into human genetic variation and population history from 929 diverse genomes. *Science*. **367**, eaay5012 (2020).
70. S. Mallick, H. Li, M. Lipson, I. Mathieson, M. Gymrek, F. Racimo, M. Zhao, N. Chennagiri, S. Nordenfelt, A. Tandon, P. Skoglund, I. Lazaridis, S. Sankararaman, Q. Fu, N. Rohland, G. Renaud, Y. Erlich, T. Willems, C. Gallo, J. P. Spence, Y. S. Song, G. Poletti, F. Balloux, G. van Driem, P. de Knijff, I. G. Romero, A. R. Jha, D. M. Behar, C. M. Bravi, C. Capelli, T. Hervig, A. Moreno-Estrada, O. L. Posukh, E. Balanovska, O. Balanovsky, S. Karachanak-Yankova, H. Sahakyan, D. Toncheva, L. Yepiskoposyan, C. Tyler-Smith, Y. Xue, M. S. Abdullah, A. Ruiz-Linares, C. M. Beall, A. Di Rienzo, C. Jeong, E. B. Starikovskaya, E. Metspalu, J. Parik, R. Villems, B. M. Henn, U. Hodoglugil, R. Mahley, A. Sajantila, G. Stamatoyannopoulos, J. T. S. Wee, R. Khusainova, E. Khusnutdinova, S. Litvinov, G. Ayodo, D. Comas, M. F. Hammer, T. Kivisild, W. Klitz, C. A. Winkler, D. Labuda, M. Bamshad, L. B. Jorde, S. A. Tishkoff, W. S. Watkins, M. Metspalu, S. Dryomov, R. Sukernik, L. Singh, K. Thangaraj, S. Pääbo, J. Kelso, N. Patterson, D. Reich, The Simons Genome Diversity Project: 300 genomes from 142 diverse populations. *Nature*. **538**, 201–206 (2016).
71. S. Mallick, A. Micco, M. Mah, H. Ringbauer, I. Lazaridis, I. Olalde, N. Patterson, D. Reich, The Allen Ancient DNA Resource (AADR): A curated compendium of ancient human genomes (2023), p. 2023.04.06.535797, , doi:10.1101/2023.04.06.535797.
72. S. Rubinacci, D. M. Ribeiro, R. J. Hofmeister, O. Delaneau, Efficient phasing and imputation of low-coverage sequencing data using large reference panels. *Nat Genet*. **53**,

- 120–126 (2021).
73. P.-R. Loh, P. F. Palamara, A. L. Price, Fast and accurate long-range phasing in a UK Biobank cohort. *Nature Genetics*. **48**, 811–816 (2016).
74. R. Pinhasi, D. M. Fernandes, K. Sirak, O. Cheronet, Isolating the human cochlea to generate bone powder for ancient DNA analysis. *Nature Protocols*. **14**, 1194–1205 (2019).
75. R. Pinhasi, D. Fernandes, K. Sirak, M. Novak, S. Connell, S. Alpaslan-Roodenberg, F. Gerritsen, V. Moiseyev, A. Gromov, P. Raczky, A. Anders, M. Pietrusewsky, G. Rollefson, M. Jovanovic, H. Trinhhoang, G. Bar-Oz, M. Oxenham, H. Matsumura, M. Hofreiter, Optimal Ancient DNA Yields from the Inner Ear Part of the Human Petrous Bone. *PLOS ONE*. **10**, e0129102 (2015).
76. I. Mathieson, S. Alpaslan-Roodenberg, C. Posth, A. Szécsényi-Nagy, N. Rohland, S. Mallick, I. Olalde, N. Broomandkoshbacht, F. Candilio, O. Cheronet, D. Fernandes, M. Ferry, B. Gamarra, G. G. Fortes, W. Haak, E. Harney, E. Jones, D. Keating, B. Krause-Kyora, I. Kucukkalipci, M. Michel, A. Mittnik, K. Nägele, M. Novak, J. Oppenheimer, N. Patterson, S. Pfrengle, K. Sirak, K. Stewardson, S. Vai, S. Alexandrov, K. W. Alt, R. Andreescu, D. Antonović, A. Ash, N. Atanassova, K. Bacvarov, M. B. Gusztáv, H. Bocherens, M. Bolus, A. Boroneanț, Y. Boyadzhiev, A. Budnik, J. Burmaz, S. Chohadzhiev, N. J. Conard, R. Cottiaux, M. Čuka, C. Cupillard, D. G. Drucker, N. Elenski, M. Francken, B. Galabova, G. Ganetsovski, B. Gély, T. Hajdu, V. Handzhyiska, K. Harvati, T. Higham, S. Iliev, I. Janković, I. Karavanić, D. J. Kennett, D. Komšo, A. Kozak, D. Labuda, M. Lari, C. Lazar, M. Leppek, K. Leshtakov, D. L. Vetro, D. Los, I. Lozanov, M. Malina, F. Martini, K. McSweeney, H. Meller, M. Menđušić, P. Mirea, V. Moiseyev, V. Petrova, T. D. Price, A. Simalcsik, L. Sineo, M. Šlaus, V. Slavchev, P. Stanev, A. Starović, T. Szeniczey, S. Talamo, M. Teschler-Nicola, C. Thevenet, I. Valchev, F. Valentin, S. Vasilyev, F. Veljanovska, S. Venelinova, E. Veselovskaya, B. Viola, C. Virag, J. Zaninović, S. Zäuner, P. W. Stockhammer, G. Catalano, R. Krauß, D. Caramelli, G. Zariņa, B. Gaydarska, M. Lillie, A. G. Nikitin, I. Potekhina, A. Papatasiou, D. Borić, C. Bonsall, J. Krause, R. Pinhasi, D. Reich, The genomic history of southeastern Europe. *Nature*. **555**, 197–203 (2018).
77. D. M. Behar, M. Van Oven, S. Rosset, M. Metspalu, E.-L. Loogväli, N. M. Silva, T. Kivisild, A. Torroni, R. Villems, A “Copernican” reassessment of the human mitochondrial DNA tree from its root. *The American Journal of Human Genetics*. **90**, 675–684 (2012).
78. H. Li, R. Durbin, Fast and accurate long-read alignment with Burrows–Wheeler transform. *Bioinformatics*. **26**, 589–595 (2010).
79. P. Skoglund, B. H. Northoff, M. V. Shunkov, A. P. Derevianko, S. Pääbo, J. Krause, M. Jakobsson, Separating endogenous ancient DNA from modern day contamination in a Siberian Neandertal. *Proceedings of the National Academy of Sciences*. **111**, 2229–2234 (2014).
80. I. Olalde, S. Mallick, N. Patterson, N. Rohland, V. Villalba-Mouco, M. Silva, K. Dulias, C. J. Edwards, F. Gandini, M. Pala, P. Soares, M. Ferrando-Bernal, N. Adamski, N. Broomandkoshbacht, O. Cheronet, B. J. Cuckle, D. Fernandes, A. M. Lawson, M. Mah, J. Oppenheimer, K. Stewardson, Z. Zhang, J. M. J. Arenas, I. J. T. Moyano, D. C. Salazar-García, P. Castanyer, M. Santos, J. Tremoleda, M. Lozano, P. G. Borja, J. Fernández-Eraso, J. A. Mujika-Alustiza, C. Barroso, F. J. Bermúdez, E. V. Mínguez, J. Burch, N. Coromina, D. Vivó, A. Cebrià, J. M. Fullola, O. García-Puchol, J. I. Morales, F. X. Oms, T. Majó, J. M. Vergès, A. Díaz-Carvajal, I. Ollich-Castanyer, F. J. López-Cachero, A. M. Silva, C.

- Alonso-Fernández, G. D. de Castro, J. J. Echevarría, A. Moreno-Márquez, G. P. Berlanga, P. Ramos-García, J. Ramos-Muñoz, E. V. Vila, G. A. Arzo, Á. E. Arroyo, K. T. Lillios, J. Mack, J. Velasco-Vázquez, A. Waterman, L. B. de L. Enrich, M. B. Sánchez, B. Agustí, F. Codina, G. de Prado, A. Estalrich, Á. F. Flores, C. Finlayson, G. Finlayson, S. Finlayson, 5 F. Giles-Guzmán, A. Rosas, V. B. González, G. G. Atiénzar, M. S. H. Pérez, A. Llanos, Y. C. Marco, I. C. Beneyto, D. López-Serrano, M. S. Tormo, A. C. Valera, C. Blasco, C. Liesau, P. Ríos, J. Daura, M. J. de P. Michó, A. A. Diez-Castillo, R. F. Fernández, J. F. Farré, R. Garrido-Pena, V. S. Gonçalves, E. Guerra-Doce, A. M. Herrero-Corral, J. Juan-Cabanilles, D. López-Reyes, S. B. McClure, M. M. Pérez, A. O. Foix, M. S. Borràs, A. C. 10 Sousa, J. M. V. Encinas, D. J. Kennett, M. B. Richards, K. W. Alt, W. Haak, R. Pinhasi, C. Lalueza-Fox, D. Reich, The genomic history of the Iberian Peninsula over the past 8000 years. *Science*. **363**, 1230–1234 (2019).
81. É. Harney, N. Patterson, D. Reich, J. Wakeley, Assessing the performance of qpAdm: a statistical tool for studying population admixture. *Genetics*. **217** (2021), doi:10.1093/genetics/iyaa045.
- 15 82. D. H. Alexander, J. Novembre, K. Lange, Fast model-based estimation of ancestry in unrelated individuals. *Genome Res*. **19**, 1655–1664 (2009).
83. N. Patterson, A. L. Price, D. Reich, Population Structure and Eigenanalysis. *PLOS Genetics*. **2**, e190 (2006).
- 20 84. V. M. Narasimhan, N. Patterson, P. Moorjani, N. Rohland, R. Bernardos, S. Mallick, I. Lazaridis, N. Nakatsuka, I. Olalde, M. Lipson, A. M. Kim, L. M. Olivieri, A. Coppa, M. Vidale, J. Mallory, V. Moiseyev, E. Kitov, J. Monge, N. Adamski, N. Alex, N. Broomandkhoshbacht, F. Candilio, K. Callan, O. Cheronet, B. J. Culleton, M. Ferry, D. Fernandes, S. Freilich, B. Gamarra, D. Gaudio, M. Hajdinjak, É. Harney, T. K. Harper, D. 25 Keating, A. M. Lawson, M. Mah, K. Mandl, M. Michel, M. Novak, J. Oppenheimer, N. Rai, K. Sirak, V. Slon, K. Stewardson, F. Zalzala, Z. Zhang, G. Akhatov, A. N. Bagashev, A. Bagnera, B. Baitanayev, J. Bendezu-Sarmiento, A. A. Bissembaev, G. L. Bonora, T. T. Chargynov, T. Chikisheva, P. K. Dashkovskiy, A. Derevianko, M. Dobeš, K. Douka, N. Dubova, M. N. Duisengali, D. Enshin, A. Epimakhov, A. V. Fribus, D. Fuller, A. 30 Goryachev, A. Gromov, S. P. Grushin, B. Hanks, M. Judd, E. Kazizov, A. Khokhlov, A. P. Krygin, E. Kupriyanova, P. Kuznetsov, D. Luiselli, F. Maksudov, A. M. Mamedov, T. B. Mamirov, C. Meiklejohn, D. C. Merrett, R. Micheli, O. Mochalov, S. Mustafokulov, A. Nayak, D. Pettener, R. Potts, D. Razhev, M. Rykun, S. Sarno, T. M. Savenkova, K. Sikhymbaeva, S. M. Slepchenko, O. A. Soltobaev, N. Stepanova, S. Svyatko, K. Tabaldiev, 35 M. Teschler-Nicola, A. A. Tishkin, V. V. Tkachev, S. Vasilyev, P. Velemínský, D. Voyakin, A. Yermolayeva, M. Zahir, V. S. Zubkov, A. Zubova, V. S. Shinde, C. Lalueza-Fox, M. Meyer, D. Anthony, N. Boivin, K. Thangaraj, D. J. Kennett, M. Frachetti, R. Pinhasi, D. Reich, The formation of human populations in South and Central Asia. *Science*. **365** (2019), doi:10.1126/science.aat7487.
- 40 85. L. Van Dorp, S. Lowes, J. L. Weigel, N. Ansari-Pour, S. López, J. Mendoza-Revilla, J. A. Robinson, J. Henrich, M. G. Thomas, N. Nunn, Genetic legacy of state centralization in the Kuba Kingdom of the Democratic Republic of the Congo. *Proceedings of the National Academy of Sciences*. **116**, 593–598 (2019).
- 45 86. B. A. Jackson, J. L. Wilson, S. Kirbah, S. S. Sidney, J. Rosenberger, L. Bassie, J. A. Alie, D. C. McLean, W. T. Garvey, B. Ely, Mitochondrial DNA genetic diversity among four ethnic groups in Sierra Leone. *American journal of physical anthropology*. **128**, 156–163

- (2005).
87. B. M. Henn, C. R. Gignoux, M. Jobin, J. M. Granka, J. Macpherson, J. M. Kidd, L. Rodríguez-Botigué, S. Ramachandran, L. Hon, A. Brisbin, Hunter-gatherer genomic diversity suggests a southern African origin for modern humans. *Proceedings of the National Academy of Sciences*. **108**, 5154–5162 (2011).
- 5 88. V. D. Blondel, J.-L. Guillaume, R. Lambiotte, E. Lefebvre, Fast unfolding of communities in large networks. *Journal of statistical mechanics: theory and experiment*. **2008**, P10008 (2008).
89. M. Bastian, S. Heymann, M. Jacomy, "Gephi: an open source software for exploring and manipulating networks" in (2009).
- 10 90. Enslaved faces from African American cemetery in Catocin, Maryland recreated - The Washington Post, (available at <https://www.washingtonpost.com/history/2021/07/09/african-american-cemetery-catocin-enslaved-faces/>).
- 15 91. A. Roberts, Historical Society unveils facial reconstructions of African-Americans once enslaved in Thurmont. *The Frederick News-Post*, (available at https://www.fredericknewspost.com/news/economy_and_business/tourism/historical-society-unveils-facial-reconstructions-of-african-americans-once-enslaved-in-thurmont/article_57a8171b-f3e2-52c8-bb8d-a6fc6d189ef2.html).
- 20 92. S. M. Fullerton, S. S.-J. Lee, Secondary uses and the governance of de-identified data: Lessons from the human genome diversity panel. *BMC Medical Ethics*. **12**, 16 (2011).
93. D. B. Resnik, The Human Genome Diversity Project: Ethical Problems and Solutions. *Politics and the Life Sciences*. **18**, 15–23 (1999).
- 25 94. J. O'Connell, T. Yun, M. Moreno, H. Li, N. Litterman, A. Kolesnikov, E. Noblin, P.-C. Chang, A. Shastri, E. H. Dorfman, S. Shringarpure, A. Auton, A. Carroll, C. Y. McLean, A population-specific reference panel for improved genotype imputation in African Americans. *Commun Biol*. **4**, 1–9 (2021).
95. E. R. Ebel, F. Reis, D. A. Petrov, S. Beleza, Historical trends and new surveillance of Plasmodium falciparum drug resistance markers in Angola. *Malaria Journal*. **20**, 175
- 30 (2021).
96. L. Sweeney, k-ANONYMITY: A MODEL FOR PROTECTING PRIVACY. *Int. J. Unc. Fuzz. Knowl. Based Syst*. **10**, 557–570 (2002).
97. E. Birney, M. Inouye, J. Raff, A. Rutherford, A. Scally, The language of race, ethnicity, and ancestry in human genetic research (2021), , doi:10.48550/arXiv.2106.10041.
- 35 98. J. K. Wagner, J.-H. Yu, J. O. Ifekwunigwe, T. M. Harrell, M. J. Bamshad, C. D. Royal, Anthropologists' views on race, ancestry, and genetics. *American Journal of Physical Anthropology*. **162**, 318–327 (2017).
99. I. Mathieson, A. Scally, What is ancestry? *PLOS Genetics*. **16**, e1008624 (2020).
100. C. Agyemang, R. Bhopal, M. Bruijnzeels, Negro, Black, Black African, African Caribbean, African American or what? Labelling African origin populations in the health arena in the
- 40 21st century. *Journal of Epidemiology & Community Health*. **59**, 1014–1018 (2005).
101. AP says it will capitalize Black but not white | AP News, (available at <https://apnews.com/article/entertainment-cultures-race-and-ethnicity-us-news-ap-top-news-7e36c00c5af0436abc09e051261fff1f>).
- 45 102. G. Coop, Genetic similarity versus genetic ancestry groups as sample descriptors in human genetics (2023), , doi:10.48550/arXiv.2207.11595.

103. A. C. F. Lewis, S. J. Molina, P. S. Appelbaum, B. Dauda, A. Di Rienzo, A. Fuentes, S. M. Fullerton, N. A. Garrison, N. Ghosh, E. M. Hammonds, D. S. Jones, E. E. Kenny, P. Kraft, S. S.-J. Lee, M. Mauro, J. Novembre, A. Panofsky, M. Sohail, B. M. Neale, D. S. Allen, Getting genetic ancestry right for science and society. *Science*. **376**, 250–252 (2022).
- 5 104. M. Miyagi, E. M. Guthman, S. D.-K. Sun, Transgender rights rely on inclusive language. *Science*. **374**, 1568–1569 (2021).
105. J. Brück, Ancient DNA, kinship and relational identities in Bronze Age Britain. *Antiquity*. **95**, 228–237 (2021).
- 10 106. S. S. Ebenesersdóttir, M. Sandoval-Velasco, E. D. Gunnarsdóttir, A. Jagadeesan, V. B. Guðmundsdóttir, E. L. Thordardóttir, M. S. Einarsdóttir, K. H. S. Moore, Á. Sigurðsson, D. N. Magnúsdóttir, H. Jónsson, S. Snorrardóttir, E. Hovig, P. Møller, I. Kockum, T. Olsson, L. Alfredsson, T. F. Hansen, T. Werge, G. L. Cavalleri, E. Gilbert, C. Lalueza-Fox, J. W. Walser, S. Kristjánsdóttir, S. Gopalakrishnan, L. Árnadóttir, Ó. Þ. Magnússon, M. T. P. Gilbert, K. Stefánsson, A. Helgason, Ancient genomes from Iceland reveal the making of a human population. *Science*. **360**, 1028–1032 (2018).
- 15 107. I. Olalde, S. Brace, M. E. Allentoft, I. Armit, K. Kristiansen, T. Booth, N. Rohland, S. Mallick, A. Szécsényi-Nagy, A. Mittnik, E. Altena, M. Lipson, I. Lazaridis, T. K. Harper, N. Patterson, N. Broomandkoshbacht, Y. Diekmann, Z. Faltyskova, D. Fernandes, M. Ferry, E. Harney, P. de Knijff, M. Michel, J. Oppenheimer, K. Stewardson, A. Barclay, K. W. Alt, C. Liesau, P. Ríos, C. Blasco, J. V. Miguel, R. M. García, A. A. Fernández, E. Bánffy, M. Bernabò-Brea, D. Billoin, C. Bonsall, L. Bonsall, T. Allen, L. Büster, S. Carver, L. C. Navarro, O. E. Craig, G. T. Cook, B. Cunliffe, A. Denaire, K. E. Dinwiddy, N. Dodwell, M. Ernée, C. Evans, M. Kuchařík, J. F. Farré, C. Fowler, M. Gazenbeek, R. G. Pena, M. Haber-Uriarte, E. Haduch, G. Hey, N. Jowett, T. Knowles, K. Massy, S. Pfrengle, P. Lefranc, O. Lemercier, A. Lefebvre, C. H. Martínez, V. G. Olmo, A. B. Ramírez, J. L. Maurandi, T. Majó, J. I. McKinley, K. McSweeney, B. G. Mende, A. Modi, G. Kulcsár, V. Kiss, A. Czene, R. Patay, A. Endrődi, K. Köhler, T. Hajdu, T. Szeniczey, J. Dani, Z. Bernert, M. Hoole, O. Cheronet, D. Keating, P. Velemínský, M. Dobeš, F. Candilio, F. Brown, R. F. Fernández, A.-M. Herrero-Corral, S. Tusa, E. Carnieri, L. Lentini, A. Valenti, A. Zanini, C. Waddington, G. Delibes, E. Guerra-Doce, B. Neil, M. Brittain, M. Luke, R. Mortimer, J. Desideri, M. Besse, G. Brücken, M. Furmanek, A. Hałuszko, M. Mackiewicz, A. Rapiński, S. Leach, I. Soriano, K. T. Lillios, J. L. Cardoso, M. P. Pearson, P. Włodarczak, T. D. Price, P. Prieto, P.-J. Rey, R. Risch, M. A. Rojo Guerra, A. Schmitt, J. Serralongue, A. M. Silva, V. Smrčka, L. Vergnaud, J. Zilhão, D. Caramelli, T. Higham, M. G. Thomas, D. J. Kennett, H. Fokkens, V. Heyd, A. Sheridan, K.-G. Sjögren, P. W. Stockhammer, J. Krause, R. Pinhasi, W. Haak, I. Barnes, C. Lalueza-Fox, D. Reich, The Beaker phenomenon and the genomic transformation of northwest Europe. *Nature*. **555**, 190–196 (2018).
- 20 25 30 35 40 45
108. “Allen Ancient Genome Diversity Project / John Templeton Ancient DNA Atlas.”
109. I. Lazaridis, D. Nadel, G. Rollefson, D. C. Merrett, N. Rohland, S. Mallick, D. Fernandes, M. Novak, B. Gamarra, K. Sirak, S. Connell, K. Stewardson, E. Harney, Q. Fu, G. Gonzalez-Fortes, E. R. Jones, S. A. Roodenberg, G. Lengyel, F. Bocquentin, B. Gasparian, J. M. Monge, M. Gregg, V. Eshed, A.-S. Mizrahi, C. Meiklejohn, F. Gerritsen, L. Bejenaru, M. Blüher, A. Campbell, G. Cavalleri, D. Comas, P. Froguel, E. Gilbert, S. M. Kerr, P. Kovacs, J. Krause, D. McGettigan, M. Merrigan, D. A. Merriwether, S. O’Reilly, M. B. Richards, O. Semino, M. Shamooun-Pour, G. Stefanescu, M. Stumvoll, A. Tönjes, A.

- Torrioni, J. F. Wilson, L. Yengo, N. A. Hovhannisyan, N. Patterson, R. Pinhasi, D. Reich, Genomic insights into the origin of farming in the ancient Near East. *Nature*. **536**, 419–424 (2016).
- 5 110. M. G. Llorente, E. R. Jones, A. Eriksson, V. Siska, K. W. Arthur, J. W. Arthur, M. C. Curtis, J. T. Stock, M. Coltorti, P. Pieruccini, S. Stretton, F. Brock, T. Higham, Y. Park, M. Hofreiter, D. G. Bradley, J. Bhak, R. Pinhasi, A. Manica, Ancient Ethiopian genome reveals extensive Eurasian admixture in Eastern Africa. *Science* (2015), doi:10.1126/science.aad2879.
- 10 111. P. de B. Damgaard, R. Martiniano, J. Kamm, J. V. Moreno-Mayar, G. Kroonen, M. Peyrot, G. Barjamovic, S. Rasmussen, C. Zacho, N. Baimukhanov, V. Zaibert, V. Merz, A. Biddanda, I. Merz, V. Loman, V. Evdokimov, E. Usmanova, B. Hemphill, A. Seguin-Orlando, F. E. Yediay, I. Ullah, K.-G. Sjögren, K. H. Iversen, J. Choin, C. de la Fuente, M. Ilardo, H. Schroeder, V. Moiseyev, A. Gromov, A. Polyakov, S. Omura, S. Y. Senyurt, H. Ahmad, C. McKenzie, A. Margaryan, A. Hameed, A. Samad, N. Gul, M. H. Khokhar, O. I. Goriunova, V. I. Bazaliiskii, J. Novembre, A. W. Weber, L. Orlando, M. E. Allentoft, R. Nielsen, K. Kristiansen, M. Sikora, A. K. Outram, R. Durbin, E. Willerslev, The first horse herders and the impact of early Bronze Age steppe expansions into Asia. *Science* (2018), doi:10.1126/science.aar7711.
- 20 112. C. Gamba, E. R. Jones, M. D. Teasdale, R. L. McLaughlin, G. Gonzalez-Fortes, V. Mattiangeli, L. Domboróczki, I. Kővári, I. Pap, A. Anders, A. Whittle, J. Dani, P. Raczky, T. F. G. Higham, M. Hofreiter, D. G. Bradley, R. Pinhasi, Genome flux and stasis in a five millennium transect of European prehistory. *Nat Commun*. **5**, 5257 (2014).
- 25 113. D. Gokhman, E. Lavi, K. Prüfer, M. F. Fraga, J. A. Riancho, J. Kelso, S. Pääbo, E. Meshorer, L. Carmel, Reconstructing the DNA Methylation Maps of the Neandertal and the Denisovan. *Science*. **344**, 523–527 (2014).
- 30 114. T. Günther, H. Malmström, E. M. Svensson, A. Omrak, F. Sánchez-Quinto, G. M. Kılınc, M. Krzewińska, G. Eriksson, M. Fraser, H. Edlund, A. R. Munters, A. Coutinho, L. G. Simões, M. Vicente, A. Sjölander, B. J. Sellevold, R. Jørgensen, P. Claes, M. D. Shriver, C. Valdiosera, M. G. Netea, J. Apel, K. Lidén, B. Skar, J. Storå, A. Götherström, M. Jakobsson, Population genomics of Mesolithic Scandinavia: Investigating early postglacial migration routes and high-latitude adaptation. *PLOS Biology*. **16**, e2003703 (2018).
- 35 115. M. Ferrando-Bernal, C. Morcillo-Suarez, T. de-Dios, P. Gelabert, S. Civit, A. Díaz-Carvajal, I. Ollich-Castanyer, M. E. Allentoft, S. Valverde, C. Lalueza-Fox, Mapping co-ancestry connections between the genome of a Medieval individual and modern Europeans. *Scientific Reports*. **10**, 6843 (2020).
- 40 116. A. Margaryan, D. J. Lawson, M. Sikora, F. Racimo, S. Rasmussen, I. Moltke, L. M. Cassidy, E. Jørsboe, A. Ingason, M. W. Pedersen, T. Korneliussen, H. Wilhelmson, M. M. Buś, P. de Barros Damgaard, R. Martiniano, G. Renaud, C. Bhérer, J. V. Moreno-Mayar, A. K. Fotakis, M. Allen, R. Allmæ, M. Molak, E. Cappellini, G. Scorrano, H. McColl, A. Buzhilova, A. Fox, A. Albrechtsen, B. Schütz, B. Skar, C. Arcini, C. Falys, C. H. Jonson, D. Błaszczyk, D. Pezhemsky, G. Turner-Walker, H. Gestsdóttir, I. Lundstrøm, I. Gustin, I. Mainland, I. Potekhina, I. M. Muntoni, J. Cheng, J. Stenderup, J. Ma, J. Gibson, J. Peets, J. Gustafsson, K. H. Iversen, L. Simpson, L. Strand, L. Loe, M. Sikora, M. Florek, M. Vretemark, M. Redknap, M. Bajka, T. Pushkina, M. Søvstø, N. Grigoreva, T. Christensen, O. Kastholm, O. Uldum, P. Favia, P. Holck, S. Sten, S. V. Arge, S. Ellingvåg, V. Moiseyev, W. Bogdanowicz, Y. Magnusson, L. Orlando, P. Pentz, M. D. Jessen, A. Pedersen, M.
- 45

- Collard, D. G. Bradley, M. L. Jørkov, J. Arneborg, N. Lynnerup, N. Price, M. T. P. Gilbert, M. E. Allentoft, J. Bill, S. M. Sindbæk, L. Hedeager, K. Kristiansen, R. Nielsen, T. Werge, E. Willerslev, Population genomics of the Viking world. *Nature*. **585**, 390–396 (2020).
- 5 117. M. Sikora, V. V. Pitulko, V. C. Sousa, M. E. Allentoft, L. Vinner, S. Rasmussen, A. Margaryan, P. de Barros Damgaard, C. de la Fuente, G. Renaud, M. A. Yang, Q. Fu, I. Dupanloup, K. Giampoudakis, D. Nogués-Bravo, C. Rahbek, G. Kroonen, M. Peyrot, H. McColl, S. V. Vasilyev, E. Veselovskaya, M. Gerasimova, E. Y. Pavlova, V. G. Chasnyk, P. A. Nikolskiy, A. V. Gromov, V. I. Khartanovich, V. Moiseyev, P. S. Grebenyuk, A. Y. Fedorchenko, A. I. Lebedintsev, S. B. Slobodin, B. A. Malyarchuk, R. Martiniano, M. Meldgaard, L. Arppe, J. U. Palo, T. Sundell, K. Mannermaa, M. Putkonen, V. Alexandersen, C. Primeau, N. Baimukhanov, R. S. Malhi, K.-G. Sjögren, K. Kristiansen, A. Wessman, A. Sajantila, M. M. Lahr, R. Durbin, R. Nielsen, D. J. Meltzer, L. Excoffier, E. Willerslev, The population history of northeastern Siberia since the Pleistocene. *Nature*. **570**, 182–188 (2019).
- 10 118. T. Kivisild, L. Saag, R. Hui, S. A. Biagini, V. Pankratov, E. D’Atanasio, L. Pagani, L. Saag, S. Rootsi, R. Mägi, E. Metspalu, H. Valk, M. Malve, K. Irtdt, T. Reisberg, A. Solnik, C. L. Scheib, D. N. Seidman, A. L. Williams, K. Tambets, M. Metspalu, Patterns of genetic connectedness between modern and medieval Estonian genomes reveal the origins of a major ancestry component of the Finnish population. *The American Journal of Human Genetics*. **108**, 1792–1806 (2021).
- 15 119. C. D. Huff, D. J. Witherspoon, T. S. Simonson, J. Xing, W. S. Watkins, Y. Zhang, T. M. Tuohy, D. W. Neklason, R. W. Burt, S. L. Guthery, S. R. Woodward, L. B. Jorde, Maximum-likelihood estimation of recent shared ancestry (ERSA). *Genome Res*. **21**, 768–774 (2011).
- 20 120. A. THOMAS, M. H. SKOLNICK, C. M. LEWIS, Genomic mismatch scanning in pedigrees. *Mathematical Medicine and Biology: A Journal of the IMA*. **11**, 1–16 (1994).
- 25 121. A. W. Wohns, Y. Wong, B. Jeffery, A. Akbari, S. Mallick, R. Pinhasi, N. Patterson, D. Reich, J. Kelleher, G. McVean, A unified genealogy of modern and ancient genomes (2021), p. 2021.02.16.431497, , doi:10.1101/2021.02.16.431497.
- 30 122. M. H. Gouveia, V. Borda, T. P. Leal, R. G. Moreira, A. W. Bergen, F. S. G. Kehdy, I. Alvim, M. M. Aquino, G. S. Araujo, N. M. Araujo, V. Furlan, R. Liboredo, M. Machado, W. C. S. Magalhaes, L. A. Michelin, M. R. Rodrigues, F. Rodrigues-Soares, H. P. Sant Anna, M. L. Santolalla, M. O. Scliar, G. Soares-Souza, R. Zamudio, C. Zolini, M. C. Bortolini, M. Dean, R. H. Gilman, H. Guio, J. Rocha, A. C. Pereira, M. L. Barreto, B. L. Horta, M. F. Lima-Costa, S. M. Mbulaiteye, S. J. Chanock, S. A. Tishkoff, M. Yeager, E. Tarazona-Santos, Origins, Admixture Dynamics, and Homogenization of the African Gene Pool in the Americas. *Molecular Biology and Evolution*. **37**, 1647–1656 (2020).
- 35 123. F. L. C. Jackson, So many Nigerians: why is Nigeria overrepresented as the ancestral genetic homeland of Legacy African North Americans? *The American Journal of Human Genetics*. **108**, 202–208 (2021).
- 40 124. A. Ko, R. Nielsen, Composite likelihood method for inferring local pedigrees. *PLOS Genetics*. **13**, e1006963 (2017).

Acknowledgments:

We acknowledge the individuals from Catoctin Furnace whose DNA we studied and recognize that they could not directly consent to participate in this study. We hope to honor the people of Catoctin and their contributions by telling their story and highlighting their ongoing legacy in the form of descendant communities. The genetic research was authorized by the Smithsonian Institution's National Museum of Natural History Department of Anthropology Collections Advisory Committee. For nearly 50 years, the Catoctin Furnace Historical Society, Inc. (CFHS) has been at the forefront of stewardship, research, and interpretation of the African American Cemetery located in Catoctin village. The CFHS has been a driving force in the effort to link the remains of deceased individuals who are yet to be fully identified to a descendant community, with the ultimate goal of using genealogical and historical research as well as DNA to establish definitive genealogies. Inquiries from those interested in learning more about the history of Catoctin Furnace, and from possible descendants interested in exploring their connections to the people who worked at the site, are welcome to contact CFHS at <https://catoctinfurnace.org/>. We thank the CFHS, the African American Resources Cultural and Heritage Society of Frederick, Maryland (AARCH), and members of descendant families for support of this research. We thank the 23andMe research participants and others who consented to participate in research for enabling this study.

Funding:

The ancient DNA analysis was funded by NIH grant HG012287; by John Templeton Foundation grant 61220; and by the Howard Hughes Medical Institute. In 2016, a \$14,000 Maryland Heritage Areas Authority grant was awarded to CFHS to fund forensic research for the African American cemetery. The Rice Family Endowment for Forensic Anthropology provided critical support for Smithsonian Skeletal Biology Program contributions.

Author Contributions:

D.R., J.M., and D.O. conceived of and supervised the study. K.S.B., K.G.B., and D.O. completed the osteological analysis spearheaded by E.C.. N.A., R.B., N.B., M.F., L.Q., K.S., N.W., F.Z., and N.R. generated the data via wet laboratory analyses. A.A., S.Ma., A.M., M.M. generated the data via bioinformatic analyses. Z.Z. and the 23andMe Research Team provided additional computational support. É.H., S.Mi., E.J., and I.O. analyzed the genetic data. É.H., S.Mi., K.S.B., W.F., K.B., E.J., E.C., H.L.G., L.H., J.T., R.C., S.A.E., K.G.B., J.S., K.S., I.O., J.M., D.O., and D.R. contributed to the interpretation of results. É.H. wrote the manuscript, with substantial input from S.Mi., K.S.B., W.F., K.B., A.A., E.J., E.C., H.L.G., L.H., J.T., R.C., S.A.E., K.G.B., J.S., K.S., J.M., D.O., and D.R. and feedback from all co-authors.

Competing Interests:

É.H., S.Mi., W.F., K.B., E.J., H.L.G., S.A.E., J.M. and members of the 23andMe Research Team are employees of and have stock, stock options, or both, in 23andMe. The remaining authors declare no competing interests.

Data Availability:

Unaligned and aligned sequences for the 27 Catoctin individuals were originally reported in Harney et al. (13) and are available from the European Nucleotide Archive under accession number PRJEB52230. Genotype files for pseudo-haploid and imputed versions of the dataset are available at <https://reich.hms.harvard.edu/datasets>. There are restrictions to the availability of 23andMe genotype data due to 23andMe consent and privacy guidelines. 23andMe agrees that the publication coauthors will rerun the comparison of historical genomic data against customer genetic data upon request by other academic and nonprofit researchers on reasonable terms to enable the results of the research activities to be replicated for at least seven years after publication or for as long as the coauthors are employed by, or otherwise affiliated with 23andMe in a capacity that allows them to rerun the analysis. Wherever possible, supplementary tables were included that report the summary statistics that were used to create figures that involved 23andMe datasets. Unless another comparable anonymizing approach was specified, these summary statistics were generated with the requirement that in all reported results, any 23andMe research participant must be indistinguishable from at least four other research participants included in the dataset. When meaningful, we repeated analyses performed on the 23andMe dataset using only the 1000 genomes and/or African American imputation panel datasets and reported these results.

Members of the 23andMe Research Team:

Stella Aslibekyan, Adam Auton, Elizabeth Babalola, Robert K. Bell, Jessica Bielenberg, Emily Bullis, Daniella Coker, Gabriel Cuellar Partida, Devika Dhamija, Sayantan Das, Sarah L. Elson, Teresa Filshstein, Kipper Fletez-Brant, Pierre Fontanillas, Karl Heilbron, Barry Hicks, David A. Hinds, Yunxuan Jiang, Katelyn Kukar, Keng-Han Lin, Maya Lowe, Jey McCreight, Matthew H. McIntyre, Meghan E. Moreno, Priyanka Nandakumar, Elizabeth S. Noblin, Jared O'Connell, Aaron A. Petrakovitz, G. David Poznik, Morgan Schumacher, Anjali J. Shastri, Janie F. Shelton, Jingchunzi Shi, Suyash Shringarpure, Vinh Tran, Joyce Y. Tung, Xin Wang, Wei Wang, Catherine H. Weldon, Peter Wilton, Alejandro Hernandez, Corinna D. Wong, Christophe Toukam Tchakouté, Alison Fitch, Alexandra Reynoso, Julie M. Granka, Qiaojuan Jane Su, Alan Kwong, Nicholas Eriksson, Dominique T. Nguyen, Bianca A. Llamas, Susana A. Tat

Supplementary Materials

Materials and Methods

Supplementary Text S1 - Extended Ethics Statement

Supplementary Text S2 - The Return of Names

5 Supplementary Text S3 - Testing the application of IBD detection methods to imputed low coverage ancient DNA using simulated data

Supplementary Text S4 - Testing the performance of Ancestry Composition on imputed low coverage ancient DNA using simulated data

10 Supplementary Text S5 - Comparison of IBD Network results of Catoctin individuals with present-day African Americans

Supplementary Text S6 - Genetic connections to African Among Catoctin individuals and 23andMe participants in the US cohort with at least 50% Sub-Saharan African ancestry

Figs. S1 to S16

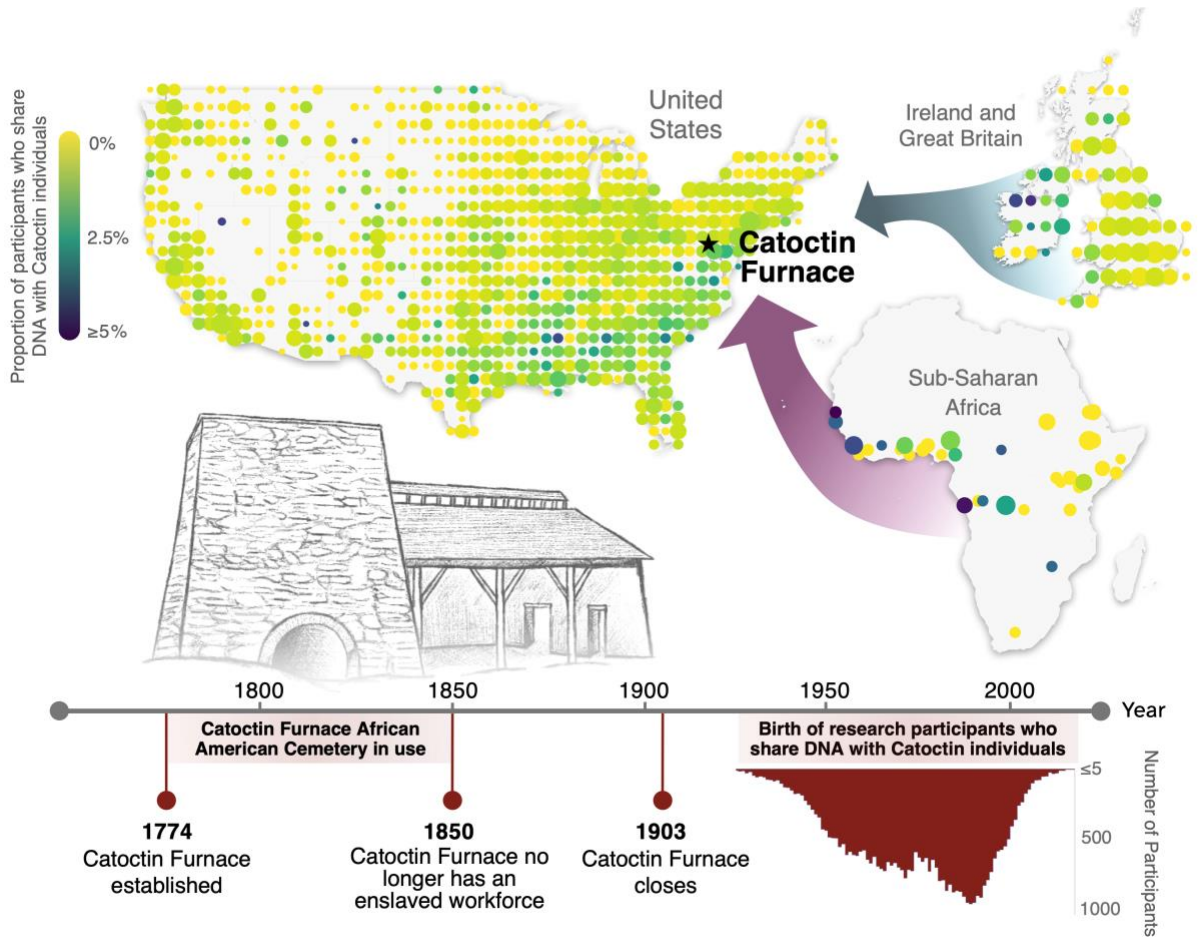
Tables S1 to S24, S1.1, S3.2 to S3.7, and S4.1

15 References 74-124

Box 1. Interpreting DNA shared between historical and present-day individuals.

- 5 The Catoctin Furnace African American Cemetery was in use between 1774–1850 (midpoint: 1812), while the average birth year of 23andMe research participants with genetic connections to Catoctin is 1974 (Table S22). The average separation between the death of the historical individuals and birth of present-day genetic relatives is ~162 years (although it is possible that as few as 70 years may have elapsed since the date of death of some of the latest Catoctin burials and the oldest research participants). The average age of reproduction among humans is 28–30 years, therefore the most likely number of generations separating the Catoctin individuals from their living relatives is about five to six generations (Fig. B1a).
- 10 The vast majority of the genetic relatives that we detected are not direct descendants of the Catoctin individuals. Instead, they are collateral relatives (i.e., relatives who are not direct ancestors or descendants) (Fig. B1b). To determine the likelihood that someone shares a direct descendant relationship with a Catoctin individual, we must consider the age of the two individuals and the amount of identical DNA (or IBD) that they share. Relatives who share very little IBD, but who
- 15 lived close together in time (as is the case for most of the connections we identified), are less likely to share a direct descendant/ancestor relationship.

Figure Captions



5 **Fig. 0. Genetic connections to individuals from Catoctin Furnace African American Cemetery in Maryland.** A timeline highlighting major events in the history of Catoctin Furnace and the birth years of research participants in the 23andMe cohort, presented alongside maps showing the proportion of 23andMe research participants associated with geographic coordinates in the United States, Sub-Saharan Africa, and Europe who share genetic connections to the Catoctin individuals.

10

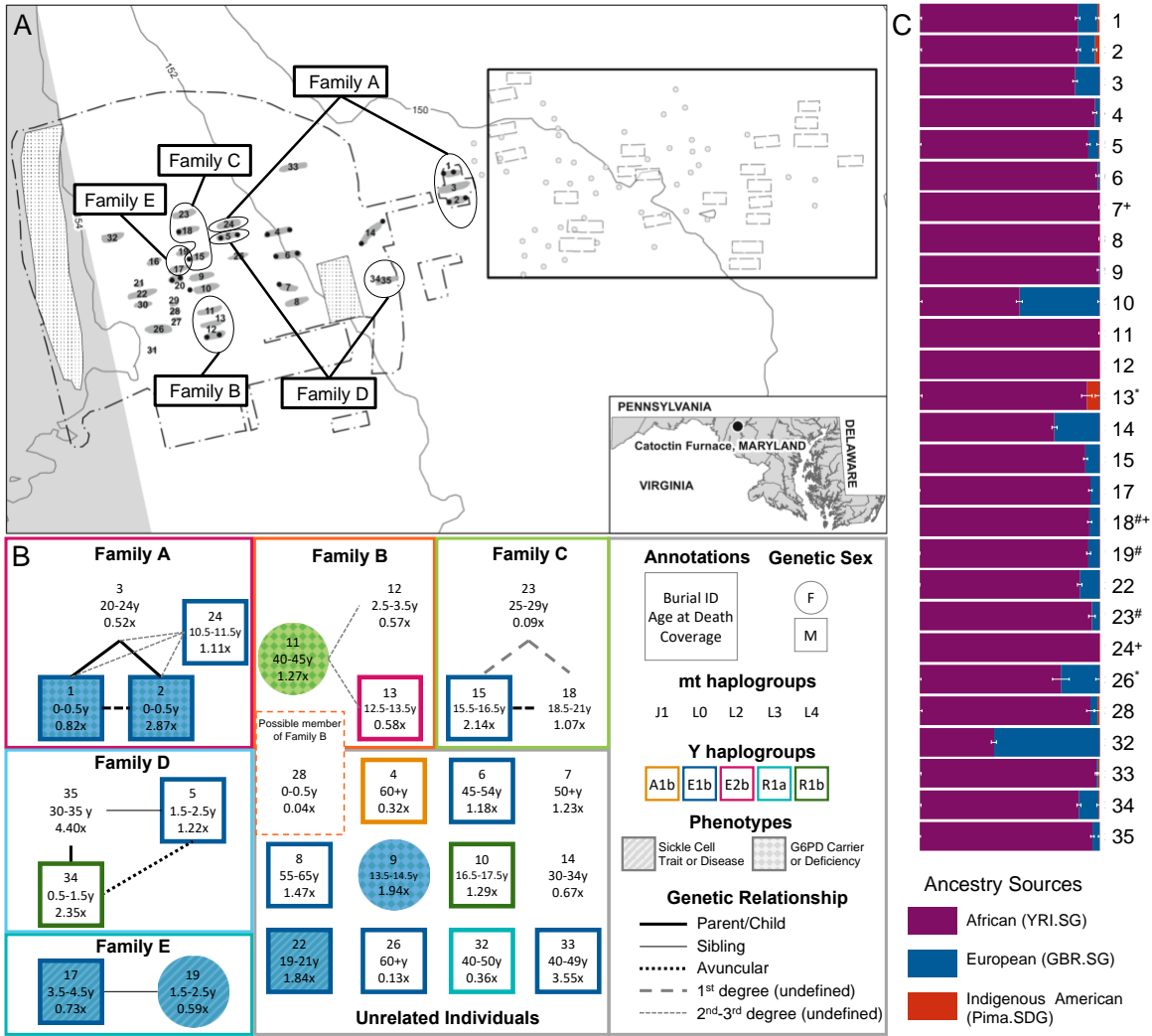


Fig. 1. Burial context, genetic kinship, and ancestry of Catoctin individuals. (A) Map showing the location of Catoctin Furnace and burials within the cemetery. Burial locations of the five genetic families are circled. The rectangle in the upper right shows a portion of the cemetery with unexcavated burials identified through ground penetrating radar (map adapted from (12), prepared by Robert Wanner). (B) Individuals, labeled according to burial ID, are grouped into families based on genetic relationships. Genetic sex, mt and Y haplogroups are indicated by marker shape, fill, and outline color, respectively. The type of genetic relationship is indicated by connector linestyle. Marker fill pattern indicates individuals with one or more copies of an allele associated with sickle cell anemia or glucose-6-phosphate-dehydrogenase (G6PD) deficiency. (C) Ancestry proportions assigned to each individual from representative African (YRI), European (GBR) and Indigenous American (Pima) populations drawn from the public dataset according to the qpAdm software. Error bars indicate one standard error. Asterisks (*) indicate cases where damage restricted data were analyzed. Hash symbols (#) and plus signs (+) indicate models with p-values <0.01 or ancestry proportion estimates that fall more than three standard errors outside the range of 0-1, respectively.

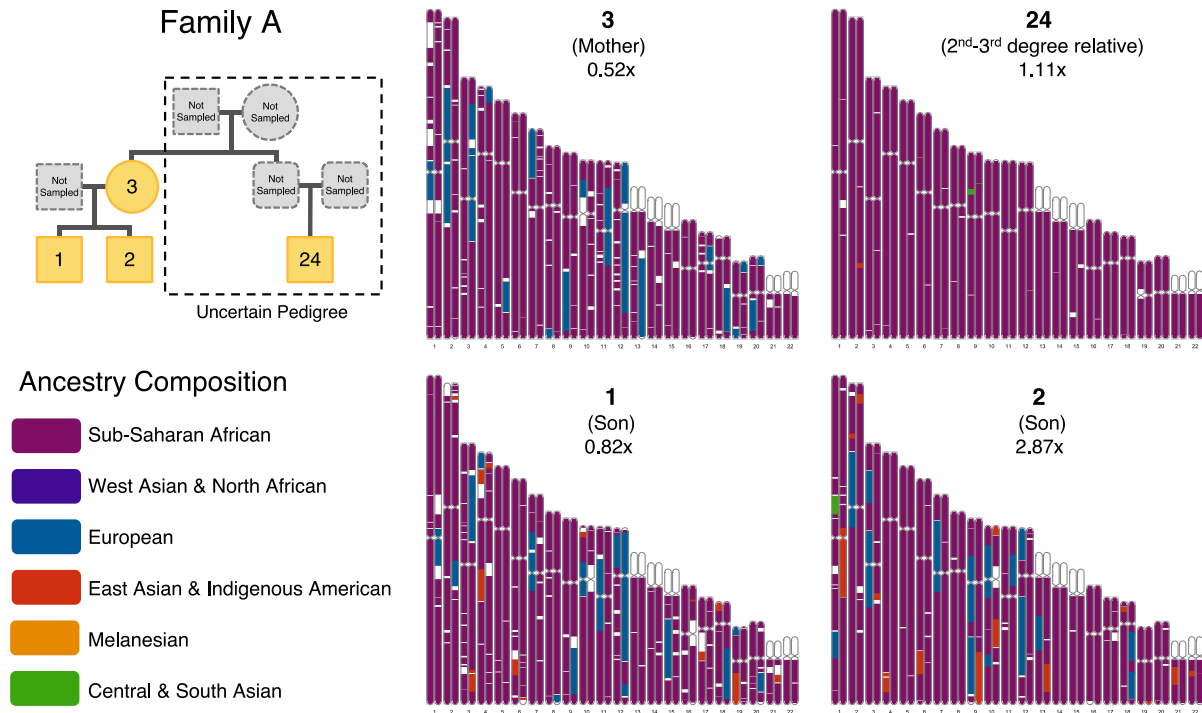


Fig. 2. Ancestry composition chromosome paintings for members of Family A. Chromosome paintings demonstrating the biogeographic ancestry assigned to portions of the autosomal chromosomes for four related Catocin individuals assigned to Family A—a mother, two sons, and their 2nd–3rd-degree relative. A likely pedigree for Family A (top left) describes their relationship to one another, although we note that the true relationship of the individuals from Burials 1, 2, and 3 to the individual from Burial 24 is uncertain. Across the genome, ancestry is assigned to one of six ancestry components defined using 23andMe reference populations: Sub-Saharan African (purple), West Asian & North African (dark blue), European (dark teal), East Asian & Indigenous American (orange), Melanesian (yellow), and Central & South Asian (green). Unassigned regions are shown in white.

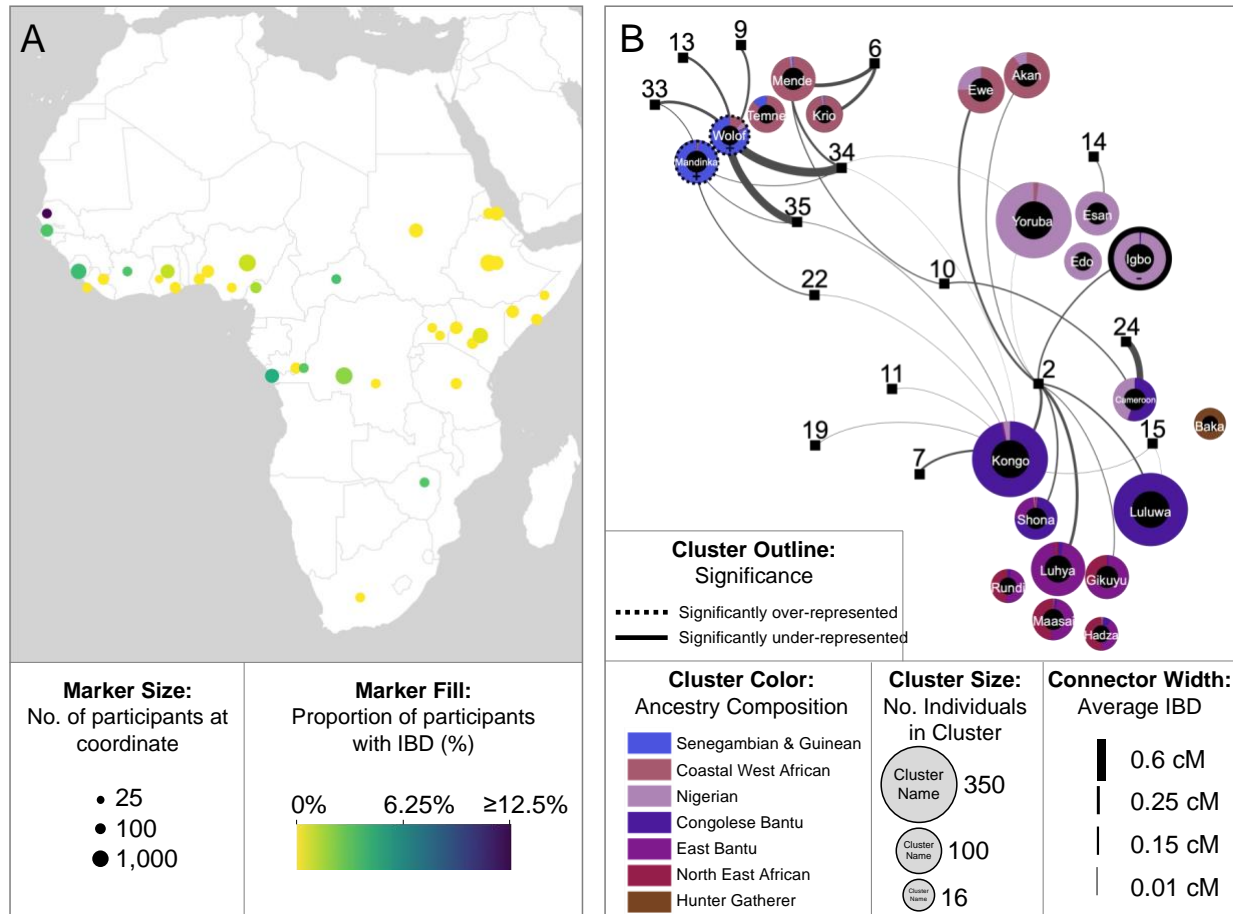


Fig. 3. Genetic connections to the Catoctin individuals among members of the African cohort. (A) The proportion of 23andMe participants in the African cohort who share IBD with Catoctin. Geographic coordinates are rounded to the nearest integer, and only coordinates that have at least 25 associated participants after 80% downsampling are shown. Marker size indicates the number of participants associated with each coordinate and color indicates the proportion of participants who share IBD with the Catoctin individuals. (B) IBD network demonstrating Catoctin individuals' connections to members of the African cohort who share less than 700 cM of IBD with one another (N = 2,807). IBD clusters (represented by circles) are filled according to members' average local African ancestry and arranged by average pairwise IBD sharing between clusters using a Force Atlas graph layout. Catoctin individuals, displayed as squares, are projected based on their average IBD shared with each cluster (shown as lines).

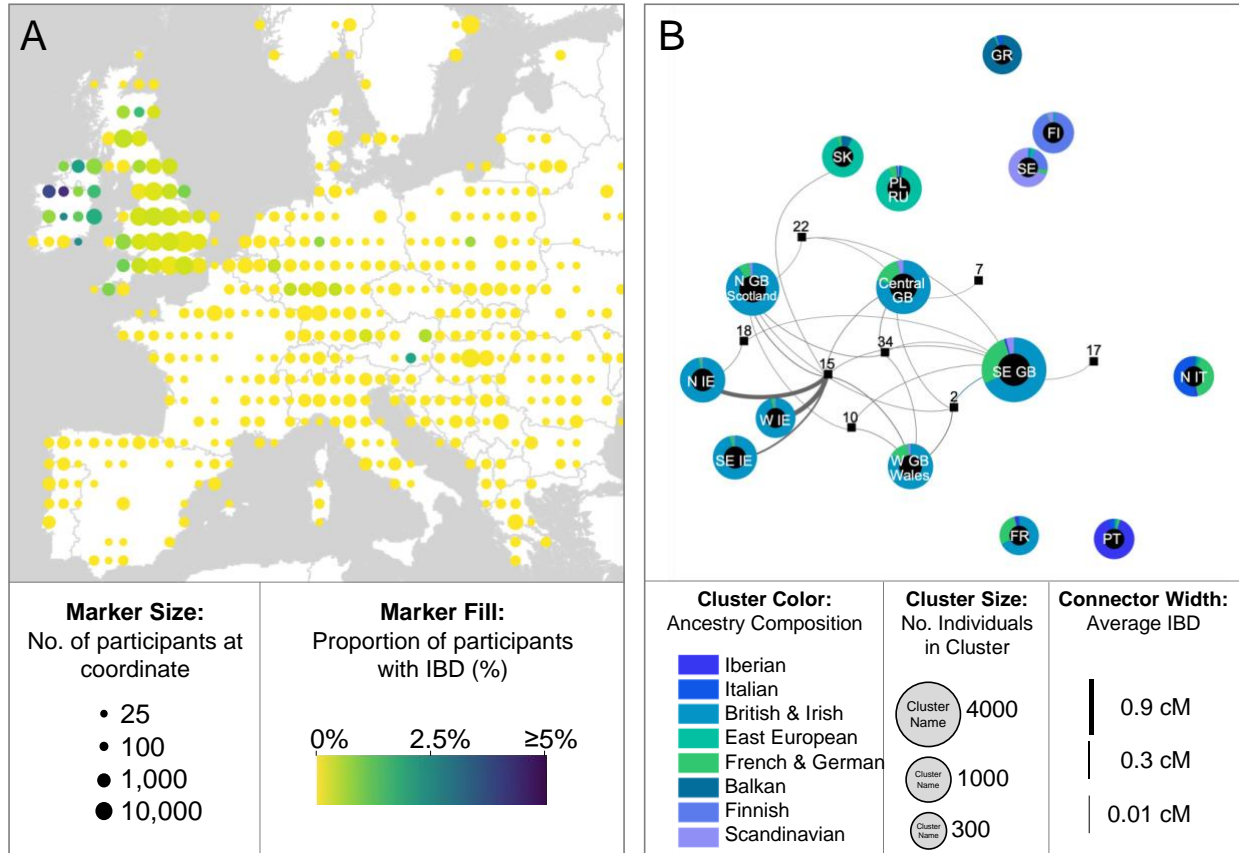


Fig. 4. Genetic connections to the Catoctin individuals among members of the European cohort. (A) Proportion of 23andMe participants in the European cohort who share IBD with Catoctin. Geographic coordinates are rounded to the nearest integer, and only coordinates that have at least 25 associated participants after 80% downsampling are shown. Marker size corresponds to the number of participants associated with each location, while the color indicates the proportion of participants who share IBD with the Catoctin individuals. (B) IBD network indicating Catoctin individuals' connections to the 23andMe participants in the European cohort who share less than 700 cM with one another. Clusters are labeled by the geographic region with which the majority of cluster members are associated using ISO2 country abbreviations and when appropriate, prefixes to indicate the cardinal directions. Clusters are arranged by the average pairwise IBD sharing between clusters using a Force Atlas graph layout, with outlines that indicate participant's average local European ancestry. Catoctin individuals, displayed as squares, are projected based on the average IBD shared with each European cluster (shown as lines).

15

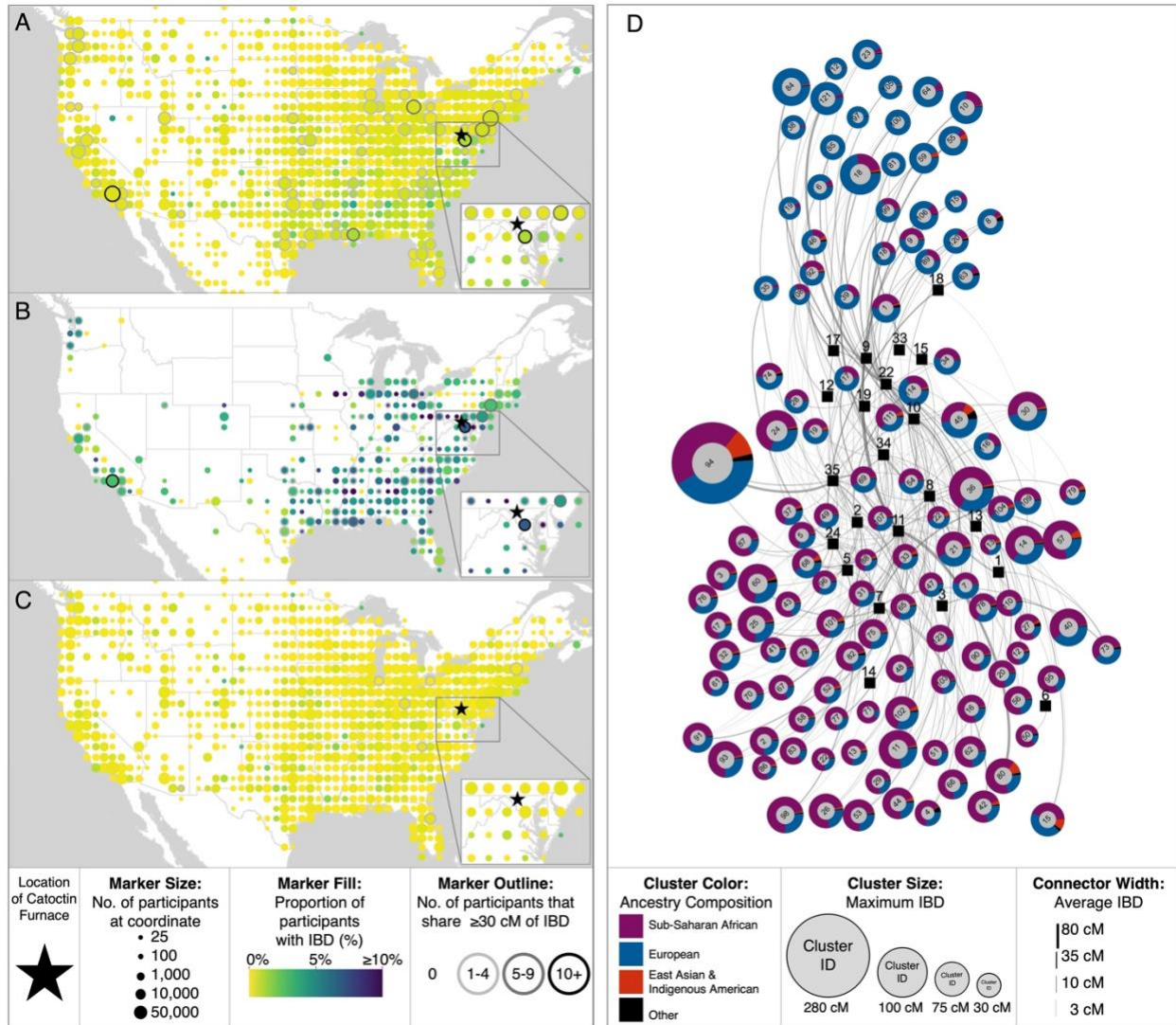


Fig. 5. Geographic distribution of distant and close relatives of the Catoctin individuals among members of the US cohort. (A) Proportion of 23andMe research participants in the US cohort who share IBD with Catoctin. Only coordinates representing at least 25 participants after 80% downsampling are shown. Marker size corresponds to the number of participants associated with each coordinate, while color indicates the proportion of participants with shared IBD. Marker outlines indicate the number of participants at each coordinate who share ≥ 30 cM of IBD with one or more Catoctin individuals. The same information is shown for (B) participants with $\geq 5\%$ Sub-Saharan African ancestry and (C) participants with $\geq 99\%$ European ancestry. (D) IBD network of the closest present-day relatives of Catoctin individuals among 23andMe research participants. Circles represent modularity clusters consisting of close Catoctin relatives (sharing ≥ 30 cM of IBD) along with their relatives (sharing ≥ 100 cM with a close relative of a Catoctin individual). Clusters are outlined according to their average ancestry and arranged by the average pairwise IBD sharing between clusters using a Force Atlas layout. Catoctin individuals, displayed as squares, are projected based on the average IBD shared with each familial group (shown as lines).

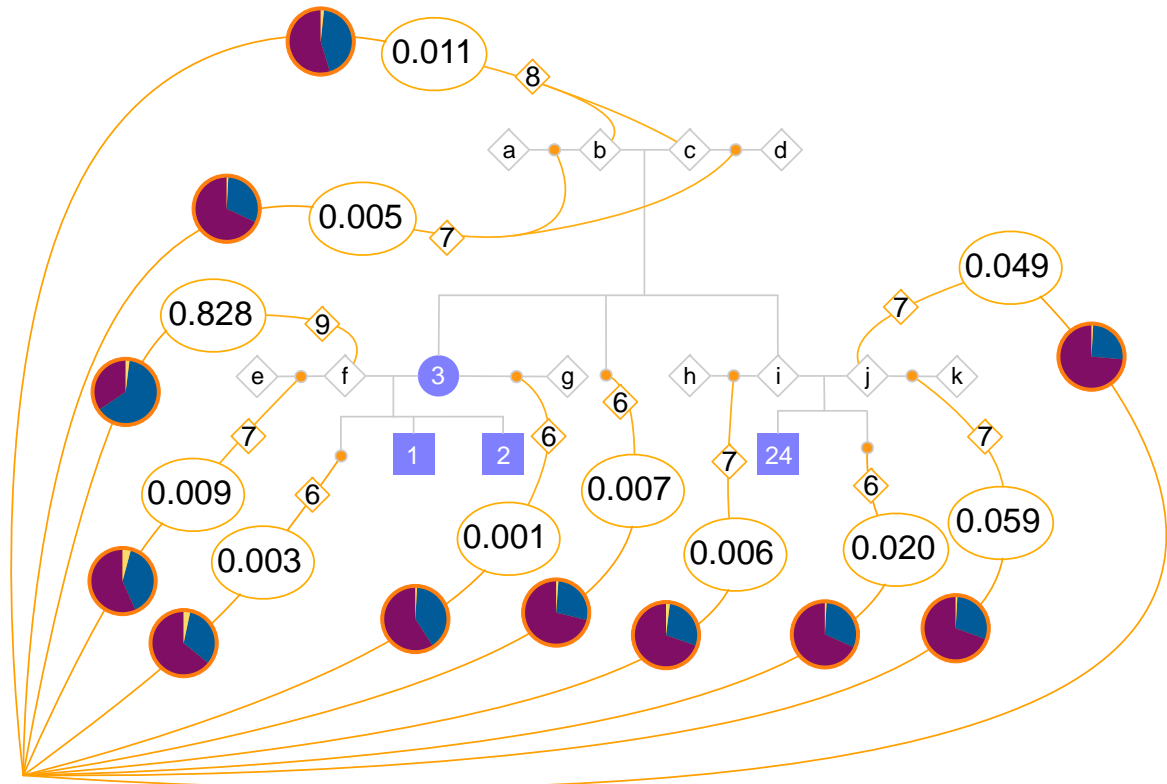


Fig. 6. Connections between Catoctin Family A and modern pedigrees. The pedigree for Catoctin Family A is shown with blue-shaded individuals connected by gray lines. Open gray diamonds indicate un-genotyped individuals, some of whom must have existed (i.e., **b**, **c**, **f**, **i**, and **j**), whereas others (i.e., **a**, **d**, **e**, **g**, **h**, **k**) are inferred to have existed. The large purple triangle represents all present-day pedigrees composed of 23andMe research participants, and the probability distribution of how these pedigrees connect to the historical pedigree is inferred. Orange dots indicate all possible points of connection of present-day pedigrees to the historical pedigree. Numbers in ovals give the percentage of present-day pedigrees whose most likely connection was to a given point on the historical pedigree. Numbers in orange diamonds indicate the average degree of a lineage connecting to a particular point. Pie charts show the average European (blue), Sub-Saharan African (purple), and Indigenous American (yellow) ancestry (normalized to sum to one) of individuals in pedigrees whose most likely point of connection was through the respective lineage leading to the present day.

15

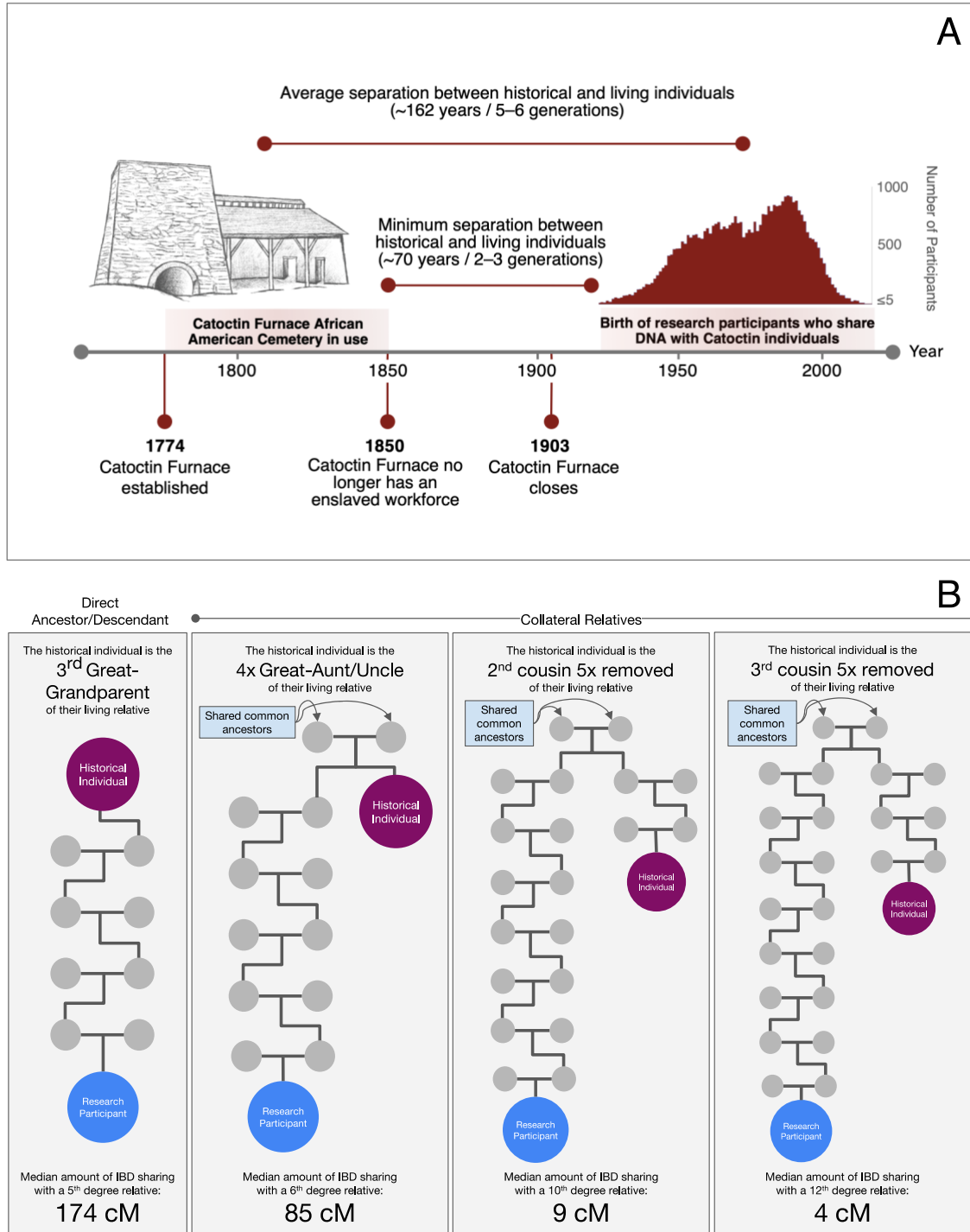


Fig. B1. (A) A timeline showing the years in which the African American Cemetery at Catoctin Furnace was active and a histogram of birth years of research participants who share IBD with Catoctin (Table S23). (B) Examples of relationships that could be shared between individuals that were born five generations apart, with varying degrees of genetic separation. Median amount of IBD is reported for pairs of present-day and historical individuals (with 2x coverage) (Table S7).

Tables

Table 1. IBD shared between 22 Catoctin individuals and 23andMe participants

23andMe Participants included in group	Number of 23andMe participants in group	Proportion of 23andMe participants in group that share IBD with Catoctin Individuals	Number of IBD segments detected	Median Length of IBD segments detected (cM)*	Maximum length of IBD segments detected (cM)*	Median total IBD in 23andMe participants with IBD detected (cM)*	Maximum total IBD shared with 23andMe participants (cM)*
All participants	9,255,493	0.45%	55,342	10	60	9.9	280
Atlantic African cohort	3,304	2.27%	85	7.4	20	7.4	30
European cohort	226,384	0.22%	519	7.6	20	7.6	25
US cohort	2,993,165	0.51%	17,854	9.7	55	9.6	280
Members of US cohort with $\geq 5\%$ Sub-Saharan African ancestry	192,880	4.25%	10,675	11	55	11	280
Members of US cohort with $\geq 99\%$ European Ancestry	1,896,655	0.26%	5,123	8.0	30	8.0	40

Summary statistics describing frequencies and amounts of IBD shared between the 22 Catoctin individuals with $>0.5x$ coverage and subsets of the 23andMe cohort. Participants were included in the US cohort either [1] if all four of their grandparents were born in the US, or [2] if they were born in the US and their grandparent birth location information was either unavailable or their grandparents were born in multiple countries. Similarly, members of the Atlantic African and European cohorts were determined using grandparent or participant birth location, with the additional requirement of $\geq 95\%$ Sub-Saharan African ancestry or $\geq 99\%$ European, respectively. Individual level results for each Catoctin individual are available in Table S5. *Values are rounded based on the magnitude of IBD sharing as follows: values >100 cM are rounded to the nearest ten, values between 30–100 cM are rounded to the nearest five, values between 10–30 cM are rounded to the nearest integer, and values <10 cM are rounded to one decimal place).



Supplementary Materials for

5 The Genetic Legacy of African Americans from Catocin Furnace

Éadaoin Harney, Steven Micheletti, Karin S. Bruwelheide, William A. Freyman, Katarzyna
Bryc, Ali Akbari, Ethan Jewett, Elizabeth Comer, Henry Louis Gates Jr., Linda Heywood, John
Thornton, Roslyn Curry, Samantha Ancona Esselmann, Kathryn G. Barca, Jakob Sedig, Kendra
10 Sirak, Iñigo Olalde, Nicole Adamski, Rebecca Bernardos, Nasreen Broomandkhoshbacht,
Matthew Ferry, Lijun Qiu, Kristin Stewardson, J. Noah Workman, Fatma Zalzal, Shop Mallick,
Adam Micco, Matthew Mah, Zhao Zhang, 23andMe Research Team, Nadin Rohland, Joanna L.
Mountain, Douglas W. Owsley, David Reich

15 Correspondence to: eadaoinh@23andme.com (E.H.); jlmountain@gmail.com (J.M.);
owsleyd@si.edu (D.W.O.); reich@genetics.med.harvard.edu (D.R)

This PDF file includes:
Materials and Methods
20 Supplementary Text S1 to S6
 Figs. S1 to S16
 References 74-124

Other Supplementary Materials for this manuscript include the following:
25 Tables S1 to S24, S3.2 to S3.7, and S4.1

Materials and Methods

In 1979–1980, the skeletons of 32 individuals were excavated from the Catoctin Furnace African American cemetery in Thurmont, Maryland, in advance of planned highway construction and were transferred into the custody of the NMNH. Sampling of 27 skeletons for ancient DNA was
5 authorized by the NMNH Department of Anthropology Collections Advisory Committee.

A report describing the generation of the genetic data was submitted to the NMNH Department of Anthropology Collections Advisory Committee (13) and the genetic data was deposited in the European Nucleotide Archive under accession number PRJEB52230 after three years had
10 elapsed following the original date of sampling, in accordance with the review committee's sampling policies. For completeness, we reprise here a description of how the DNA data was prepared.

Ancient DNA Sequencing:

We performed all ancient DNA sampling work in dedicated ancient DNA facilities at Harvard
15 Medical School, following standard guidelines for ancient DNA laboratory setup and cleaning.

We sampled bone powder from the petrous portion of the temporal bone (74, 75) from a total of 27 Catoctin individuals. When sampling from intact skulls, we used a minimally destructive cranial base drilling approach (59). We extracted DNA from ~37 mg of bone powder using published
20 methods (60–62) and created dual-barcoded, double stranded DNA libraries treated with a partial uracil-DNA glycosylase (UDG) approach that reduces characteristic ancient DNA damage (63, 6).

To maximize the amount of endogenous human DNA sequenced, we used an in-solution targeted enrichment capture approach. We enriched for sequences that overlap the mitochondrial genome and ~1.24 million (1240k) single nucleotide polymorphisms (SNPs) from the nuclear genome (24–26, 76). Following enrichment, we added unique seven base pair long indexing barcodes to each molecule in the library and performed paired-end sequencing using either an Illumina HiSeq10 or NextSeq500 instrument with 2x101 or 2x76 cycles, respectively, and with 2x7 cycles to read the library indices. We also performed a relatively small amount of shotgun sequencing for each library, which we used to assess DNA quality.

10 We trimmed the molecular adapters and barcodes from sequenced reads, and merged paired-end reads (requiring an overlap of 15 base pairs with up to 3 mismatches in low quality bases (<20) or 1 mismatch of a high quality base (≥ 20) using custom software (<https://github.com/DReichLab/ADNA-Tools>). We mapped the merged sequences to both the mitochondrial (mt) consensus sequence (RSRS) (77) and the human reference genome (version 15 hg19) using *samse* in BWA (v0.6.1) (78). We identified duplicate molecules using Picard MarkDuplicates (<http://broadinstitute.github.io/picard/>), defining reads with identical start and end positions, orientation, and identical DNA barcodes as duplicates, and retaining only the highest quality duplicate sequence.

20 We assessed ancient DNA authenticity and considered the following criteria when deciding if the data were suitable for analysis. Typically, requiring a minimum rate of 3% cytosine-to-thymine substitutions at the 5' end of each molecule is recommended to establish ancient DNA authenticity (63). However, based on the relatively recent age of the Catocin skeletal samples, versus the

considerably more ancient samples upon which this recommendation was based, we considered all of the Catoctin individuals (minimum 2.3% terminal damage rate) to have sufficient damage rates to be suitable for analysis (63). Next, we quantified the mt contamination rate using contamix v1.0-12 (26), requiring libraries to have 95% confidence intervals for their inferred contamination rate to be entirely greater than 5%. Additionally, we used ANGSD (65) to estimate contamination on the X-chromosomes of genetic males, requiring contamination rates below 3%.

The libraries generated from two individuals (Burials 13 and 25) had somewhat elevated levels of estimated contamination when we considered the upper bounds of the 95% confidence intervals of the mt match to consensus and ANGSD contamination rates. Therefore, we restricted to sequences that showed evidence of having ancient DNA damage, using the damage restriction approach described in PMDtools (79). The damage restricted version of each library passed all authenticity metrics and was used to create pseudo-haploid genotype calls (described later) used for preliminary population genetic analyses. However, since we do not expect such low rates of contamination to significantly impact the accuracy of imputed genotype calls, all sequences were used during the imputation process.

Imputation

Imputation was performed using GLIMPSE (72) (v1.0.0) using the 1000 Genomes project phase 3 dataset as the reference panel (68). Diploid genotype calls were generated using bcftools mpileup (v1.10.2). All the autosomal biallelic SNPs and indels in 1000 Genomes project phase 3 have been imputed. Only biallelic genotype likelihoods for SNPs, generated by mpileup were used as input to build the phasing and imputation model, and genotype likelihoods for indels were ignored

because of more severe reference bias. Unless otherwise noted, the data were filtered to remove genotype calls with an estimated maximum genotype posterior below a minimum threshold (henceforth referred to as the “max (GP) threshold”) of 0.95.

Genetic Sex and Uniparental Haplogroups

5 We determined the genetic sex of each individual by calculating the ratio of the number of shotgun sequences that align to the X chromosome versus the Y chromosome. Individuals for whom we detected a ratio of approximately 1:1 shotgun sequences aligning to the X and Y chromosomes were assigned a genetic sex of male, while individuals for whom we detected a ratio of approximately 1:0 were assigned a genetic sex of female (66). To identify mitochondrial
10 haplogroups, we considered reads that aligned to the RSRS mitochondrial genome with MAPQ \geq 30 and base quality \geq 20. Haplogroups were determined with haplogrep2 (67), using Phylotree version17. Y-chromosome haplogroups were called from reads that aligned to the Y-chromosome with MAPQ \geq 30 and base quality \geq 30. The most derived mutation for each individual was used to determine the Y-haplogroup, using the nomenclature defined by the International Society of
15 Genetic Genealogy (ISOGG) (<http://www.isogg.org>) version 14.76 (April 2019). Assigned genetic sex, mt and Y haplogroups for each individual are reported in Fig. 1B and Table S1.

Genetic relatedness between Catoctin Individuals

We identified genetic relatives of first, second, and third degree using a previously described method based on comparing the rate of matching across individuals to the rate of matching of the
20 maternal and paternal chromosomes of the same individual (80). We identified 15 related individuals, belonging to 5 distinct families. Another individual (Burial 28) did not have sufficient coverage to conclusively determine whether they should be included in genetic Family B. Using

the estimated degree of relatedness, genetic sex, uniparental haplogroups and age of death of each individual we further resolved the relationship shared between each pair of related individuals, as shown in Fig. 1B. While IBD comparisons between the Catoctin individuals (described later) were not used to determine these genetic relationships, the results of this analysis are consistent with these predicted relationships considering that we expect to underestimate the total amount of IBD shared between historical individuals (Fig. S16).

Comparison to publicly available data

We determined pseudo-haploid genotype calls for the non-imputed dataset by randomly sampling a single sequence to represent each position. We merged previously reported, publicly available, genome-wide data from present-day individuals from 12 populations (BantuSA.SDG, CHB.SG, ESN.SG, FIN.SG, GBR.SG, GWD.SG, Khomani_San.DG, Mandenka.SDG, Mbuti.SDG, MSL.SG, Pima.SDG, and YRI.SG) (68–71) with the newly generated pseudo-haploid dataset containing 27 Catoctin individuals. We refer to this dataset as “the public dataset.” The resulting merged dataset contained information at 1,233,013 SNPs. We also created a version of this publicly available dataset using the imputed genotype calls for the Catoctin individuals (filtering out all genotype calls with a maximum genotype posterior below 0.95), to show the impact of imputation on the Catoctin dataset. This dataset contained information at 1,083,703 SNPs.

qpAdm estimates of mixture proportions

We used the software qpAdm (81) (version 960) to estimate the proportion of ancestry that derived from African, European and Indigenous American sources for each Catoctin individual, using default parameters and the option “allsnps:YES”. Since the purpose of this analysis was to broadly estimate ancestry proportions and not to identify the best possible model for each individual’s

ancestry, we selected a single population to represent each ancestry type: YRI.SG (African), GBR.SG (European), and Pima.SDG (Indigenous American). An advantage of qpAdm is that it does not require access to reference data from individuals from the true source population to give unbiased and accurate results; instead, it works well if the set of samples used to represent each

5 ancestry type are descended from the same ancestral population (perhaps distantly in time) as the true source population. We selected four reference populations that are differentially related to each of these source populations and that we considered unlikely to be more closely related to the Catoctin individuals than chosen source populations: Mubti.SDG, Khomani_San.DG, CHB.SG, FIN.SG. We considered all models with p-values >0.01 to be plausible. Additionally we

10 considered models that assigned ancestry proportions outside the range of 0–1 to be plausible if the assigned proportions were within 3 standard errors of this range. Applying this approach to the non-imputed dataset, we could plausibly model the ancestry of 22 of the 27 Catoctin individuals tested. Two of the individuals whose ancestry could not be plausibly modeled using this approach were assigned over 100% YRI.SG ancestry, indicating that they likely have fully African ancestry

15 but that YRI.SG is not a good proxy for this ancestry with respect to the reference populations included in the model. We could plausibly model the ancestry of all Catoctin individuals using this approach when using the imputed dataset.

ADMIXTURE

We used the clustering tool ADMIXTURE (82) to assign the ancestry of the Catoctin individuals

20 and representative African (GWD.SG, Mandenka.SDG, MSL.SG, YRI.SG, ESN.SG and BantuSA.SDG), European (GBR.SG) and Indigenous American (Pima.SDG) populations to k theoretical ancestral populations. We pruned SNPs in linkage disequilibrium using PLINK with

parameters --indep-pairwise 200 25 0.4 and performed ADMIXTURE analysis on the remaining 1,095,120 SNPs for values of k between 2 and 10, with 10 replicates for each value of k . The highest likelihood replicate at each k was retained and we display results for $k=4$, which was the most visually informative for distinguishing broadly between African, European and Indigenous American ancestry in the Catoctin individuals. We also repeated this analysis using the public dataset with imputed versions of the Catoctin individuals. The pruned dataset consisted of 1,021,850 SNPs.

PCA

We performed principal components analysis (PCA) using smartpca (83) with default parameters in addition to the settings lsqproject:YES, numoutlier:0, shrinkmode:YES and ellconf: 0.95. We projected the Catoctin individuals onto a PCA plot created using representative African (YRI.SG), European (GBR.SG) and Indigenous American (Pima.SGD) populations. This PCA was designed to reveal a cline of European-related ancestry among self-identifying African Americans (ASW.SG). The PCA plot was created using both the non-imputed and imputed versions of the Catoctin dataset to show the impact of imputation.

DATES

We estimated the date of European and African admixture for each of the Catoctin individuals using the tool DATES (84) using the non-imputed dataset, with default parameters in addition to the settings mincount: 2 and minparentcount: 0. The populations YRI.SG and GBR.SG were used to represent the European and African admixture sources.

23andMe dataset

We compared the Catoctin dataset with data from 9,255,493 participants (elsewhere referred to as the “23andMe cohort”) who had been genotyped by 23andMe, Inc., a consumer personal genetics company, by July 28th, 2020. Participants provided informed consent and participated in the
5 research online, under a protocol approved by the external AAHRPP-accredited IRB, Ethical & Independent Review Services (E&I Review). Participants were included in the analysis on the basis of consent status as checked at the time data analyses were initiated. The name of the IRB at the time of the approval was Ethical & Independent Review Services. Ethical & Independent Review Services was recently acquired, and its new name as of July 2022 is Salus IRB
10 (<https://www.versiticlinicaltrials.org/salusirb>). We also included data from the 1000 Genomes Project (68) (Table S24), the Human Genome Diversity Project (69), and previously published data from people from Angola (22), the Democratic Republic of the Congo (85) and Sierra Leone (86), in addition to Khoe-San speaking people (87) in these comparisons.

15 We considered a participant to be associated with a particular geographic location based on their answers to questions about where they and their grandparents were born. In cases where all four grandparents were born in the same location, we prioritized this information over participant birth location. Additionally, in cases where participant birth location and grandparent birth location was the same, and where we had finer resolution for participant birth location (*i.e.*, we know that all
20 four grandparents and the participant were born in the same country and we also have information about the participant’s birth state) we prioritized birth location information. We grouped participants associated with the US in the “US cohort.” We grouped participants associated with European countries (including the following countries, as denoted by their ISO2 country codes:

AD, AL, AT, AX, BA, BE, BG, BY, CH, CZ, DE, DK, EE, ES, FI, FO, FR, GB, GG, GI, GR, HR, HU, IE, IM, IS, IT, JE, LI, LT, LU, LV, MC, MD, ME, MK, MT, NL, NO, PL, PT, RO, RS, RU, SE, SI, SJ, SK, SM, UA, VA, and XK) into a “European cohort,” with the additional requirement that participants in this cohort are assigned $\geq 99\%$ European ancestry by Ancestry Composition.

5 Similarly, we grouped participants associated with African countries (including the following countries, as denoted by their ISO2 country codes: AO, BI, CD, CM, CF, TD, CG, GQ, GA, KE, NG, RW, ST, TZ, UG, SD, SS, DJ, ER, ET, SO, BW, KM, LS, MG, MW, MU, MZ, NA, SC, ZA, SZ, ZM, ZW, BJ, ML, BF, CV, CI, GM, GH, GN, GW, LR, MR, NE, SN, SL, and TG) into an “African cohort,” requiring that participants in this cohort were assigned $\geq 95\%$ Sub Saharan-
10 African ancestry by Ancestry Composition. Finally we grouped participants associated with Atlantic African countries (including the following countries, as denoted by their ISO2 country codes: AO, CD, CF, CI, CM, GH, GM, GN, LR, NG, SL, SN, TG, and ZA) into an “Atlantic African cohort,” again requiring that participants in this cohort were assigned $\geq 95\%$ Sub-Saharan African ancestry by Ancestry Composition.

15 ***Ancestry Composition***

We performed ancestry prediction using 23andMe’s Ancestry Composition tool (42) for each of the 22 Catocin individuals with $>0.5x$ coverage, using a max (GP) threshold of 0.00, reporting results with a 90% confidence threshold. In Supplementary Text S4, we tested the performance of ancestry composition on an imputed test dataset of high coverage ancient individuals, which was
20 originally described in Supplementary Text 3. We find that Ancestry Composition performs better when poorly imputed genotypes are retained (i.e. no max (GP) threshold is used) than when these genotypes are considered missing. We therefore rephased the unfiltered imputed Catocin

genotypes against the panel of 23andMe research participants genotyped on the version 5 23andMe sequencing platform, as described previously, and performed Ancestry Composition analysis on the resulting dataset. We also found that while the broadest level Ancestry Composition assignments (e.g., Sub-Saharan Africa, East Asia & the Americas, West Asia & North Africa) were consistently assigned, even to the lowest coverage, imputed ancient DNA data, the more specific assignments (e.g., British & Irish versus Italian) were not reliably assigned. We therefore only considered the broadest level Ancestry Composition assignments for each Catoctin individual.

Identity-by-Descent

To search for portions of the genome that are identical by descent between the Catoctin individuals and members of the 23andMe cohort, we filtered out genotype calls that were assigned a max (GP) of less than 0.95. This threshold was chosen based on extensive testing of the performance of TPBWT comparisons between ancient individuals and 23andMe participants, described in Supplementary Text S3. After filtering, we then rephased the imputed data using EAGLE, with default settings and optional parameter `--allowRefAltSwap`. We created two rephased datasets using a reference panel of either 691,759 23andMe research participants at 454,507 SNPs or 706,995 23andMe research participants at 541,948 SNPs for subsequent analysis of participants genotyped on the versions 1-4 or version 5 23andMe genotyping platforms, respectively. Missing genotypes, including those that were filtered out when the minimum genotype posterior threshold was applied, were not re-imputed.

We ran TPBWT with default parameters, comparing the 22 Catoctin individuals with sequencing coverage of at least 0.5x and the 23andMe cohort. While TPBWT reports IBD segments as short as 3cM, we restricted our analyses to segments that exceeded minimum length thresholds. These thresholds were defined for each Catoctin individual based on average chromosomal coverage at 1240k sites to reduce the frequency of false positive IBD calls to ~10% in the shortest IBD segments that we consider (Supplementary Text S3). We used average chromosomal coverage at 1240k sites, rather than the overall coverage on 1240k sites (which does not consider coverage on each chromosome separately) to best match the coverage estimates used in the down-sampling tests described in Supplementary Text S3. References to “coverage” in this manuscript refer to average chromosomal coverage at enriched autosomal positions. For individuals with >2x average chromosomal coverage (n=5), we considered segments as short as 6 cM. For individuals with 1-2x average chromosomal coverage (n=10), we considered segments as short as 9cM and for individuals with 0.5-1x average chromosomal coverage (n=7), we considered segments as short as 10cM.

15

We interpreted IBD shared between the Catoctin individuals and participants by generating summary statistics that group participants based on their geographic location (provided by participants through surveys) and their ancestry composition (assigned by 23andMe’s Ancestry Composition tool (42)). We generated metrics including the proportion of participants that shared IBD with the Catoctin individual(s) of interest, the average total IBD shared between participants and the Catoctin individual(s) of interest (where average is calculated across all participants, and only those participants who shared some amount of IBD with the Catoctin individual(s) of interest), the maximum amount of IBD shared between a single participant and Catoctin individual

(rounded to 1 digit when IBD sharing is <10cM, 0 digits when IBD sharing is between 10-100cM, and to the nearest 10 when IBD sharing exceeds 100cM), and the number of participants that shared at least 30 cM of IBD with the Catoctin individual (s) of interest. Results are reported for participants grouped based on associated geographic coordinates (rounded to the nearest integer)
5 for participants in the US, European and African cohorts.

To ensure participant anonymity, coordinate level results are reported only for locations that have at least 25 associated participants. Additionally, we randomly downsampled our 23andMe cohort to include only results for 80% of participants to provide further anonymity. In the US and
10 European maps, we show data only for participants who provided county or state level information, respectively, while in Africa we also include participants who provided only country level information, in which case we assigned them to the geographic centroid of the country.

Randomization Tests

We performed randomization tests in order to determine whether cases where elevated rates of
15 IBD sharing with the Catoctin individuals among specific subsets of research participants were observed could be explained by random chance. In each case, we randomly sampled participants (with replacement) from the larger participant cohort of interest (e.g. participants in the US with over 5% Sub-Saharan African ancestry) to create 1000 random subsets of participants that were equal in size to specific subsets of participants of interest (e.g. participants with over 5% Sub-
20 Saharan African ancestry from the southern US [i.e., Alabama, Arkansas, Delaware, Florida, Georgia, Kentucky, Louisiana, Maryland, Mississippi, North Carolina, Oklahoma, South Carolina, Tennessee, Texas, Virginia, West Virginia and the District of Columbia]). For each replicate, we

counted the number of participants in the subset who shared any IBD with a Catoctin individual, or at least 30 cM in the case of the Maryland randomization test. We calculated p-values as the proportion of sampled subsets in which more individuals shared matches to Catoctin than were observed among participants from the true subset of participants under consideration. We
5 considered all p-values <0.01 to be significant.

IBD Networks

To identify Catoctin individuals' distant and recent connections to genetic groups, we first performed community detection using the Louvain Method (88). The Louvain Method uses a
10 heuristic model to optimize modularity, a value that represents the number of connections inside proposed groups with respect to connections to outside groups. Optimizing this value results in a natural grouping of participants of a given cohort. In the context of this study, the Louvain Method determines genetic clusters of participants by placing individuals into groups that maximize IBD sharing within a group after assessing pairwise IBD shared between all individuals in the cohort.
15 We applied this method to unrelated Atlantic Sub-Saharan Africans with $\geq 99\%$ Sub-Saharan African ancestry (N = 2,807), unrelated Europeans with $\geq 99\%$ European ancestry (N = 23,092), and a partially-related cohort of individuals that share >30 cM with any Catoctin individual (N = 4,828). Unrelated cohorts are filtered so that no two individuals share ≥ 700 cM, whereas partially-related cohorts contain no IBD filters. In each of the three cohorts, we identified the groupings of
20 participants that maximize modularity and found any enrichment of geographical or ethnolinguistic terms within each group using survey answers provided by participants. After identifying the optimal clusterings, based on modularity, we determined the average amount of IBD each Catoctin individual shares with each of the groups. We used these data to display each

Catoctin individual's connections to each group in the form of a graph layout. To achieve this, we first arranged groups within each of the cohorts, using the Force Atlas layout(89). Force Atlas is an algorithm that situates groups (or nodes) in a graph using a physical magnetic model. In this case, groups with more IBD sharing will be attracted to one another and groups with less IBD sharing are repelled. Force Atlas runs until balance between repulsion and attraction is achieved, essentially illustrating the structure of groups via their IBD sharing. After Force Atlas was run on each of the participant cohorts, we independently ran Force Atlas between each Catoctin individual and the pre-arranged graph of participants, projecting Catoctin individuals onto the structure of each cohort, thus illustrating where Catoctin individuals physically fell into the structure of each cohort.

Pedigree Reconstruction

Pedigrees were inferred between Catoctin families and modern pedigrees using a modified version of the Bonsai pedigree inference algorithm that is used to reconstruct research participant pedigrees at 23andMe (43). The algorithm was modified to use likelihoods adjusted for low coverage individuals (Supplementary Text S6).

Biologically Significant Variants

We determined the number of reference and alternative alleles observed in unique reads that overlap positions of phenotypic interest, including those known to be associated with sickle cell anemia and G6PD deficiency. While sequencing coverage was not high enough for any of the Catoctin individuals to make diploid genotype calls, the presence of causal alleles that are associated with phenotypes of interest suggests that the Catoctin individuals were either homozygous or heterozygous at these sites

Supplementary Text S1: Extended Ethics Statement

S1.1 Permissions for this and prior related studies

The Catoctin Furnace cemetery was excavated during a Maryland state highway project in 1979-1980 and the remains were subsequently transferred to the care of the Smithsonian National
5 Museum of Natural History (NMNH). Authorization for the ancient DNA analysis of 27 Catoctin individuals was provided by the NMNH Department of Anthropology Collections Advisory Committee. In fulfillment of DNA sampling requirements, the genetic data were made fully publicly available on European Nucleotide Archive after 3 years had elapsed after the initial date
10 of sampling. A technical report that describes the methods used during sampling, data generation, and bioinformatic processing and that details the results of the genetic analyses that had already been publicly presented during the community outreach events described below was returned to the Collections Advisory Committee and posted publicly at the same time (13).

The Catoctin Furnace Historical Society, Inc. (CFHS) and the African American Resources
15 Cultural and Heritage Society (AARCH) are considered organizations with a vested interest in the research, and were consulted throughout the study. Members of two families that can genealogically trace their ancestry to enslaved and free African Americans who labored at Catoctin Furnace were also consulted. Each group directly supported the decision to collaborate with the direct to consumer genetic testing company, 23andMe, Inc., in order to compare the DNA of the
20 Catoctin individuals to research participants in the 23andMe cohort.

S1.2 Community outreach

The community outreach efforts included in this study built upon a foundation established by co-author Elizabeth Comer (current President of the Catoctin Furnace Historical Society). For further information about the history of CFHS please refer to <https://catoctinfurnace.org/>.

5

A major goal of CFHS is to identify a descendant community of the African American individuals buried at Catoctin Furnace. Despite extensive efforts to identify such a community, CFHS has only recently been successful in identifying one family who can trace their ancestry back to an enslaved person at Catoctin Furnace. They have also identified a family who can trace their ancestry to a free African American ironworker who labored at the furnace. The search for the broader descendant community was therefore one of the primary drivers of this genetic study.

10

Although identifying a descendant or direct biological kinship community for the enslaved and free African Americans buried at Catoctin Furnace is a goal for CFHS, multiple groups have served as community stakeholders for these individuals, including:

15

- **The Catoctin Furnace Historical Society, Inc. (CFHS).** This society was established in 1972 and among its members are descendants of the paid laborers of primarily European ancestry who worked at (but did not own) the Furnace. Many of these descendants still reside in Thurmont, Maryland in dwellings associated with Catoctin Furnace and their lives are deeply intertwined with the village's history.
- **The African American Resources Cultural and Heritage (AARCH) Society, Frederick, Maryland.** AARCH was officially incorporated in 2009, and its mission is to

20

“identify, collect, preserve and exhibit the cultural objects, artifacts, and stories that tell and celebrate the unique history, culture, and heritage of African Americans in Frederick County, Maryland for the purpose of educating the general public and deepening our understanding of how the African American past can shape and enrich the present and the future.” Members of AARCH have worked closely with CFHS to ensure that the portrayal and study of African Americans at Catoctin Furnace is done sensitively and appropriately.

- **Members of descendant families.** Historical research led by CFHS has recently identified two descendant families whose ancestry can be directly traced to enslaved and free African American ironworkers who labored at Catoctin Furnace.

Interaction with these stakeholder communities and others with an interest in the history of Catoctin Furnace has involved a variety of engagement events and activities, during which we shared findings from the study and gathered community feedback on the project. These events and activities include:

- **The Catoctin Furnace African American Cemetery Interpretive Trail.** Visitors to Catoctin Furnace (both in person and virtual) can learn about the role that enslaved and free African Americans played at Catoctin Furnace during its early history by participating in a self-guided tour that leads participants from the ruins of Catoctin’s “Isabella” Furnace to an observation area that overlooks the site of the African American cemetery. Along the trail are 11 informational panels that describe the site and various aspects about the lives of the enslaved and free African American laborers at Catoctin. We contributed to panel 9 of the interpretive trail by reporting the genetic relationships identified among the 27

individuals included in this study. More information about the interpretive trail is available here: <https://catoctinfurnace.org/african-american-cemetery/>

- **Facial Reconstruction Unveiling Event.** In June of 2021, the CFHS held an event during which facial reconstructions that had been created of two African Americans buried at Catoctin were unveiled to members of CFHS and other interested members of the Frederick community. The evening included readings by Elayne Bond Hyman from her collection of poems, *Catoctin SlaveSpeak*, performances by Joseph Ngwa, a master ancestral drummer, and a reading of the names of the enslaved individuals at Catoctin, which paid tribute to the idea that “A person is not forgotten until his or her name is forgotten” (Supplementary Text S2). Also among the events of the evening were two talks in which representatives of our research team shared preliminary genetic results from our study, including a description of the genetic relationships that were identified, preliminary estimates of ancestry, and discussion of the possible identification of several individuals who may have been carriers of or had sickle cell disease. Media coverage of the evening is available in *The Washington Post* (90) and in *The Frederick News-Post* (91). Placards describing the results presented during this evening are now on display in the Museum of the Ironworker at Catoctin Furnace.
- **Tours of the NMNH Collections for Catoctin Stakeholders.** Co-authors affiliated with the NMNH hosted multiple tours of the NMNH collections for members of CFHS and AARCH, as well as students and teachers from the Silver Oak Academy, a school for at-risk youth in Keymar, Maryland affiliated with CFHS. The most recent of these tours occurred in April, 2022.

- **Screening of “America’s Hidden Stories: Forged In Slavery.”** CFHS and members of the study team helped to organize a screening of this Smithsonian Channel documentary in Frederick Maryland in June, 2022. The documentary spotlights the ongoing research into the lives and legacies of the Catoctin African Americans. Additionally, several members of the study team were interviewed about the genetics of the Catoctin individuals as part of the documentary.
- **Virtual meeting with members of the descendant families.** In June, 2022, members of the research team virtually met with representatives from the two descendant families to discuss the results of this study.

10 *S1.3 Informed Consent Provided by Present-day Research Participants*

In this study, we compared the Catoctin individual’s genomes to that of present-day research participants whose genetic data was obtained from a variety of sources. Here, we outline the different datasets used and provide an overview of the informed consent that was provided with each of these datasets. In Table S1.1 we specify which datasets were used in each analysis and indicate whether the results of those analyses can be reproduced using publicly available data.

- **Non-23andMe datasets:**

- **1000 Genomes Project**

Individual’s whose genetic data is included in the 1000 Genomes Project (68) dataset provided broad consent to allow individual level data generated from the samples that they provided to be made publicly available on online scientific databases, provided that no individual identifiers or medical information was associated with the samples. The 1000 Genomes dataset can be used for a variety

of purposes, including studying population history and relatedness, and it may be accessed by academic, commercial and government entities. The sampling protocol for all samples included in the dataset was required to be approved by local Internal Review Boards (IRB) or Research Ethics Committees (REC), while also fulfilling the requirements of the 1000 Genomes Samples and ELSI group. For more information about the 1000 Genomes Project consent process, see: https://www.internationalgenome.org/sample_collection_principles/.

5

- **The Human Genome Diversity Project**

Like the 1000 Genomes Project dataset, individual's whose genetic data is included in the Human Genome Diversity Project (HGDP) dataset provided broad consent to allow individual level data generated from the samples that they provided to be made publicly available on online scientific databases. The HGDP dataset was generated with the intention of providing a resource that could be used to study human genetic variation, including studies of human evolutionary history and/or ancestry. In this study, the HGDP dataset is used to learn about the ancestry of the Catoctin individuals, an aim that falls within the intended use case. However, a number of criticisms have emerged since the release of the HGDP dataset regarding sampling procedures and informed consent, as the majority of samples included in the dataset came from existing collections that were not originally sampled with the intent of creating a public database of global human genetic variation (e.g. 92, 93).

10

- **Simons Genome Diversity Project**

We considered individuals whose genetic data was included in the Simons Genome Diversity Project dataset. Only genetic data from individuals who provided

informed consent that was consistent with fully public data release on the EBI European Nucleotide Archive was considered. Data uploaded to the European Nucleotide Archive may not be subject to any usage restrictions and must remain permanently accessible as part of the scientific record. For more information about the Simons Genome Diversity Project and the European Nucleotide Archive policies, see: Mallick et al, 2016 and

<https://www.ebi.ac.uk/ena/browser/about/policies>

- **23andMe datasets:**

- **23andMe Research participants**

This study (like all 23andMe Research studies) only considered the data of 23andMe customers who had actively provided consent to participate in 23andMe Research at the time of study onset (July 28th, 2020). More than 80% of 23andMe customers have provided informed consent to participate in research via a protocol that was approved by an external AAHRPP-accredited IRB, Ethical & Independent Review Services (E&I Review), now known as Salus IRB. Consenting participants provide broad consent to allow 23andMe researchers to study and publish on a wide variety of research topics, including, but not limited to, “The history of peoples across the world, including how they migrated and intermixed in the past.” In order to protect participant privacy, 23andMe researchers do not have access to identifying information, such as participants’ names and contact information. Additionally, all research results are reported as combined summaries that do not allow identification of any particular individual. Participants are informed that they are unlikely to directly benefit from participation and that they should not expect to

receive individual results that are learned through 23andMe Research discoveries. However, they or people with shared ancestry may indirectly benefit if these 23andMe Research discoveries go on to be incorporated into the 23andMe product in the future. 23andMe Research participants have the option to change their consent choice at any time. For more information about the 23andMe Research consent process, see: <https://www.23andme.com/about/consent/>

5

- **23andMe’s African American Sequencing Project imputation panel:**

The 23andMe African American Sequencing Project imputation panel reported in O’Connell et al (94) is composed of 23andMe Research participants who provided additional informed consent to allow their individual level genetic data to be uploaded to the database of Genotypes and Phenotypes (dbGap), where it may be accessed by qualified researchers conducting human genetic variation research. The study design and consent were approved by Ethical & Independent Review Services (E&I Review), now known as Salus IRB. For more information about the panel, see O’Connell et al (94).

10

- **23andMe Population Collaboration Datasets:**

The following datasets were generated as part of collaborations between 23andMe and academic institutions with the purpose of increasing global representation of genetic databases:

- 15
- 299 individuals from Angola (22, 95). Sampling was conducted and consented for following a research protocol that was approved by ethics committees at the University 11th of November (Universidade 11 de

Novembro), Cabinda, Angola (REf: GD-FM/UoN/2016) and the University of Leicester ethics committee (REf: 11334-sdsb1-genetics).

- 605 individuals from The Democratic Republic of the Congo (85). Sampling was conducted and consented for following a protocol that was approved by the Harvard Internal Review Board (IRB00000109; Protocol 24087).
- 225 individuals from Sierra Leone (86). Sampling was conducted and consented for following a protocol that was approved by IRBs obtained by Boston University and the University of South Carolina.
- 95 Khoe-San speaking people (87). Sampling was conducted and consented for following a protocol that was approved by an IRB obtained from Stanford University.

The 23andMe Population Collaboration Program provided support to 23andMe collaborators to genotype research participants from populations that are understudied in terms of genetics. The exact research protocols and consent procedures used in each study was developed in collaboration between 23andMe and the external collaborators who were leading the study. In all cases, informed consent was received that permitted researchers to collect a saliva sample and for 23andMe to store, access and analyze the sample and resulting data. Additionally, collaborating researchers were responsible for gathering demographic information, including participant age, sex, birthplace, ethnic affiliations and languages to be shared with 23andMe. For more information about the 23andMe Population

Collaborations Program, see: <https://blog.23andme.com/articles/23andme-population-collaboration-program-supports-research-in-understudied-groups>

S1.4 Strategies to Ensure 23andMe Participant Anonymity

5 23andMe Research participants provided informed consent for their data to be used in 23andMe Research studies with the understanding that 23andMe would not release individual level data to outside collaborators or include it in publications without their explicit and separate consent. Instead, under the 23andMe Research Consent Document (<https://www.23andme.com/about/consent/>), 23andMe researchers may only share research
10 participant data in a combined format that does not identify any particular individual. We applied several anonymization strategies throughout the study that were created in order to fulfill this requirement, while also enabling us to share fine grained results. Here, we outline the strategies used for each analysis involving 23andMe Research participants:

- **Default approach: k-anonymity ($k \geq 5$):**

15 Unless otherwise noted, all results generated using the 23andMe dataset were required to meet the requirement of k-anonymity, where $k \geq 5$ (96). This means that any reported counts that were less than 5 were excluded or masked (i.e. reported as " ≤ 5 "). This anonymization strategy greatly reduces the chance that individual-level data could be discerned from the reported results.

20 ***Applies to results reported in:*** Table 1, Figs 3b, 4b, 5b, 6 and associated Supplementary Tables

- **Rounding of IBD segment lengths and total IBD:**

While individual-level results about genetic connections to the Catoctin individuals were not returned to research participants as part of this study, we wanted to ensure that if these results were to be returned in the future, that this information would not make it possible to determine whether specific research participants were included in the study. While it would be difficult to discern whether or not a particular participant was included in the dataset when considering values like average IBD sharing or the proportion of participants in a particular subset, the maximum IBD segment length and maximum total IBD could be more easily linked to a particular research participant if that participant's results were known. We rounded the maximum IBD segment length and total IBD sharing using the following approach to unlink individual results from the values provided in these tables: Values >100 cM were rounded to the nearest ten, values between 30–100 cM were rounded to the nearest five, values between 10–30 cM were rounded to the nearest integer, and values <10 cM were rounded to one decimal place.

Applies to results reported in: Table 1, Figs 3a, 4a, 5a and associated Supplementary Tables

- **Downsampling to 80% and only reporting coordinates with at least 25 associated participants:**

Many of the geographic signals that we identify in this study would not have been possible to discern using a strategy where counts ≤ 5 were masked for k-anonymity, particularly at geographic coordinates where there were only a small number of associated individuals. We therefore adopted the following strategy in order to report meaningful results, involving counts ≤ 5 that were associated with specific geographic coordinates.

First, we downsampled the entire dataset to 80% of its original size, meaning that 1 in 5 research participants were excluded from the analysis. Next, we only reported results from geographic coordinates where there were at least 25 associated participants (after downsampling). This means that on average, there were at least 5 individuals from each coordinate that were not included in the analysis. Following this anonymization strategy, it would not be possible to determine whether a particular research participant was included in the analysis, even if their birth or grandparental birth location and the exact amount of IBD they shared with a Catoctin individual were known.

5
10 *Applies to results reported in:* Figs 3a, 4a & 5a and associated Supplementary Figs and Tables

- **Pedigree Figures:**

To ensure the anonymity of research participants in the display of pedigree structures, we did not show pedigrees containing relationships among present-day research participants. We only displayed the relationships among historical individuals along with summary information depicting the connections between historical and modern pedigrees. This ensures that pedigrees with unusual structures, which could be identified as belonging to one or few present-day families, were not depicted. In cases where five or fewer research participants shared a unique connection to the historical pedigree, we masked the exact count and instead reported “ ≤ 5 ”.

15
20 *Applies to results reported in:* Fig. 6 and associated Supplementary Figs and Tables

S1.5 Terminology Choices

Discussions involving topics such as race, ancestry and gender require careful consideration of terminology. In what follows, we outline choices that we made regarding the terminology that is used throughout the manuscript. In some cases, we used terms that are imprecise in order to maintain the ease of readability of the manuscript, so we have provided a detailed explanation of how these terms should be interpreted.

- **Ancestry, Race and Ethnicity**

Although they are often incorrectly used interchangeably, the terms ancestry, race and ethnicity have distinct definitions in the fields of anthropology and genetics that researchers must be careful not to conflate (97). In genetics, the term “ancestry” refers to one’s biological ancestors and their genetic connections to groups of people or places in the past. In contrast, the terms “race” and “ethnicity” are not biologically defined categories. Race is a socially constructed category that is often associated with shared physical characteristics. Members of the same race often share social experiences, while the term ethnicity refers to self-identified cultural groups. Each of these terms and how they are used (correctly and incorrectly) by researchers in the fields of anthropology and genetics are discussed in detail in Birney et al (97), Wagner et al (98) and Mathieson and Scally (99).

The term “African American” is often associated with descendants of enslaved individuals of Sub-Saharan African ancestry in the US, while the term “Black” is applied more broadly, also encompassing individuals whose ancestors (or who themselves) moved to the US more recently and individuals who live outside the US (100). As this study is specifically focused on individuals buried in the Catoctin Furnace African American Cemetery, the majority of

whom were enslaved, we primarily use the term “African American” throughout the manuscript. However, we also use the term “Black” where it is more appropriate, such as to match how race-based information was collected by outside sources (such as the US census) or when paired with the term “white” (to maintain linguistic continuity). We follow the Associated Press style guidelines, which recommend that the term “Black” be capitalized while “white” not be when referring to race (101). When discussing genetic ancestry, we refer to continental-level ancestry categories, either defined in relation to one or more representative populations sampled from each region (as in the qpAdm, ADMIXTURE and PCA analyses) or to assignments made by the 23andMe Ancestry Composition algorithm (42), whose categories are also defined using a panel of representative individuals with deep ancestral ties to known geographic regions. We do not use genetic ancestry to assign the Catoctin individuals or research participants to specific racial or ethnic groups (i.e. African American) and instead refer to their continental-level ancestry assignments (i.e. participants with at least 5% Sub-Saharan African ancestry). In cases where we do refer to research participants as African American, we are referring specifically to their self-reported ethnicity.

Race and ethnicity are not defined by genetic ancestry, and continental-level ancestry categories can obfuscate the differences (and similarities) that exist between different groups of people (e.g. 102, 103). However, there are correlations between people who identify as African American and genetic ancestry (39), and we believe that it is important to highlight the historical associations between these distinct categories in cases where genetic signatures may reflect or shed new light on historical events and/or patterns that were known to have impacted African American individuals. For instance, we observe a

higher number of European-associated Y-haplogroups among the Catoctin individuals relative to the number of European-associated mt-haplogroups. This is a likely a genetic signature of historically well-documented patterns in which white men raped enslaved Black women (38). These acts have left a genetic signature that is detectable in the DNA of many historic and present-day individuals in the US with African ancestry.

- **Genetic sex and gender**

We determine the genetic, or chromosomal, sex of the Catoctin individuals based on X to Y-chromosome ratios. Throughout the manuscript, we refer to individuals who are determined to have XY sex chromosomes as male and those who have XX sex chromosomes as female. We chose to use the singular, gender-neutral pronoun ‘they’ when referring to individuals, in acknowledgement that although genetic sex and gender are often correlated, gender is not defined by genetic sex (104).

- **Genetic relatedness and kinship**

We use kinship-based terminology to describe the genetic relationships detected between the Catoctin individuals, referring to groups of individuals with close genetic relationships as genetic families and using terms such as mother and child/son/daughter to refer to specific genetic relationships that are shared between individuals in each family. We acknowledge that genetic relatedness does not necessarily dictate how kin relationships were defined between the Catoctin individuals (105). Therefore, in all cases, any terms that we use to define relatedness refer specifically to genetic relatedness (i.e., “mother” may be read as “genetic mother” or “biological mother”), rather than to kinship.

Supplementary Text S2: The Return of Names

An overlook located close to the Catoctin Furnace cemetery includes three interpretive panels. The panels provide information about the erasure and rediscovery of the cemetery, and a list of 271 given names found in land records, probate inventories, church records, diaries, and freedom-seeker ads, which we list below.

5 Notice the number of names listed simply as “unknown” and the absence of any last names. As we read their names, which are listed on the following pages, these people are remembered.

“a person is not forgotten until his or her name is forgotten”

In reading these names to you, you ensure enslaved workers at Catoctin Furnace are not forgotten:

10

Jack	Janey	Mary
Jaines	Joe	Daniel
Milly	Larkin	Anne
Phil	Len	Anthony
Ben	Lewis	Richard
Nelly	Liddy	James
Sam	Little Bill	Patsy
John	Lock	Nace
Thomas	Lorena	Rachel
John	Lusinda	Ann
Clemens	Magdeline	Bill
Jenny	Maria	Bob
Polly	Mary	Charity
Rachel	Mary	Christiana
Samuel Hercules	Mattie	David
Caty	Mill	Eliza
Clemens	Milly	George
Maria	Mingo	George
Petty	Nanny	Harrison
Sammy	Ned	Harry
Susanna	Nell	Henry
Ally	Old Hanna	Isaac
Anne	Old Jack	Leonard
Ben	Old Will	Lucky
Betty	Parris	Lucy
Betty	Priss	Peter
Big Dick	Resey	Sarah
Bill	Romeo	Stacy
Bill	Rose	Wally
Bill	Sal	Sarah
Cate	Sam	Leonard
Charlot	Sam	Jeremiah
Christina	Samuel	Henry
Cloay	Sue	Peter
Elsey	Sue	Nathaniel
Estor	Toby	Ruth
Farm Jacob	Wally	Polly
Frederick	Will	Richard
George	Yellow Girl	William
Harriet	Hanson	Priscilla
Harry	Big Bill	Phebe
Harvey	Daniel	George
Henry	Isaac	Jessee
Hetty	John	Thomas
Humbert	William	James
Jack	William of Elizabeth	Richard
Jacob	Jacob	Richard Jr
Jane	Moses	Thomas
Jane	Nicholas	Henry
Jane	Richard	Peter

Celeste	Otho	John
Benjamin	Anna	Julia
Unknown	Ann	Julia
Unknown	Archibald	Nick
Unknown	Bisi	Peter
Unknown	Daniel	Sarah
Unknown	Elias	Simon
Unknown	Lulian [Julian]	Andrew
Unknown	Mary	Julia
Unknown	Mary	Lucy
Unknown	Mary	Mary
Unknown	Merideth	Peter
Unknown	Savilla [Sasilla]	Sarah
Unknown	Susan	Sylvester
Unknown	Thomas	Andrew
Unknown	William	Eliza
Unknown	Carlline [Caroline]	John
Unknown	Ellen	John
Unknown	James	Joseph
Unknown	John	Mary
Unknown	Mary	William
Charles	Sarah	
Elias	William	Total 271
Rebecca	Zachariah	
Isabella	John	
John	Annenise	
Elizabeth	Emiley	
James	Georgeana	
Joseph	James	
Maria	Daniel	
Nathan	Martin	
William	Sylvester	
George	Caroline	
Milly	Henry	
William	Jane	
Eliza	Joseph	
Joseph	Lucy	
Ann	Martha	
Elias	Philip	
Elizabeth	Sarah	
Hesekiah	Henry	
Hesekiah	Elizabeth	
James	Hezakiah	
John	John	
John	Nathan	
John	Otho	
Mary	Sarah	
Mary	Susan	
Mary	Ann	
Nathaniel	Isaac	

Supplementary Text S3. Testing the application of IBD detection methods to imputed low coverage ancient DNA using simulated data

S3.1 Data preparation

5 We selected 32 high coverage ancient genomes from varying time periods and regions across the globe in order to test the performance of TPBWT(41) when applied to imputed genotypes from low coverage, captured ancient DNA data. The imputation was performed using the tool GLIMPSE (40) with an approach that has been optimized for low-coverage, capture-based ancient DNA data. All 32 individuals included in this test dataset are of at least 20x coverage, 10 except for two individuals (I6714.SG and I3388.SG) that were included as they are first degree relatives of two other high coverage individuals (Table S3.1).

Table S3.1. Ancient Individual Background

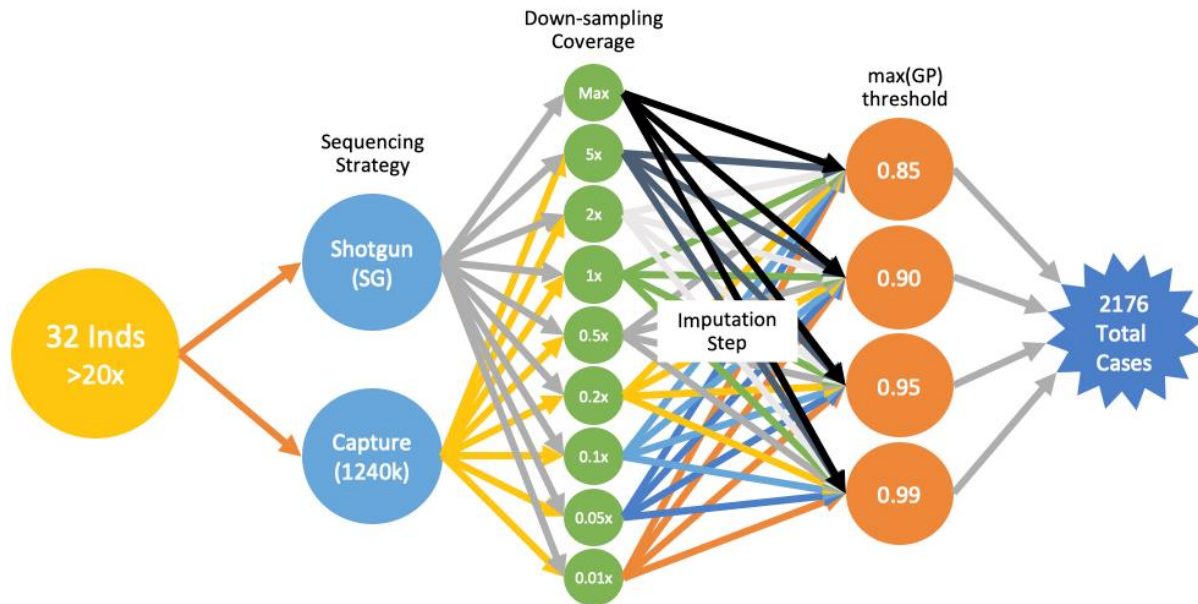
Individual ID	Genetic Sex	Country where individual was excavated	Average age (years before present)	Coverage (average autosomal)	Original Publication	Publication of High Coverage Shotgun Data	Notes
HSJ-A-1_38.SG	M	Iceland	1015	34.68	(106)	(106)	
I2861.SG	F	Great Britain	2853	20.54	(107)	(108)	
I1053.SG	M	Russia	3793	20.22	(84)	(108)	
I5835.SG	M	Germany	4200	23.75	(107)	(108)	
I2514.SG	M	Iran	4341	21.30	(84)	(108)	
I1633.SG	F	Armenia	4465	20.89	(109)	(108)	
I5950.SG	M	Ethiopia	4472	22.68	(110)	(108)	
I6714.SG	M	Russia	4495	17.95	(84)	(108)	Afanasievo Family – Son B
I3388.SG	F	Russia	4600	8.95	(84)	(108)	Afanasievo Family – Mother
I3949.SG	M	Russia	4618	22.78	(84)	(108)	Afanasievo Family – Son A
I3950.SG	M	Russia	4707	23.33	(84)	(108)	Afanasievo Family – Father
Yamnaya.SG	M	Kazakhstan	4903	27.32	(111)	(111)	
I5279.SG	M	Russia	4905	24.58	(84)	(108)	
I2935.SG	M	Great Britain	5123	23.95	(107)	(108)	
I2978.SG	M	Great Britain	5129	30.90	(107)	(108)	
I2520.SG	M	Bulgaria	5132	22.41	(76)	(108)	
I2980.SG	F	Great Britain	5181	26.20	(107)	(108)	
I3133.SG	M	Great Britain	5455	26.27	(107)	(108)	
I1631.SG	F	Armenia	6100	29.62	(109)	(108)	

I5077.SG	M	Croatia	7026	24.24	(76)	(108)	
I1496.SG	M	Hungary	7052	26.07	(112)	(108)	
I4438.SG	M	Latvia	7291	20.63	(76)	(108)	
I4878.SG	M	Serbia	7803	22.62	(76)	(108)	
I4873.SG	F	Serbia	7872	21.95	(76)	(108)	
I4596.SG	M	Latvia	7976	20.27	(76)	(108)	
I4914.SG	M	Serbia	8123	22.19	(76)	(108)	
I1960.SG	F	Russia	8166	20.40	(84)	(108)	
I1583.SG	M	Turkey	8281	21.50	(23)	(113)	
I4877.SG	F	Serbia	8505	23.33	(76)	(108)	
SF12.SG	F	Sweden	8895	65.47	(114)	(114)	
I5236.SG	M	Serbia	10008	23.10	(76)	(108)	
I5235.SG	M	Serbia	10835	20.12	(76)	(108)	

We used samtools view (v1.10.2) to subsample reads and create bam files with coverages of 0.01x, 0.05x, 0.1x, 0.2x, 0.5x, 1x, 2x, 5x, max (the max case was only generated for shotgun-style simulations) (Fig. S3.1). For shotgun (SG) and 1.2 million SNP capture (1240k) simulations we only keep reads that overlap with 1000 Genomes project phase 3 (68) and the 1.2 million sites targeted during enrichment capture (23–25), respectively. These bam files were used as input to the imputation pipeline to estimate the Genotype Posterior (GP=[GP0, GP1, GP2]) for each genotype. The genotype with highest GP value was used as the imputed genotype.

Following imputation, the data were filtered to remove genotype calls with an estimated maximum genotype posterior below a minimum threshold (henceforth referred to as the “max(GP) threshold”) of 0.85, 0.90, 0.95 or 0.99, resulting in 2,176 simulated test cases. We also considered the non-imputed versions of the original 32 individuals in our analyses, using the most likely genotype calls generated by bcftools mpileup (v1.10.12) prior to imputation. In cases where no genotype could be predicted or two genotypes were equally likely, the genotype was considered missing. All data were then rephased with EAGLE (73) using a panel of 706,995 23andMe

research participants at 541,948 SNPs, with default settings and optional parameter --allowRefAltSwap. Missing genotypes were not re-imputed.



5 **Fig. S3.1. Schematic of simulated data processing strategies.** The schematic shows the various conditions that were generated at each stage of processing. Starting with 32 high coverage ancient individuals, the data modified to mirror shotgun (SG) and capture (1240k) sequencing strategies. Then the data were downsampled to coverages between 0.1x-5x (also retaining the max coverage case for shotgun data). Next, data was filtered to retain sites with a max(GP)
10 threshold between 0.85-0.99, resulting in a total of 2,176 cases.

S3.2 Impact of data quality reduction on total IBD sharing

While IBD-based tools have previously been applied to ancient DNA (115–118), these analyses have been restricted to shotgun sequence data. In order to ensure that the process of imputation
15 on low-coverage, captured sequence data did not introduce substantial biases, we explored the

impact of data generation strategy (i.e., capture versus shotgun) and down-sampling coverages on IBD segment detection. For each case, we used TPBWT (41) to detect IBD shared with a panel of ~470,863 23andMe research participants who indicated having 4 grandparents that were born in the same region, including ~200,000 research participants whose grandparents were born in the same US state and an additional ~270,000 research participants whose grandparents were born in a single country. We emphasize that imputation is an essential step in our process, not only because it allows inference of diploid genotypes, but also because only 22.3% (146,701/656,786) of the version 5 panel of SNPs genotyped by 23andMe were targeted in the 1240k capture process.

10

We detected 229,492,064 IBD segments shared between all the downsampled cases and the 23andMe panel, ranging in size from 3cm (the minimum segment length output by TPBWT) to 32 cM (Fig. S3.2a; Table S3.2). The majority of IBD segments (71.8%) were between 3-4cm in length, while fewer than 0.5% of segments exceeded 8cm. The relative abundance of short IBD segments is expected, as shorter IBD segments reflect more distant relatedness (119, 120).

15

Because imputation can potentially introduce false positive IBD segments, particularly for the lowest coverage cases, we determined the rate of false positive IBD detected across all scenarios. We assumed that IBD segments detected between 23andMe research participants and the highest coverage cases (i.e. DP max) represented true IBD segments, while segments only observed in lower coverage cases represented false positive segments introduced by imputation. We defined false positive rate (FPR) as the number of false positive IBD segments detected in a lower coverage case divided by the total number of segments detected in that case. In our calculations, segments

20

that overlapped at any position were considered to be the same segment. In Fig. S3.2b (Table S3.3) we present the weighted average of the FPR for each case, where the relative weight of each ancient individual is determined based on the number of IBD segments detected in the highest coverage (DP max) condition.

5

We found that FPR increases as coverage decreases with a higher rate of increase in capture data. The difference in performance of capture versus shotgun data is unsurprising as coverage measurements are not equivalent between the two data types—for shotgun sequenced data, coverage refers to the average number of reads aligning to every site in the human genome, while
10 only the targeted sites are considered in measurements of coverage for capture data. The large amount of data from non-targeted SNPs available from shotgun data greatly increases the precision with which we can make genotype inferences at all SNP positions including targeted ones. We also found that the FPR was generally similar across the various max(GP) thresholds, with slightly higher FPRs typically associated with max(GP) threshold of 0.99, particularly in lowest coverage
15 cases. This likely reflects the relative increase in missing data associated with using a more stringent filtering threshold. In order to strike a balance between the number of reliably imputed genotype calls and the amount of missing data, we chose to apply a max(GP) threshold of 0.95 going forward. However, we note a minimal impact of varying max(GP) threshold across subsequent analyses. We also focus on the capture-style data going forward in order to mirror the
20 data available for study in the main text, again noting that we observe similar trends in the shotgun style data.

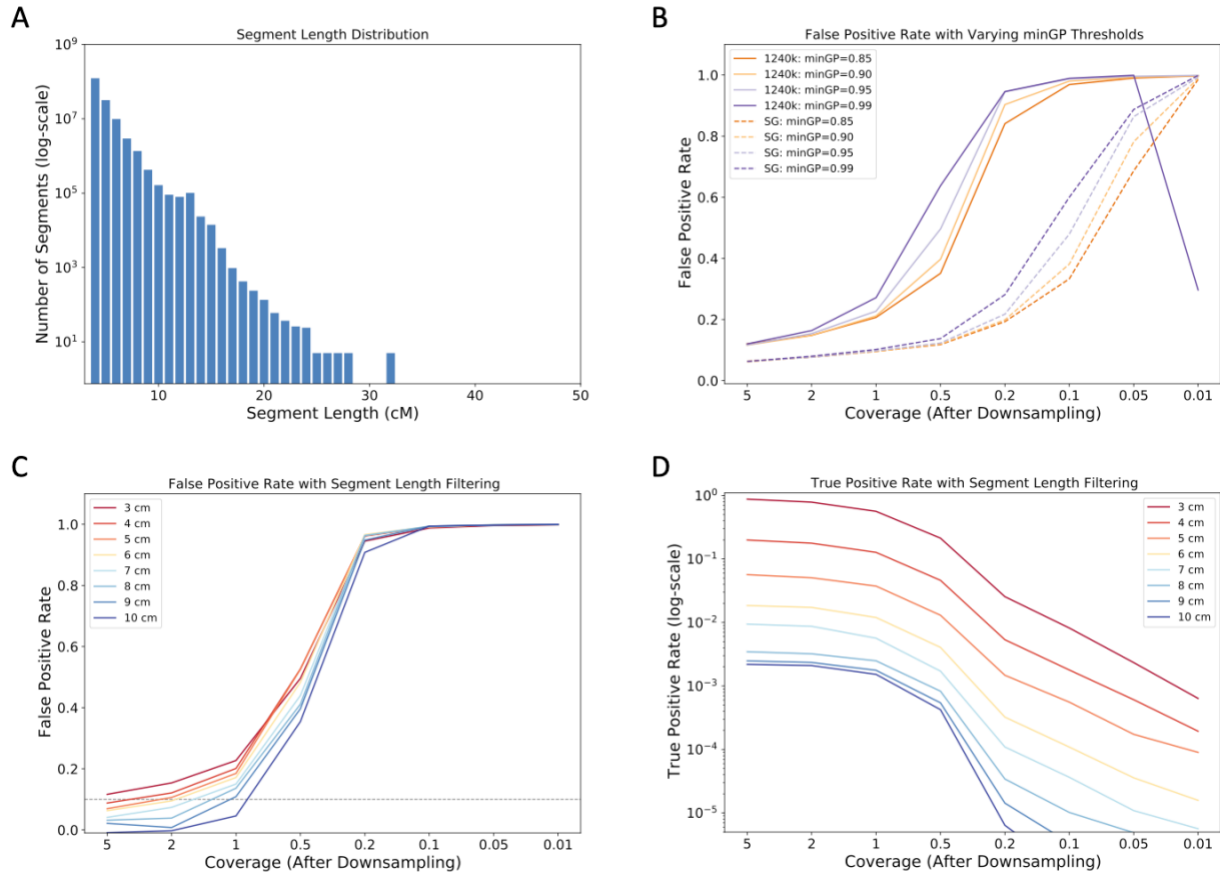


Fig. S3.2 IBD Segment Authenticity [A] Histogram of IBD segment lengths shared with 23andMe research participant panel across all simulated cases. x-axis labels indicate the upper bound of each size bin (i.e. 4cM indicates the 3-4cM bin). Segment counts are shown on the y-axis using a log scale. [B] FPR for shotgun (dotted line) and 1240k capture (solid line) style sequence data, with varying max(GP) thresholds (as indicated by line color). FPR was calculated as the proportion of IBD segments in a specified case that do not occur in the corresponding highest coverage (DP max) case. We present the weighted average of the FPR for each case, where the relative weight of each ancient individual is determined based on the number of IBD segments detected in the highest coverage (DP max) condition. [C] Weighted average FPR for the max(GP) threshold = 0.95 for 1240k capture style data after filtering using a variable minimum segment length threshold between 3-10cM (as indicated by line color). [D] Weighted average TPR for the

max(GP) threshold = 0.95 for 1240k capture style data after filtering using a variable minimum segment length threshold between 3-10cM (as indicated by line color). The TPR was calculated as the proportion of IBD segments that are detected in the max coverage case that are also detected in the lower coverage case. TPR is shown on the y-axis using a log scale.

5

To minimize the FPR while maximizing the true positive rate (TPR) when studying capture-style sequenced ancient DNA we explored the impact of filtering IBD segments based on length, with the hypothesis that shorter reads are more likely to be false positives. We find that the FPR decreases as more stringent minimum IBD segment length filters are applied (Fig. S3.2c, Table 10 S3.3). At 5x coverage, a minimum segment length threshold of 4cm is sufficient to reduce the weighted average FPR to 9.8%. However, as coverage decreases, longer minimum segment length thresholds are required to reach the 10% FPR threshold.

While length thresholding reduces FPR, it also dramatically reduces the number of true IBD 15 segments detected. Therefore, we considered the impact of length filtering on the true positive rate (TPR)—the proportion of IBD segments that are detected in the max coverage case that are also detected in the lower coverage case. Mirroring trends observed with FPR, when using the standard minimum segment length threshold of 3cM TPR is maximized in the highest coverage cases and dramatically declines as coverage decreases (Fig. S3.2d, Table S3.3). Applying a more stringent 20 minimum length threshold dramatically reduces the TPR, even in the highest coverage cases, indicating that many of the shorter IBD segments removed by length filtering are real.

In order to balance the reduction in false positive IBD with the loss of true IBD associated with length filtering, we chose to apply a sliding scale minimum segment length threshold to our TPBWT results, selecting the minimum segment length threshold at each coverage that is closest to a 10% FPR. For empirical analyses we applied the following thresholds:

5

Coverage (x)	Minimum IBD Segment Length
>5	4 cM
[2,5)	6 cM
[1,2)	9 cM
<1	10 cM

We note that at 0.5x coverage and below, none of the thresholds that we tested substantially reduced the FPR. We therefore chose to apply a minimum segment length threshold of 10 cM for the purposes of testing.

10

S3.3 Exploring broad geographic signals of IBD sharing

In order to assess whether the IBD segments detected between the ancient individuals and the panel of 23andMe participants reflect known historical patterns, we considered the geographic distribution of IBD sharing. Since each country in our dataset has a different number of associated participants who report ancestry from the region, we considered the average total IBD shared with 23andMe participants from each country in each case. To protect individual research participant privacy, we only report results for countries with a minimum of 5 associated 23andMe research

15

participants. Here we highlight the results of 3 ancient individuals who serve as representative examples of general trends that we observed in this dataset.

5 First, we considered individual HSJ-A-1_38.SG. This individual was excavated in Iceland and dates to approximately 1015 years before present (*106*), making them the most recent individual in our test dataset. The highest average IBD is shared between this individual and 23andMe participants with 4 grandparents from Iceland for all cases with at least 0.2x coverage, including the non-imputed case (Fig. S3.3a-e, Table S3.4). Research participants with ancestry from Northwestern Europe, including Scandinavian countries, Great Britain and Ireland also show a
10 high rate of IBD sharing with this ancient Icelander. This pattern of IBD sharing directly matches our historical expectations, as Iceland was colonized by populations with ancestry from these regions. Further, ancient Icelanders have previously been shown to be even more genetically similar to present-day Scandinavian, British and Irish populations than present-day Icelandic people, likely due to the genetic drift that inhabitants of the region have undergone in the
15 millennium since this ancient individual lived (*106*). The most total IBD is observed in the 5x coverage case, even relative to the non-imputed dataset. We believe that the relative increase in IBD detected in the high coverage imputed dataset versus the non-imputed dataset is due to the greater accuracy of genotype calls in this dataset, as the non-imputed dataset did not undergo any filtering based on the likelihood of the genotype calls and likely includes more incorrect genotype
20 calls than the high coverage imputed dataset. Similarly, we observe a relative decrease in total IBD for the imputed cases down-sampled to lower coverages, in part due to the higher minimum segment length thresholds that we apply in the lower coverage cases. However, this decrease in IBD is relatively uniform across the entire 23andMe cohort, therefore the geographic pattern is

apparent even in the 0.2x coverage case. In the 0.1x coverage case and below, the geographic pattern is lost, as almost no IBD is detected between any 23andMe participants.

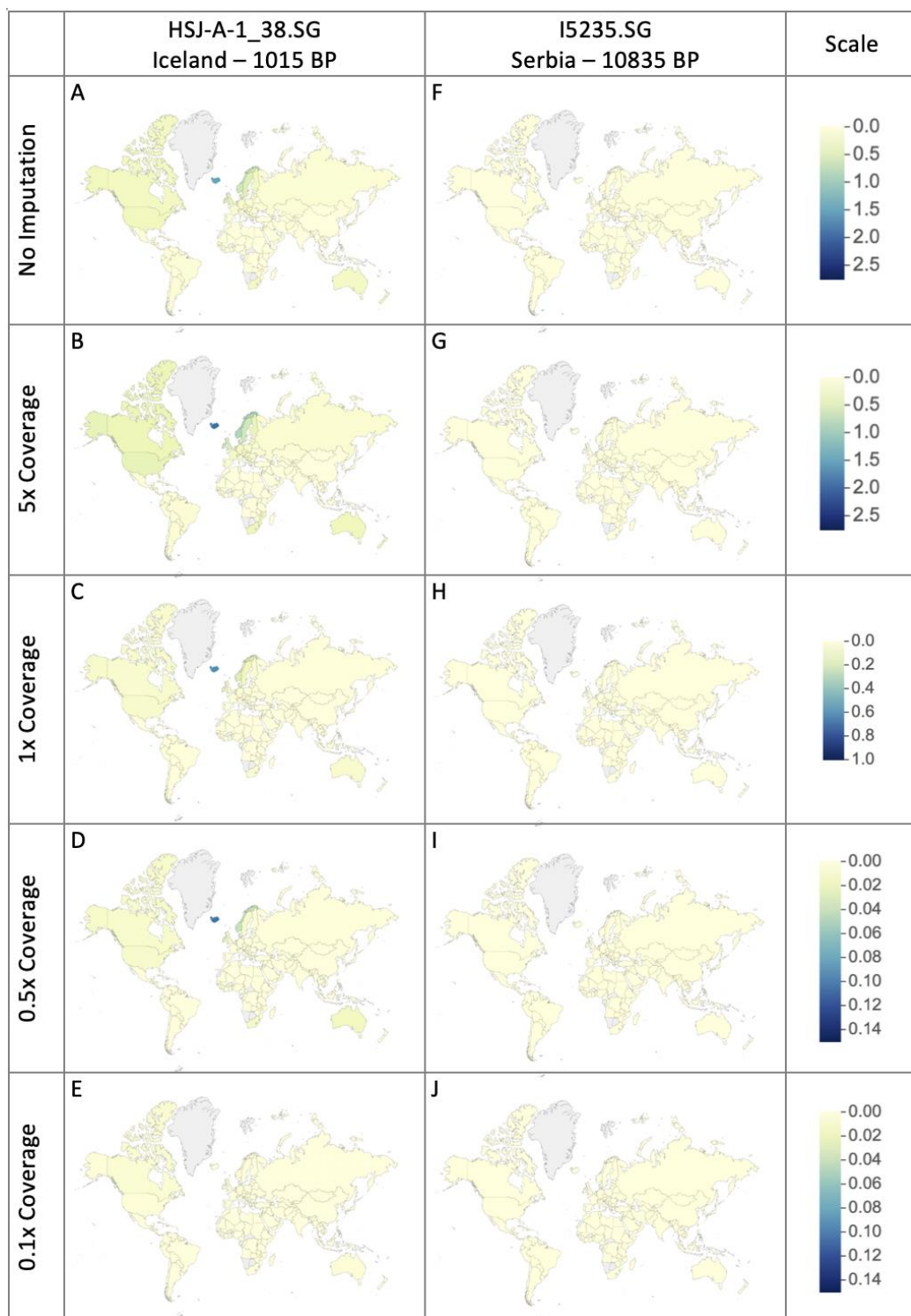


Fig. S3.3. Geographic distribution of average IBD sharing. Average IBD shared between an ancient individual and 23andMe research participants with 4GP from each country. Higher average IBD is highlighted in blue, while lower average IBD is shown in yellow. Countries with fewer than 5 associated 23andMe research participants are shown in gray. Average IBD shared with each of three ancient individuals is shown in each column, while varying coverages are shown in each row. In all cases, except for the non-imputed version, results for the 1240k capture style data filtered using a max(GP) threshold of 0.95 is shown, with minimum IBD segment length thresholds applied based on coverage. The color scale used for each coverage varies and is indicated by the scale bar to the right of each row.

10

In contrast, we detect very little IBD shared between the oldest ancient individual in the test dataset—a 10,835 year old individual from present-day Serbia (76)—and the panel of 23andMe research participants for any case (Fig. S3.3 f-j). This failure to detect IBD shared between 23andMe research participants and an ancient individual of this age is expected, as IBD breaks down over time due to recombination. The likelihood of an IBD segment over 4 cM in length being shared between individuals that are separated in time by almost 11 thousand years is nearly negligible (119).

15

S3.4 Detecting relatedness between ancient individuals

20 Among the 48 high coverage ancient individuals used for testing are 4 individuals that form a genetically related family unit, consisting of a biological father (I3950.SG), mother (I3388.SG) and two sons (I3949.SG and I6714.SG). These individuals were originally described and identified as relatives in Narasimhan et al. (84), and the shotgun sequencing data are reported in Wohns et

al. (121) The inclusion of these related individuals in our test dataset provided the opportunity to determine how well TPBWT can detect IBD in known relatives.

We therefore compared all 32 individuals to one another using TPBWT. In order to understand the impact of imputation of low coverage data, we compared cases with 0.1-5x coverage (with the same coverage used for each individual in the comparison) and included comparisons with the highest coverage shotgun case. At the highest coverage, first-degree relatives in the Afanasievo family share substantially more IBD than any other pair of individuals (Fig. S3.4a, Table S3.5). Further, the total IBD detected between the related Afanasievo family members is highly dependent upon coverage, with the most total IBD detected at 5x coverage. These results indicate that total IBD detected between ancient individuals depends on both the degree of relatedness and coverage, and therefore the degree of closeness of a relationship cannot be directly inferred from the total IBD measured between two individuals without taking the coverage of those individuals into consideration. Further, we observe an increase in total IBD detected between unrelated individuals at lower coverages. By 0.2x coverage it is not possible to distinguish between the known 1st degree relatives and random pairs of unrelated individuals. We therefore caution that total IBD measured between two ancient individuals with less than 1x coverage should be interpreted with extreme caution.

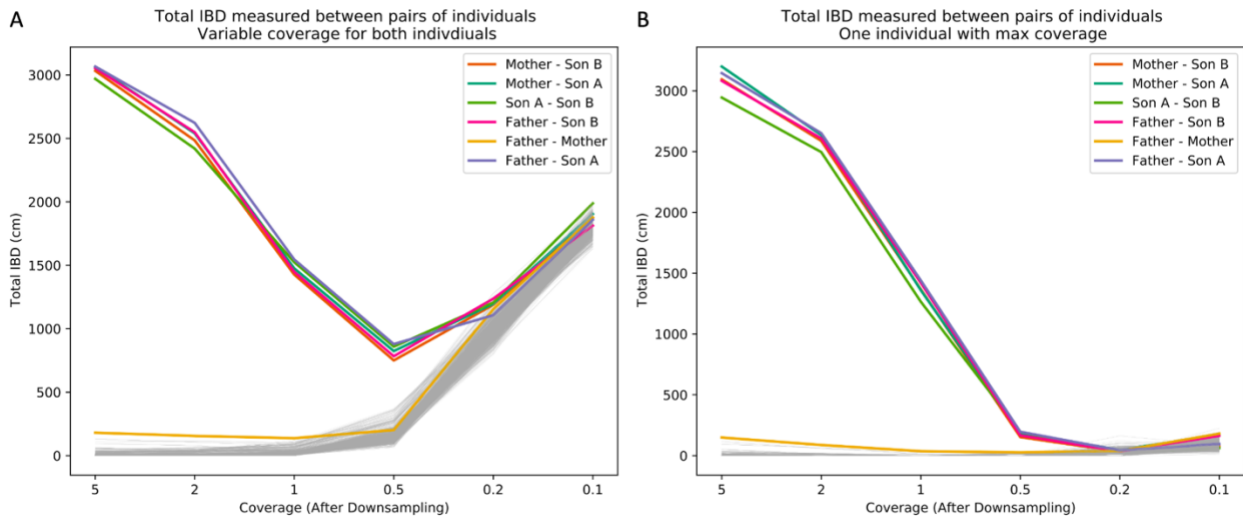


Fig. S3.4. Total IBD detected between ancient individuals. Total IBD measured by TPBWT in pairwise comparisons of all ancient individuals. Comparisons between members of the Afanasievo family are shown in varying colors (see legend) while all other comparisons are shown in gray.

5 We show the change in total IBD detected at varying down-sampling coverages, where either both individuals are down-sampled to the same coverage [A] or a single down-sampled individual compared with the highest coverage (DP max) case.

In comparisons between 23andMe participants and ancient individuals, only the ancient
10 individuals will be impacted by reduced data quality, as the diploid genotypes of 23andMe research participants are called with a high degree of confidence. We therefore decided to repeat our comparison of the ancient individuals while only downsampling a single ancient individual and using the highest coverage version (DP max) of the second individual (Fig. S3.54b, Table S3.6) in order to better mirror this scenario. In this case, we find a more rapid decline in total IBD detected
15 between the first-degree relatives as coverage decreases; however, we do not detect substantial IBD between the unrelated pairs of individuals, even at the lowest coverage threshold. These

results suggest that when substantial IBD is detected between an ancient individual with at least 0.5x coverage and a 23andMe participant, it likely reflects a true genetic relationship. Again, however, it is not possible to directly translate the total amount of IBD shared into a specific degree of relatedness without taking the coverage of the ancient individual into consideration.

5

Finally, in order to understand how the distribution of IBD segments detected between relatives changes as coverages decreases, we mapped the genetic positions of the IBD segments detected between the two highest coverage members of the Afanasievo family—I3950.SG (Father) and I3949.SG (Son A). In a comparison between the highest coverage cases (DP max), we detect IBD
10 across almost the entire genome (Fig. S3.5, Table S3.7). Additionally, we observed relatively few instances where two IBD segments were detected in the same region (i.e., full IBD), consistent with the distribution of IBD segments expected between a father and son pair. In the few cases where we do detect full IBD, many of these regions are also areas where we detect IBD shared
15 between the father and mother. Thus, these may represent true instances of full IBD sharing between the father and son, as the son may have also inherited an identical segment from the mother. When we reduce the coverage of a single individual (I3949.SG), we again show that as coverage decreases we fail to detect additional true IBD.

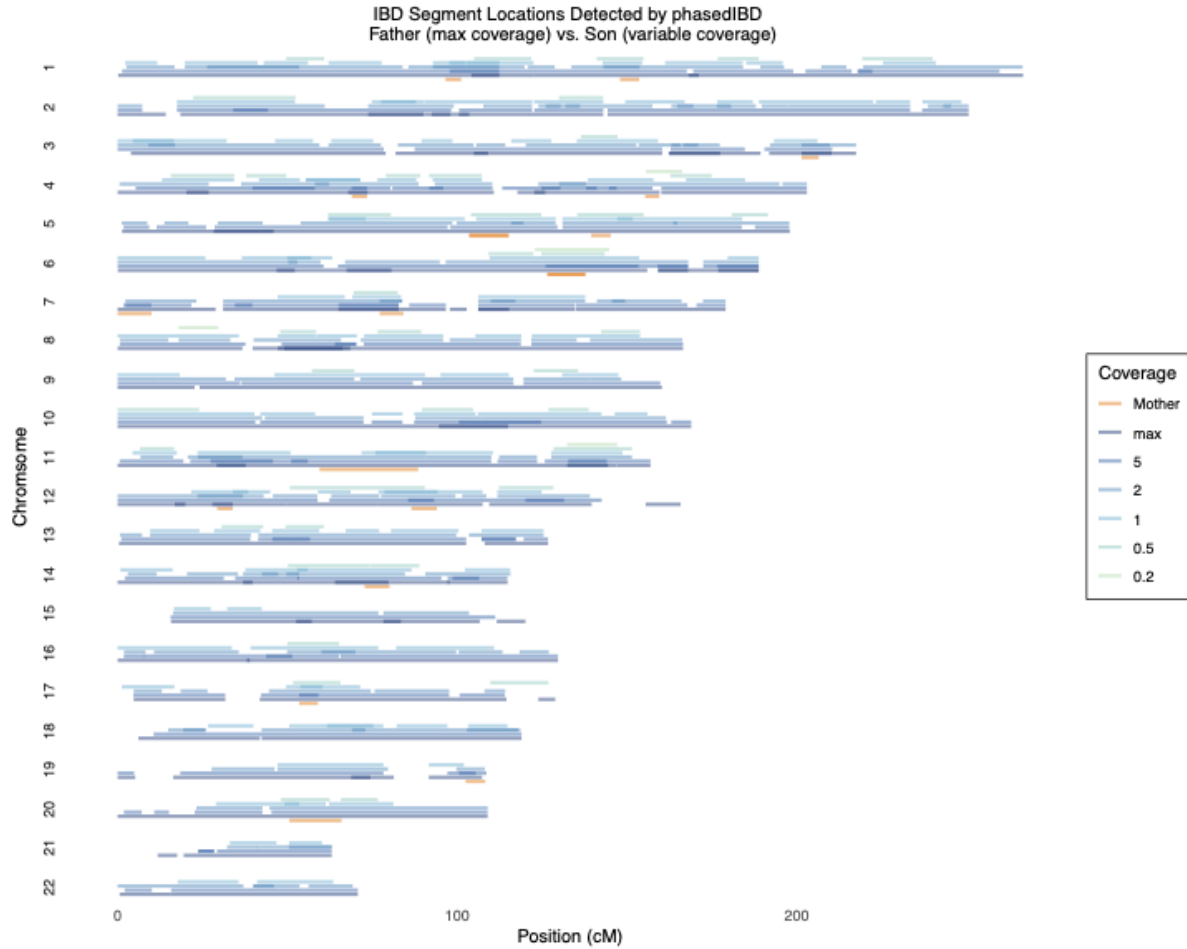


Fig. S3.5. Location of IBD segments detected between Father (I3950.SG) and Son A (I3949.SG) at varying coverages. In all cases, the highest coverage version (DP max) of the father is compared with Son A, downsampled to varying coverages, as specified by segment color. Positions where full IBD is detected (i.e. two overlapping IBD segments are detected in single pair) are indicated by darker colors. Positions where IBD is detected between the mother and father (in the max case for both individuals) are shown in orange.

S3.6 Guidelines for IBD analysis of imputed ancient DNA

10 Taken together, these results suggest several guidelines for IBD analysis of imputed data which we will follow for all analyses in the main text. First, we require an absolute minimum coverage

of 0.5x for ancient individuals sequenced using a 1240k capture-based approach (in cases where shotgun sequenced data is considered, a threshold of 0.05x is acceptable), and will interpret results for individuals with <1x coverage with caution. In order to maximize genotype call quality while minimizing missing data, we filter all imputed data using a max(GP) threshold of 0.95. Finally, in
5 order to reduce false positive IBD, while still capturing as much true IBD as possible, we only consider IBD segments that exceed a minimum length threshold, as defined by the coverage of the individual.

Supplementary Text S4: Testing the performance of Ancestry Composition on imputed low coverage ancient DNA using simulated data

23andMe's Ancestry Composition (42) algorithm infers local ancestry in genomic windows across
5 each chromosome. Ancestry Composition was designed to predict local ancestry using high
coverage genotypic data from present-day individuals. Consequently, there are several factors that
might impact the performance of Ancestry Composition when applied to aDNA data, such as
biases caused by imputation and the presence of missing data (even at the rate that it is present in
an imputed dataset that has been filtered to remove low confidence genotype calls). Therefore,
10 using the test dataset described in Supplementary Text S4, we evaluated Ancestry Composition
applied to imputed ancient genomes generated from low-coverage capture-based sequence data.

Since Ancestry Composition was not designed for use with missing data, we also created an
unfiltered dataset for which we did not perform any filtering based on the quality of the inferred
15 genotype. We refer to this unfiltered dataset as having a minimum maximum genotype posterior
(max(GP) threshold) of 0.00, and compared this dataset to the max(GP) thresholds of 0.85, 0.90,
0.95 and 0.99 datasets described in Supplementary Text S3.

Ancestry Composition predicts local ancestry using present-day reference populations which may
20 not be applicable to very ancient individuals. We therefore chose to focus our tests on the most
recently deceased of the 32 individuals in our test dataset for whom these assignments would be
most meaningful. The current version of Ancestry Composition assigns windows of each
chromosome to one of 45 leaf populations. These populations are nested within a hierarchical
structure (Fig. S4.1). The broadest level assignments are divided into 6 categories (which we will

refer to as “level 1”): “Sub-Saharan African”, “East Asian & Indigenous American”, “Melanesian”, “Central & South Asian”, “Western Asian & North African” and “European”. Within each of the level 1 (Continental) categories, there are up to two additional levels of nested classifications, referred to as “level 2” (Regional) and “level 3” (Population) assignments. For instance, within the Sub-Saharan African level 1 category are the nested “African Hunter-Gatherer”, “Congolese & Southern East African”, Northern East African, and “West African” level 2 categories, and each of these (except for “African Hunter Gatherer”) contains its own nested level 3 categories. It is also possible for a proportion of an individual's genome to be classified as "Unassigned" (i.e., level 0) when a genomic window cannot be confidently assigned to a single ancestry across all levels.

We hypothesized that there were two likely ways in which Ancestry Composition assignments could be impacted by data of reduced quality, like that observed in aDNA data: (1) the total amount of ancestry assigned to any category could be reduced. This could mean that a large proportion of the individual's ancestry would be considered “Unassigned” or their ancestry would be assigned to a lower level category, such as “Sub-Saharan African” and not to a more granular higher-level category, like “Congolese & Southern East African,” which are more difficult to predict. Although it would be ideal to have as much ancestry assigned to the highest-level category possible, we view this potential impact as preferable to the alternative option, (2) that portions of the genome would be assigned to the incorrect ancestry category (e.g., “European” instead of “Sub-Saharan African”).

Level 0	Level 1	Level 2	Level 3
Unassigned			
	Sub-Saharan African		
		West African	
			Senegambian & Guinean
			Ghanaian, Liberian & Sierra Leonean
			Nigerian
		Northern East African	
			Sudanese
			Ethiopian & Eritrean
			Somali
		Congolese & Southern East African	
			Angolan & Congolese
			Southern East African
		African Hunter-Gatherer	
	East Asian & Indigenous American		
		Japanese & Korean	
			Japanese
			Korean
		Chinese & Southeast Asian	
			Chinese
			Chinese Dai
			Vietnamese
			Filipino & Austronesian
			Indonesian, Thai, Khmer & Myanma
		Northern Asian	
			Manchurian & Mongolian
			Siberian
		Indigenous American	
	Melanesian		
	Central & South Asian		
		Central Asian, Northern Indian & Pakistani	
			Central Asian
			Northern Indian & Pakistani
			Bengali & Northeast Indian
			Gujarati Patidar
		Southern Indian Group	
		Southern South Asian	
			Southern Indian & Sri Lankan
			Malayali Subgroup
	Western Asian & North African		
		Northern West Asian	
			Cypriot
			Anatolian
			Iranian, Caucasian & Mesopotamian
		Arab, Egyptian & Levantine	
			Peninsular Arab
			Levantine
			Egyptian
			Coptic Egyptian
		North African	
	European		
		Northwestern Europe	
			British & Irish
			French & German
			Scandinavian
			Finnish
		Southern European	
			Spanish & Portuguese
			Sardinian
			Italian
			Greek & Balkan
		Eastern European	
			Ashkenazi Jewish

Fig. S4.1 Nested Ancestry Composition Categories. The hierarchical structure of Ancestry Composition (ac45), with higher level (more granular) categories nested beneath and to the right of the corresponding lower level (less granular) categories. Ancestry Composition categories are colored using a color palette that is consistent in all subsequent plots.

In order to understand whether either of these two types of errors occurred when Ancestry Composition is applied to imputed aDNA data, we first focused our analysis on individual HSJ-A-1_38.SG (a ~1015 year old individual from Iceland). As in Supplementary Text 4, we assumed that the Ancestry Composition results assigned to the highest quality versions this individual (i.e. the shotgun maximum coverage versions) represented the most accurate Ancestry Composition assignments, and that any changes to these assignments at lower coverages represented an error. We computed Ancestry Composition assignments for HSJ-A-1.SG across a variety of downsampled coverages and max(GP) thresholds. For all max(GP) thresholds, the maximum coverage versions of individual HSJ-A-1.SG are assigned 100% European ancestry (Fig. S4.2a, Table S4.1). This level 1 ancestry assignment appears most stable across all coverages at the max(GP) threshold 0.00 (i.e., without filtering out low confidence genotype calls). At 1x coverage and below an increasing proportion of the individual's ancestry could not be assigned to a level 1 category; however, very little ancestry was mis-assigned to a non-European category, even at the lowest coverages. In contrast, data produced with the other max(GP) thresholds produced deviating results at much higher coverages (Fig. S4.2b-e, Table S4.1). We therefore use the max(GP) threshold 0.00 data for the remainder of our analyses.

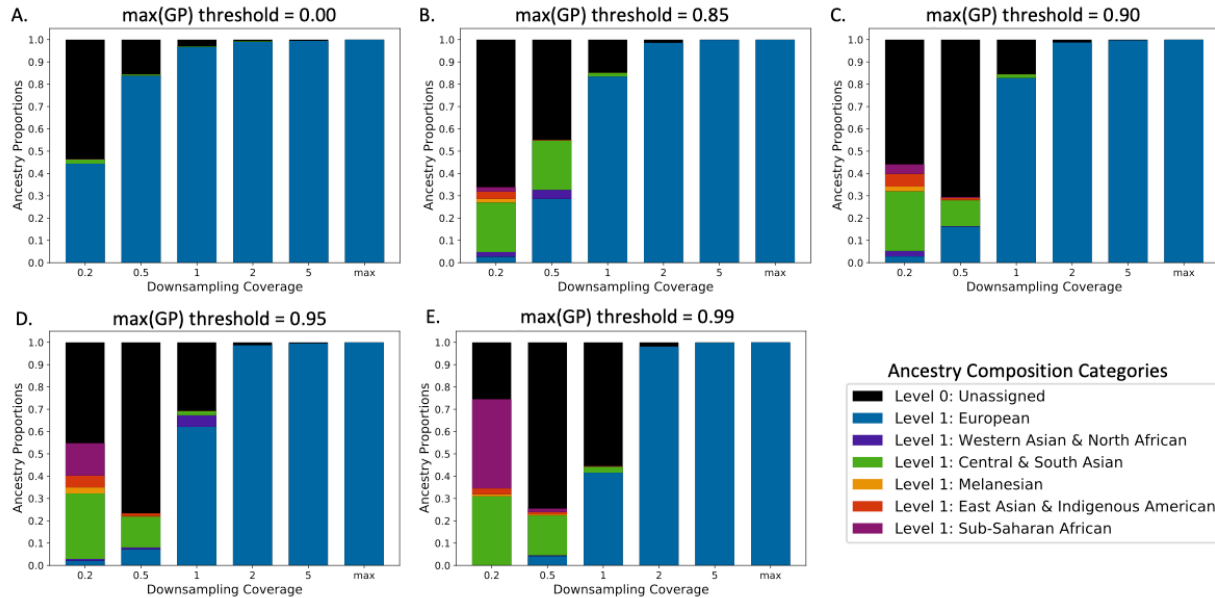


Fig. S4.2 - Level 1 Ancestry Composition Assignments for a single ancient individual (HSJ-A-1_38.SG) across multiple $\max(\text{GP})$ thresholds. Each panel shows the total proportion of ancestry assigned to each Level 1 Ancestry Composition categories across the genome of a single ancient individual (HSJ-A-1_38.SG) at a variety of sequencing approaches and coverages (Shotgun max coverage, 1240k 5x coverage, 1240k 2x coverage, 1240k 1x coverage, 1240k 0.5x coverage, 1240k 0.2x coverage). Panels A-E show the Ancestry Composition assignments using $\max(\text{GP})$ thresholds of 0.00, 0.85, 0.90, 0.95 and 0.99, respectively.

10 In order to study this stability of the level 1 Ancestry Composition assignments across a variety of ancestry types, we generated Ancestry Composition assignments for 6 additional individuals across multiple downsampled coverages and again found that level 1 Ancestry Composition results can be reliably generated for ancient individuals with coverage great than or equal to 1x (Fig. S4.3, Table S4.1). For several individuals at coverages below this threshold we observe more

15 appreciable amounts of ancestry mis-assigned to Ancestry Composition categories that differ from

the highest coverage assignments, suggesting that we should exercise caution when interpreting Ancestry Composition results for imputed ancient individuals with less than 1x coverage.

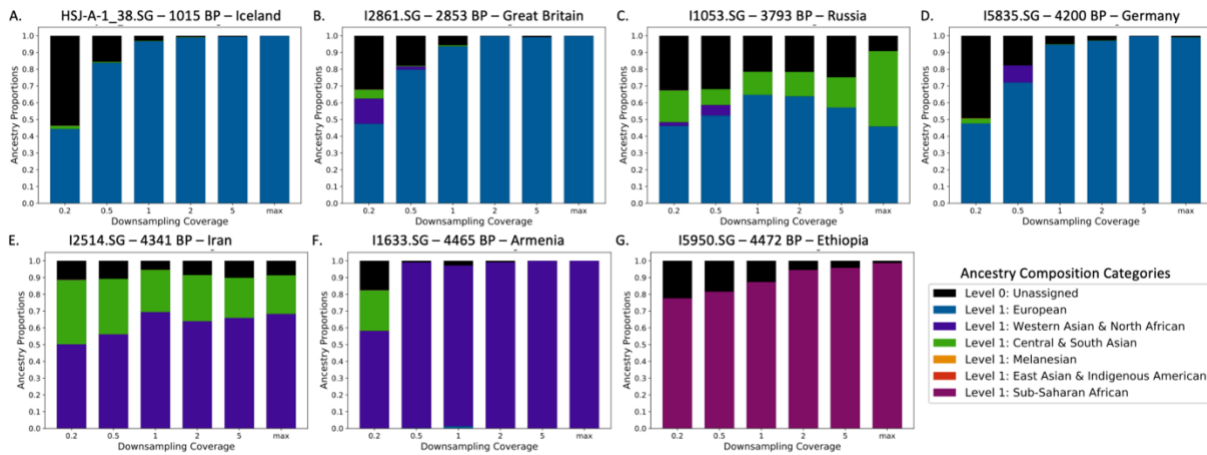


Fig. S4.3 - Level 1 Ancestry Composition Assignments for multiple ancient individuals. The total proportion ancestry assigned to each Level 1 Ancestry Composition categories across the genome of multiple ancient individuals at a variety of sequencing approaches and coverages (Shotgun max coverage, 1240k 5x coverage, 1240k 2x coverage, 1240k 1x coverage, 1240k 0.5x coverage, 1240k 0.2x coverage). Each panel displays the assignments for a different ancient individual: (A) HSJ-A-1_38.SG, (B) I2861.SG, (C) I1053.SG, (D) I5835.SG, (E) I2514.SG, (F) I1633.SG and (G) I5950.SG.

Since Ancestry Composition not only determines the overall proportion of ancestry assigned to each category, but also assigns ancestry to specific regions of the genome, we next painted the chromosomes of several individuals using their ancestry composition assignments at a variety of coverages and found that these level 1 ancestry assignments occurred in stable locations throughout the genome (Fig. S4.4, Table S4.1).

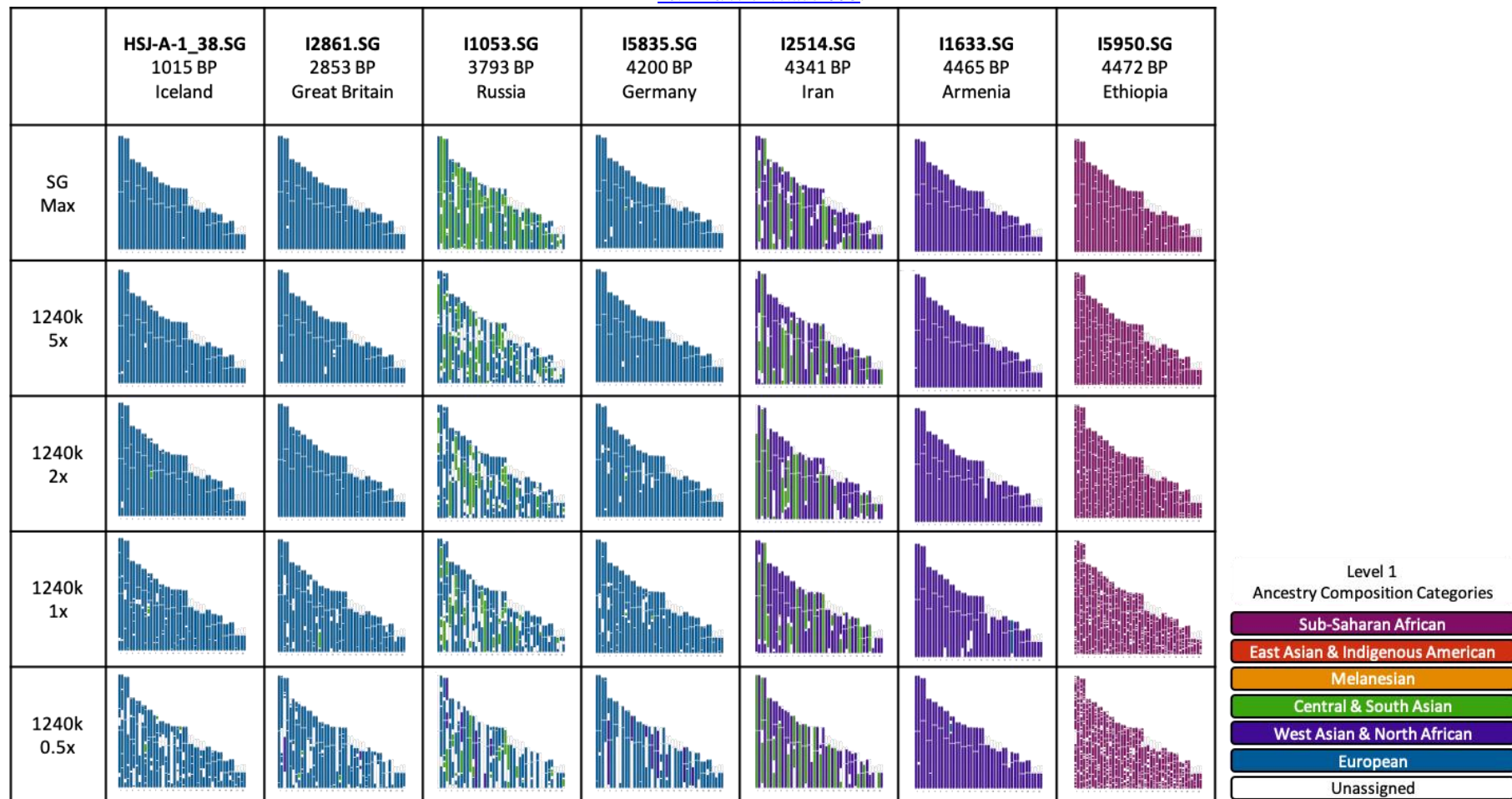


Fig. S4.4 - Chromosome paintings at a variety of coverages. Level 1 Ancestry Composition assignments visualized across the genome of seven historical individuals (left to right: HSJ-A-1_38.SG, I2861.SG, I1053.SG, I5835.SG, I2514.SG, I1633.SG, I5950.SG), at a variety of sequencing approaches and coverages (top to bottom: Shotgun max coverage, 1240k 5x coverage, 1240k 2x coverage, 1240k 1x coverage, 1240k 0.5x coverage). Chromosomes are colored according to their Level 1 Ancestry Composition category, with unassigned portions of the genome shown in white.

5

Next, we next considered the higher level Ancestry Composition assignments. We first considered the Icelandic individual (HSJ-38-1_A.SG) (Fig. S4.5a, Table S4.1). While only the highest coverage cases received level 2 assignments for their whole genomes, for all coverages, the only level 2 assignment was to the “Northwestern European” category. The level 3 assignments were somewhat less stable, with some ancestry assigned to the categories “British & Irish” and “Scandinavian” categories at the highest coverages. At 2x coverage and below, some ancestry was assigned to the level 3 category “French & German” suggesting that the level 3 category assignments are not reliable, even at modest (2x) coverages. Further, when we explored the Ancestry Composition assignments for individual 15950.SG—a ~4472 year old Ethiopian individual—we observed a steady increase in the amount of ancestry assigned to the level 2 “West African” category across all downsampled coverages (Fig. S4.5b, Table S4.1), suggesting that level 2 ancestry assignments are also unreliable for imputed, ancient DNA data. The reliability of level 2 and 3 Ancestry Composition assignments on aDNA data likely varies depending on the ancestry and imputation quality of the data, therefore further work may reveal that some level 2 and 3 Ancestry Composition assignments can be reliably inferred; however, in our analysis of the Catocin individuals, we favored a conservative approach and only reported the level 1 ancestry assignments.

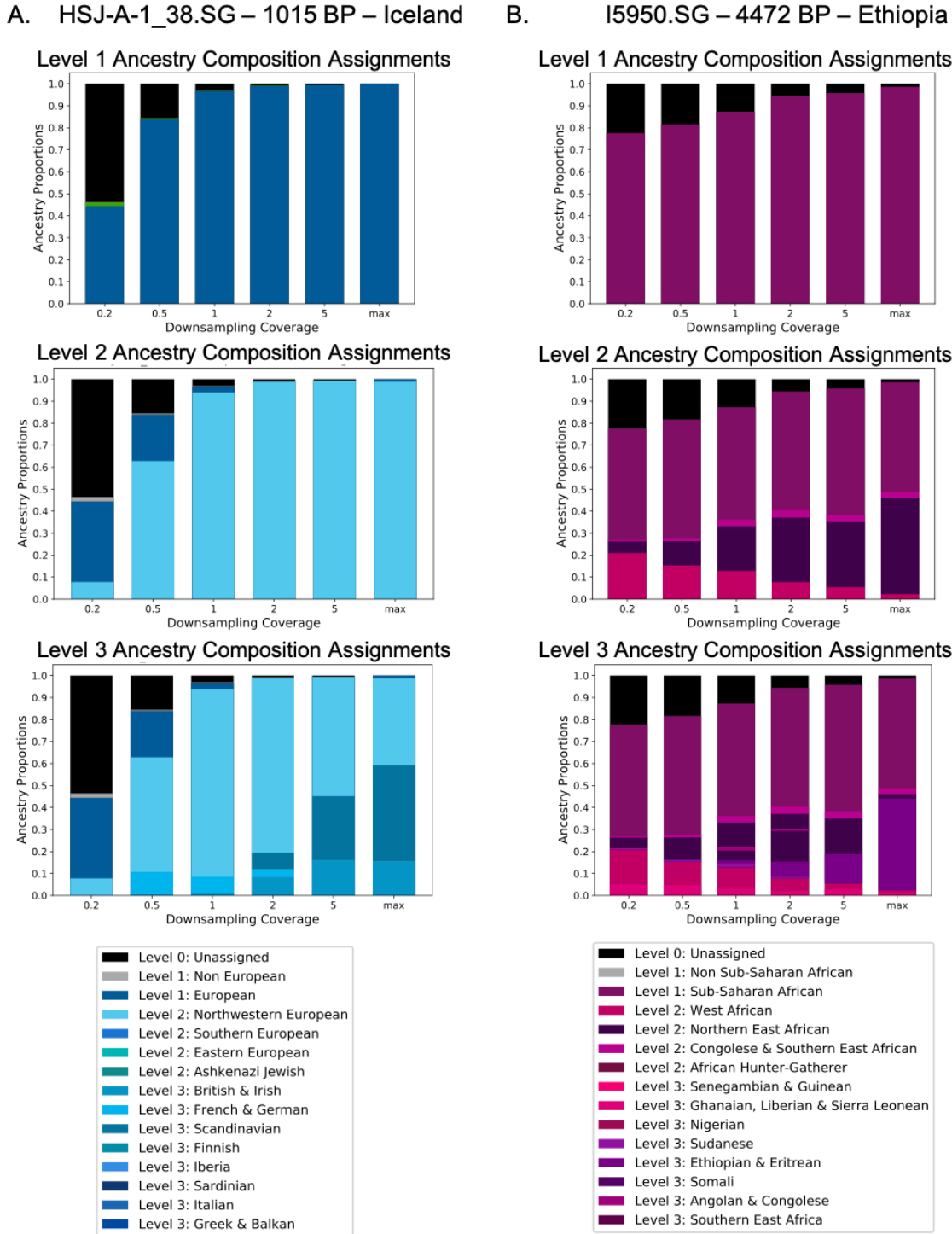


Fig. S4.5 - Level 1-3 Ancestry Composition Assignments for two ancient individuals. The total proportion ancestry assigned to Ancestry Composition categories with varying granularity across the genome for two ancient individuals (HSJ-A-1_38.SG (left) and I5950.SG (right)) at a variety

This is the author's version of the work. It is posted here by permission of the AAAS for personal use, not for redistribution. The definitive version was published in Science on August 4th, 2023, DOI: [10.1126/science.ade4995](https://doi.org/10.1126/science.ade4995).

of sequencing approaches and coverages (Shotgun max coverage, 1240k 5x coverage, 1240k 2x coverage, 1240k 1x coverage, 1240k 0.5x coverage, 1240k 0.2x coverage). (Top row) Panels show Level 1 Ancestry Composition assignments. (Middle row) Panels show Level 2 Ancestry Composition assignments, in addition to Level 1 assignments for portions of the genome that could not be assigned to a Level 2 category. (Bottom row) Panels show Level 3 Ancestry Composition assignments, in addition to Level 1 and 2 assignments for portions of the genome that could not be assigned to a higher level category.

Supplementary Text S5. Genetic connections to African Among Catoctin individuals and 23andMe participants in the US cohort with at least 50% Sub-Saharan African ancestry

S5.1 The impact of applying minimum IBD segment size thresholds.

5 Catoctin individuals share segments of DNA that are identical-by-descent (IBD) with present-day individuals from African genetic groups that are associated with ethnolinguistic affiliation and geography (Fig. 3, Table S11). Given that Catoctin individuals were estimated to have died in Maryland between 1776-1850, they are likely recent descendants of enslaved Africans from specific regions of Africa who were forced into the Americas between the 16th and 19th century as
10 part of the transatlantic slave trade. If Catoctin individuals are fewer generations removed from their African ancestors, they are expected to share more recent common ancestors with African genetic groups from which their ancestors were kidnapped.

To test this, we compared the IBD connections between Catoctin individuals and unique African
15 genetic groups to the IBD connections observed between 23andMe participants in the US cohort with substantial Sub-Saharan African ancestry and unique African genetic groups. We constructed a cohort of present-day participants who have at least 50% Sub Saharan African ancestry, as estimated by 23andMe's Ancestry Composition algorithm (42), and who reported that all four of their grandparents were born within the United States (N = 43,696), henceforth referred to as the
20 “US Sub-Saharan African ancestry cohort.”

Using the templated positional Burrows-Wheeler transform (TWBWT) we can accurately detect small IBD segments in genotyped present-day participants (41); however, we set minimum segment size thresholds to identify IBD between Catoctin individuals and present-day individuals

to decrease false positive segments that can occur due to variable depths of coverage in historical samples (Fig. S3.2). Unsurprisingly, increasing the minimum IBD segment size threshold decreased the number of unique African groups an individual has connections with, on average (Fig. S5.1). This is expected as small segments can indicate connections to more distant common ancestors that may have existed prior to, or in the initial stages of the transatlantic slave trade. These temporally distant connections become undetectable as smaller IBD segments are pruned and connections become focused on the African groups with whom individuals share more recent common ancestors (22).

10

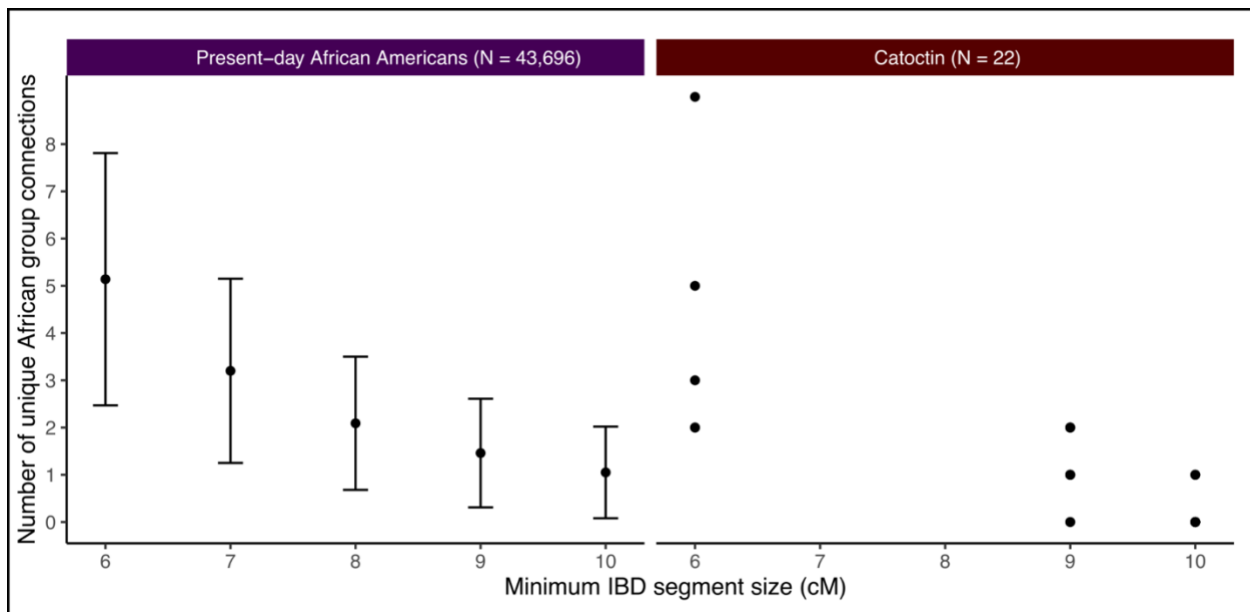


Fig. S5.1. Relationship between minimum IBD segment size threshold and number of unique African group connections. The left panel shows the mean number of connections with standard deviation bars of the US Sub-Saharan African ancestry cohort. The right panel shows the number of connections for independently plotted Catocotin individuals.

15

To account for biases that IBD segment size may have on the number of connections to African groups, we ran IBD analyses between the US Sub-Saharan African ancestry cohort and African genetic groups using 6,7,8,9, and 10 cM minimum segment size thresholds. To explore the effects African ancestry proportions may have on the number of connections to African genetic groups we parsed the US Sub-Saharan African ancestry cohort into different bins based on minimum African ancestry: $\geq 50\%$ (N=43,696), $\geq 75\%$ (N=28,763), and $\geq 95\%$ (N=421). Together, these cohorts cover the range of African ancestry and minimum IBD segment size observed in Catoctin individuals. However, the minimum IBD segment size thresholds are variable among Catoctin individuals, depending on their depth of coverage, making direct comparisons more nuanced. To address variability in filtering thresholds, we also ran analyses on a present-day lookalike cohort whose Ancestry Composition and IBD segment size thresholds match those in the Catoctin cohort at the same frequency. In this special instance, 22 individuals (to match the sample size of Catoctin) whose ancestry and minimum IBD segment size thresholds match those of the Catoctin cohort (Table S1) were resampled 1000 times from the total present-day cohort to ensure that patterns seen in Catoctin individuals were not being driven by African ancestry proportion and segments size thresholds.

S5.2 Exploring number of connections to African genetic groups between US Sub-Saharan African ancestry cohort and Catoctin individuals

We compared the number of unique connections to African genetic groups between Catoctin individuals and various subsets of the US Sub-Saharan African ancestry cohort (Fig. S5.2). In addition to including all Catoctin individuals, we investigated the distribution of connections in Catoctin individuals that have $>90\%$ African ancestry. Catoctin individuals with more African

ancestry are expected to have had more recent African ancestors and therefore may share common ancestors with fewer present-day African groups.

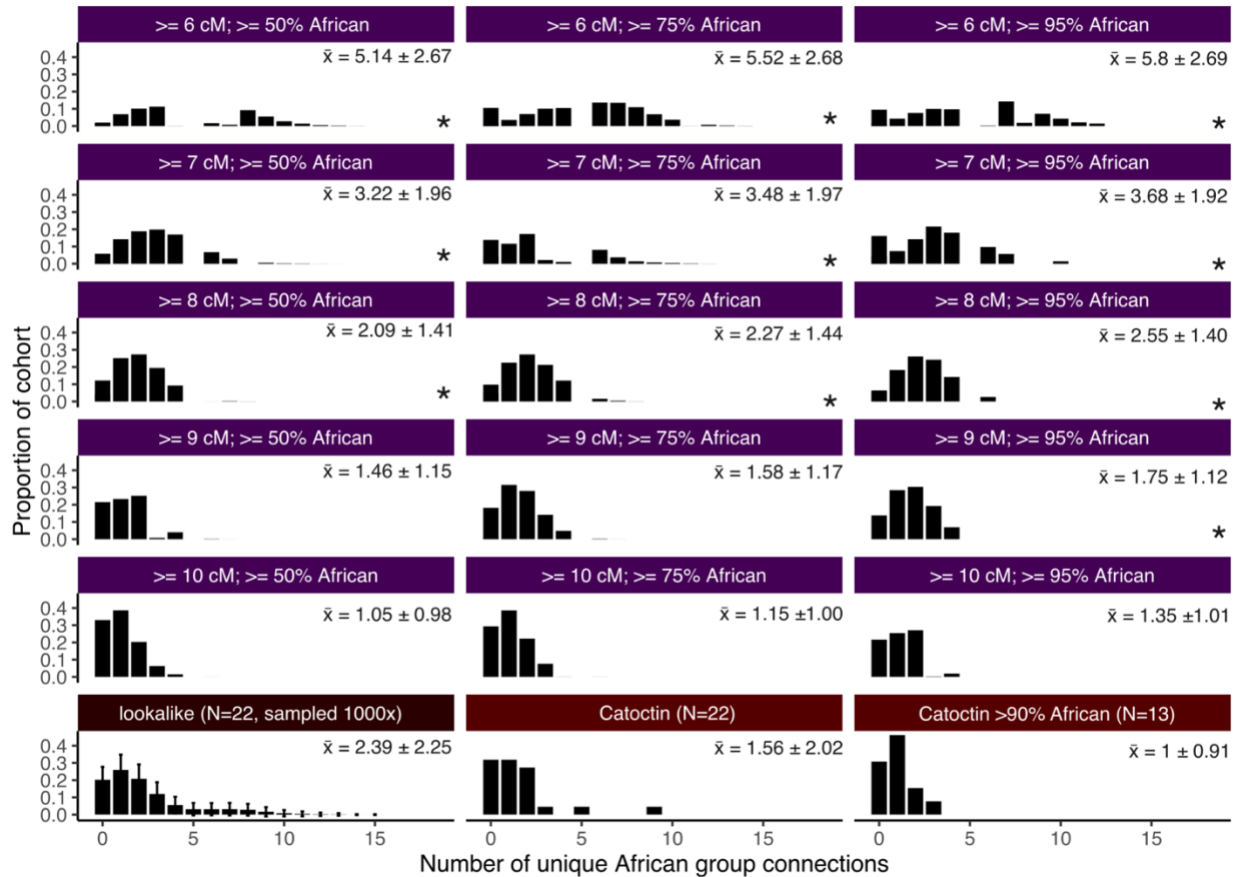


Fig. S5.2. The distribution of the number of unique African group connections in various

5 **cohorts.** The mean and standard deviation of the number of unique hits are displayed in the top right of each panel. Asterisks indicate a significant ($p \leq 0.05$) difference in means between the Catoctin cohort and the corresponding panel using either a Student's t-test or Welch's t-test (depending on equal or unequal variances between datasets, respectively). The lookalike panel demonstrates the mean distribution of connections of 22 members of the US Sub-Saharan African

10 ancestry cohort, sampled 1000 times, whose Sub-Saharan African Ancestry and minimum cM thresholds mimic those of the Catoctin cohort.

As expected, the distribution of unique connections to African genetic groups is widespread in present-day cohorts when retaining smaller IBD segments and skewed towards smaller values when restricting to larger segment sizes. From comparing the mean number of connections across all cohorts using a t-test, the Catoctin distribution is most similar to the $\geq 75\%$ African cohorts at 9 cM ($p = 0.96$) and 10 cM ($p = 0.83$) thresholds and least similar to the $\geq 95\%$ African cohort at 6 cM ($p = 5.6e-13$)

To determine if the distribution of connections to African genetic groups in Catoctin is smaller than expected among members of the US Sub-Saharan African ancestry cohort, we resampled the lookalike cohort 1000 times and determined the number of times the distribution of connections was significantly larger ($p < 0.05$; t-test) than that of Catoctin. Though the raw mean of number of connections was higher 100% of the time, this was only significant ($p < 0.05$) 50% of the time. When performing the same analysis on the Catoctin 90% African cohort, the mean of connections was higher 100% of the time and significant 84.5% of the time, indicating that individuals with more African ancestry in the Catoctin cohort tended to have fewer connections to African groups. In contrast, subsetting the US Sub-Saharan African ancestry cohort by increasing African ancestry *increased* the mean number of unique connections to African groups in every instance. This may indicate that the Catoctin individuals with high African ancestry had ancestors from the few groups they connect to, whereas members of the US Sub-Saharan African ancestry cohort have a greater chance of connecting with multiple African groups that may have admixed during and after the slave trade.

S5.3 Connections to specific African groups.

Self-identifying African Americans in the United States tend to have African ancestry from multiple regions of Atlantic Africa, presumably due to migrations and admixture that occurred during and after the colonial slave trade in the US (22). Studies have also noted an over-
5 representation of ancestry from Nigeria when considering embarkation rates from ports along present-day Nigeria documented during the transatlantic slave trade (22, 122). In general this over-representation of Nigerian ancestry is thought to be a consequence of events that occurred during the colonial slave trade, such as forced breeding in certain US states (123). Catoctin individuals are expected to deviate from African group connection patterns seen among members
10 of the US Sub-Saharan African ancestry cohort because they existed prior to many migrations and admixture events.

We investigated shared IBD connections between Catoctin and African groups and found that the largest proportion of Catoctin individuals have connections to the Kongo (36%), Wolof
15 (22%), and Mandinka (18%) groups (Fig. S5.3). Contrastingly, the largest proportion of individuals in present-day cohorts have connections to the Igbo and Kongo groups consistent with previous studies (22, 122).

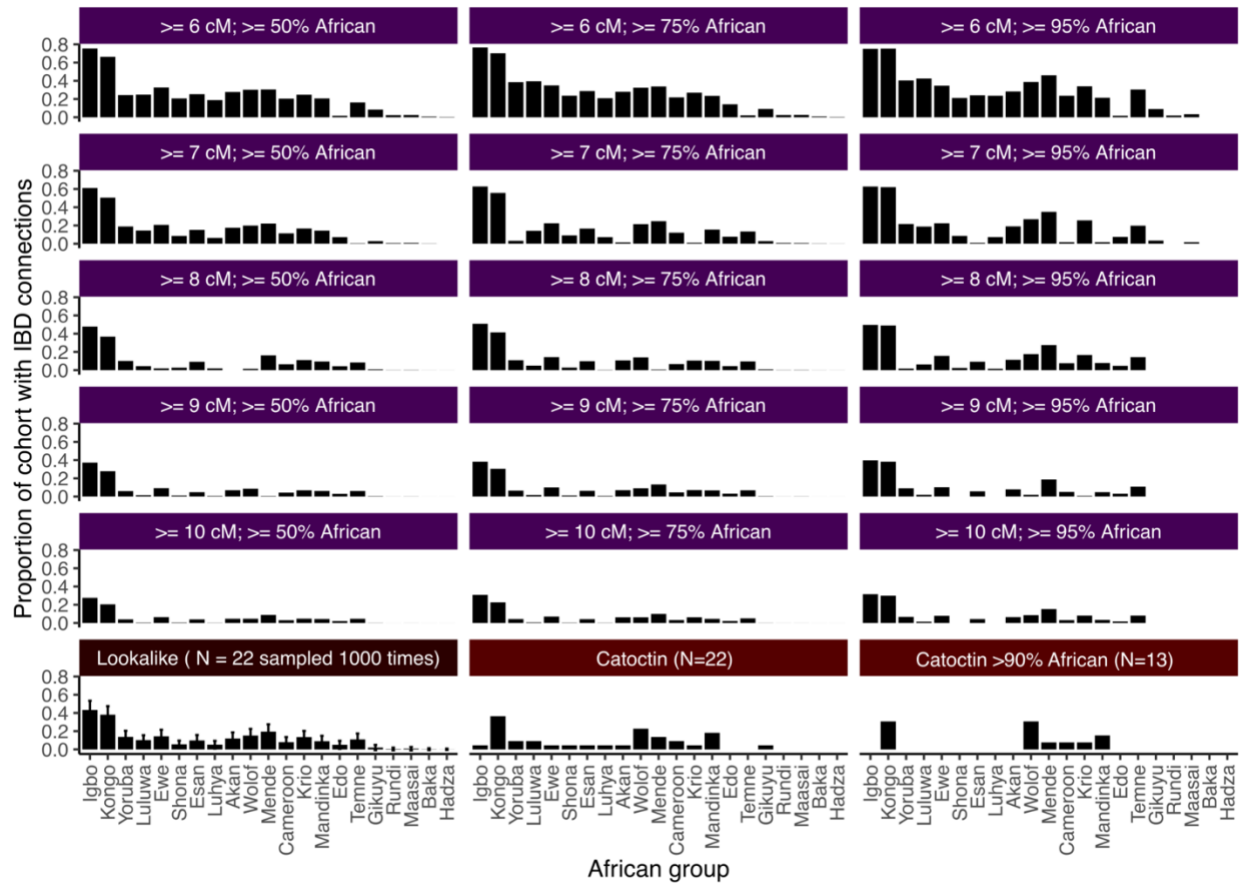


Fig. S5.3. The proportion of individuals with connections to specific African groups across all tested cohorts. The lookalike panel demonstrates the mean proportion of African group connections of 22 members of the US Sub-Saharan African ancestry cohort, sampled 1000 times, whose African Ancestry and minimum cM thresholds mimic those of the Catocin cohort.

To test if the distribution of African connections seen in Catocin is significantly enriched for specific African groups, we calculated the number of times the count of individuals with connections to each African group connection was matched both between Catocin and the lookalike dataset across 1000 iterations. From this analysis, the most striking difference between the distributions is the underrepresentation of connections to the Igbo group in Catocin individuals ($p < 0.001$; Table S5.3). That is to say, the distribution of Igbo connections seen in the

Catoctin cohort (just a single connection) was observed 0 times across all subsampling analyses. Though the Catoctin group shows enrichment for the Mandinka, Kongo, and Wolof groups, it is not until the Catoctin cohort is subset to >90% African ancestry that these groups are significantly enriched.

5

Records from the transatlantic slave trade indicate that the majority of enslaved Africans brought to Maryland embarked from Senegambia and West Central Africa (*I*) (Table S9). Comparing these records to connections to African groups provides support that at least a portion of the Catoctin individuals had recent African ancestors brought to the US from Senegambia (where Wolof
10 ancestors would have disembarked from) and West Central Africa (where Kongo ancestors would have disembarked from). It is more likely that the Catoctin individuals with more African ancestry and less European admixture were those with the recent ancestors embarking from the central and northwestern coasts of Africa.

African Group	Catoctin (N=22)		Catoctin >90% African (N=13)	
	<i>p higher rep</i>	<i>p lower rep</i>	<i>p higher rep</i>	<i>p lower rep</i>
Akan	0.958	0.231	0.777	0.578
Baka	1	0.964	1	0.991
Cameroon	0.571	0.743	0.256	0.945
Edo	1	0.284	1	0.535
Esan	0.909	0.337	0.681	0.718
Ewe	0.969	0.149	0.845	0.481
Gikuyu	0.404	0.902	0.183	0.993
Hadza	1	0.98	1	0.988
Igbo	1	<0.0001	0.998	0.009
Kongo	0.659	0.517	0.079	0.971
Krio	0.961	0.168	0.879	0.437
Luhya	0.729	0.671	0.441	0.933
Luluwa	0.735	0.592	0.269	0.961
Maasai	1	0.837	1	0.892
Mandinka	0.112	0.968	0.008	1
Mende	0.838	0.364	0.523	0.731
Rundi	1	0.89	1	0.968
Shona	1	0.24	1	0.577
Temne	1	0.067	1	0.174
Wolof	0.213	0.917	0.027	0.992
Yoruba	0.838	0.376	0.509	0.802

Table S5.3. Significant over- and under-representation of African groups that Catoctin

(N=22) and Catoctin > 90% African ancestry (N=13) connected to. *p higher* represents the

proportion of times the present-day lookalike cohort had the exact same number or fewer number

5 of individuals with connections to each African group over 1000 iterations (lower values

correspond to higher representation in Catoctin) ; proportions less than <0.05 are bolded *p lower*

represents the proportion of times the present-day lookalike cohort had the exact same number or

greater number of individuals with connections to each African group over 1000 iterations (lower values correspond to lower representation in Catocin); proportions less than <0.05 are bolded.

5 **Supplementary Text S6. A method for inferring relationships and pedigrees when individuals have low coverages**

S6.1 Likelihoods for low-coverage pedigrees

The most likely ways of connecting historical and present-day pedigrees were inferred using a composite
10 likelihood approach. First, pedigrees connecting present-day 23andMe research participants were inferred using the software Bonsai (Jewett et al, 2021). We then considered all plausible ways of connecting the most recent common ancestral node in each present-day pedigree to a node on the historical pedigree (Fig. S6.1). All possible points of connection on the historical pedigree were considered, assuming outbred pedigrees, and a broad range of possible connection degrees, d , covering the range of realistic historical-to-
15 present-day connecting lineage degrees.

For each possible point of connection and degree, d , we computed the composite likelihood, L_A , of the arrangement, A , as

$$L_A = \prod_{i,j} \hat{L}_{i,j}^{g,c} L_{i,j}^a, \quad (\text{Eq. 6.1})$$

20 Where $L_{i,j}^a = f(a_i - a_j | R_{i,j})$ is the probability density function of the difference in ages a_i and a_j of individuals i and j and $L_{i,j}^{g,c} = Pr(I_{i,j} | R_{i,j}, c)$ is the probability of the observed IBD $I_{i,j}$ between individuals i and j , given that their pairwise relationship is $R_{i,j}$ and given that the genotypes of one of the individuals were obtained from sequencing data with coverage c . $\hat{L}_{i,j}^{g,c}$ is the composite likelihood approximation of $L_{i,j}^{g,c}$ given by

25

$$\hat{L}_{i,j}^{g,c} = Pr(N_{i,j} | R_{i,j}, c) Pr(T_{i,j} | R_{i,j}, c), \quad (\text{Eq. 6.2})$$

where $N_{i,j}$ is the number of segments observed between individuals i and j and $T_{i,j}$ is the total length of IBD observed between individuals i and j . When computing the approximation $\hat{L}_{i,j}^g =$
5 $Pr(N_{i,j} | R_{i,j}) Pr(T_{i,j} | R_{i,j})$, we used the analytical formulas for $Pr(N_{i,j} | R_{i,j})$ and $Pr(T_{i,j} | R_{i,j})$ derived by Huff et al (119), but we corrected these formulas to account for the fact that the genomic data for the historical individuals was low coverage, as described in section S6.2. The pairwise age likelihoods were computed using distributions trained with 23andMe research participant data as described in Jewett et al (43). Age distributions were extended to arbitrarily distant relationships as follows: denote a relationship
10 between i and j by $R_{i,j} = (u, d, n)$ using the notation of Ko and Nielsen (124). Here, u is the number of meioses between i and their common ancestor with j , d is the number of meioses between j and their common ancestor with i , and n is the number of common ancestors of i and j . If $E[\Delta a_{p,c}]$ and $var(\Delta a_{p,c})$ are the empirically observed mean and variance of the difference in age between a parent and child, then the age difference distribution between a pair, i and j , with relationship $R_{i,j}$ is modeled as a Gaussian
15 random variable with mean $(u - d)E[\Delta a_{p,c}]$ and variance $(u + d)var(\Delta a_{p,c})$.

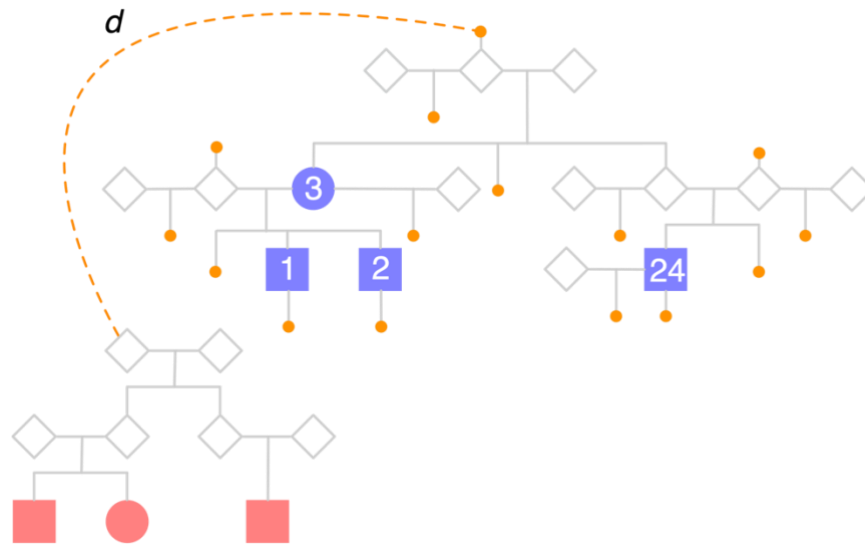


Fig S6.1: Determining the most likely way of connecting a present-day and historical pedigree. Genotyped individuals in the present-day pedigree are shaded in red. Genotyped individuals in the historical pedigree are shaded in purple. The lineage connecting the present-day and historical pedigrees is shown as a dashed orange line. All locations where this lineage can attach to the historical pedigree are shown as small orange dots. The degree of the lineage is denoted as d . We connected the present-day and historical pedigrees through each possible attachment point and a range of values for d . The composite likelihood (Equation SE6.1) was computed for each connection point and value of d .

S6.2: Correcting IBD probabilities for low coverage data

Here, we derive the probabilities $Pr(N_{i,j} | R_{i,j}, c)$ and c of the number and total length of segments shared between a pair of individuals i and j when the genotypes of one individual were obtained from low coverage
5 imputed sequencing data with coverage c .

Low coverage imputed data introduces both false negative and false positive segments. False negative segments arise because missing genotypes or genotyping errors occur within true IBD (or identical-by-state) segments, causing them to be missed by an IBD detection algorithm. For low coverage imputed data,

false positive segments arise largely due to imputation, which can cause two regions to be identical-by-state over a region that is longer than the minimum threshold set by the IBD detection algorithm. Thus, when considering IBD called on genotypes inferred from imputed low coverage data, we must jointly model the IBD arising from Mendelian inheritance, as well as missing and spurious IBD arising from the low coverage
5 data.

Huff et al (119) derived a formula for $Pr(N_{i,j} | R_{i,j})$ for the case in which the observed IBD $I_{i,j}$ between individuals i and j was the true IBD without false positive or false negative segments and they derived a joint likelihood for the total number of segments together with the set of segment lengths, allowing for a
10 given false positive segment rate and mean false positive segment length. In contrast to the approach by Huff et al, we don't consider individual segment lengths, which can be noisy in the case of low coverage DNA. Thus, we do not include a term in the genetic likelihood for the probability of all observed segment lengths, and instead consider the total IBD length, which may be more robust to IBD inference errors such as the fragmentation of segments.

15 We take the alternate approach of incorporating the false negative rates into the formulas for $Pr(N_{i,j} | R_{i,j})$ and $Pr(T_{i,j} | R_{i,j}, c)$ directly. We assume that the false positive rate based on coverage is small and only exerts a significant influence on the likelihood of a pairwise relationship when the two individuals are truly unrelated. This assumption is reasonably well justified by the low observed average false positive rate of <
20 0.2 false positive segments per pair, shown in Fig. S6.4A. Using this assumption, we derive one set of formulas for $Pr(N_{i,j} | R_{i,j}, c)$ and $Pr(T_{i,j} | R_{i,j}, c)$ for the case in which $R_{i,j}$ denotes an unrelated pair and we derive a separate set of formulas for $Pr(N_{i,j} | R_{i,j}, c)$ and $Pr(T_{i,j} | R_{i,j}, c)$ for the case in which $R_{i,j}$ denotes a pair of truly related individuals. For the case in which i and j are unrelated, the influence of low coverage on the distributions of $N_{i,j}$ and $T_{i,j}$ comes solely from false positive segments arising from the

imputation process. For the case in which i and j are related, the influence of low coverage on the distributions of $N_{i,j}$ and $T_{i,j}$ comes solely from false negative segments arising from genotype error.

S6.3: The distributions of $N_{i,j}$ and $T_{i,j}$ for related individuals

5 In deriving formulas for $Pr(N_{i,j} | R_{i,j}, c)$ and $Pr(T_{i,j} | R_{i,j}, c)$, we will use two results that we demonstrate in Section S6.4. First, the false negative rate for a segment of length l – i.e., the probability that a segment of true length l is unobserved when one individual has coverage c – can be modeled as

$$Pr(O | c, l) \approx 1 - e^{-qcl}, \quad (\text{Eq. 6.3})$$

10

for some constant q . Second, we demonstrate that the average observed length l_o of a segment with true length l_t is approximately given by

$$E_c[l_o | l_t] \approx (1 - e^{-pc})(l_t - \tau) + \tau, \quad (\text{Eq. 6.4})$$

15

for some constant p , where τ is the minimum threshold length for an IBD segment to be called. Using Equations (Eq. 6.3) and (Eq. 6.4), we now derive $Pr(N_{i,j} | R_{i,j}, c)$ and $Pr(T_{i,j} | R_{i,j}, c)$.

As in Huff et al (119), we model the number $N_{i,j}$ of segments shared between individuals i and j as a Poisson random variable. The parameter $\lambda_{R,c}$ of the Poisson distribution is equal to the expected number of segments shared between individuals of relationship $R = (u, d, n)$ when one of the individuals has coverage c . The expected number of segments when the coverage is c is equal to the expected number of segments at full coverage, times the probability that a segment is observed between two people with relationship $R_{i,j}$ when the coverage of one of them is c . Let O_R be the event that a given segment is observed between a pair of individuals with relationship R . Then we have

20

$$\lambda_{R,c} = \lambda_R Pr(O_R | R, c),$$

where Huff et al (119) showed that

5

$$\lambda_R \approx n \frac{((u+d)r + 22)}{2^{(u+d)-1}} e^{-(u+d)\tau/100}, \quad (\text{Eq. 6.5})$$

where $r \approx 35.5$ is the expected number of meioses in the autosomal genome, 22 is the number of autosomes, and τ is the threshold in cM below which IBD segments are not considered. The probability

10 $Pr(O_R | R, c)$ can be obtained by integrating over the true length of the segment:

$$\begin{aligned} Pr(O_R | R, c) &= \int_{l=0}^{\infty} Pr(O | l, c) f_R(l) dl \\ &= \int_{l=0}^{\infty} (1 - e^{-qc l}) 1_{l \geq \tau} f_R(l) dl \\ &= \int_{l=\tau}^{\infty} (1 - e^{-qc l}) \frac{(u+d)}{100} e^{-(u+d)l/100} dl \\ &= e^{-(u+d)\tau/100} - \int_{l=\tau}^{\infty} \frac{(u+d)}{100} e^{-(\frac{u+d}{100} + qc)l} dl \\ &= e^{-(u+d)\tau/100} - \frac{(u+d)}{100} \left(\frac{u+d}{100} + qc \right)^{-1} e^{-(\frac{u+d}{100} + qc)\tau}, \end{aligned} \quad (\text{Eq. 6.6})$$

15

20

where the density $f_R(l)$ comes from Huff et al (119) and $1_{l \geq \tau}$ is the indicator function taking the value 1 whenever $l \geq \tau$ and 0, otherwise. In the second equality, we have assumed that the observed segment is not longer than the true segment because we are only considering false negative rates. Thus, the true segment must be longer than τ to be observed.

We can check the formula for $Pr(O_R | R, c)$ by noting that as the coverage approaches infinity, the formula for $Pr(O_R | R, c)$ approaches $e^{-(u+d)\tau/100}$, which is the probability that the true segment has at least length τ . As the relationship $R = (u, d, n)$ becomes increasingly distant – i.e., as $u + d$ goes to infinity – the formula for $Pr(O_R | R, c)$ approaches $e^{-(u+d)\tau/100}(1 - e^{-qc\tau})$, which is the probability that the true segment has length at least τ and that the segment of length τ is observed between the low coverage individuals, regardless of the relationship.

To find the expected total IBD length $T_{R,c}$ between two individuals separated by relationship $R = (u, d, n)$ when one individual is full coverage and the other individual has coverage c , let $\mu_{R,c}$ be the mean segment length observed between the two individuals. Then we can approximate $E[T_{R,c}]$ by the product of $\mu_{R,c}$ and the expected number of segments $\lambda_{R,c}$:

$$E[T_{R,c}] \approx \mu_{R,c} \lambda_{R,c}. \quad (\text{Eq. 6.7})$$

Using the relationship $E_c[l_o | l_t] \approx (1 - e^{-pc})(l_t - \tau) + \tau$ from Equation (Eq. 6.4) we find that

$$\begin{aligned} \mu_{R,c} &= (1 - e^{-pc})(E_R[L_t] - \tau) + \tau \\ &= (1 - e^{-pc})\left(\frac{100}{u+d} - \tau\right) + \tau, \end{aligned} \quad (\text{Eq. 6.8})$$

where the formula $E_R[L_t] = \frac{100}{u+d}$ comes from the result that segments between two individuals of relationship $R = (u, d, n)$ have expected length $\frac{100}{u+d}$ when expressed in centimorgans (119).

To derive an approximation of the variance of the observed total IBD $T_{R,c}$, we make the simplifying assumption that all variability in $T_{R,c}$ arises from the lengths of the true segments T_R . In other words, we

assume that $l_o \approx (1 - e^{-pc})(l_t - \tau) + \tau$, so that $T_{R,c} \approx (1 - e^{-pc})(T_R - N\tau) + N\tau$, where N is the number of segments. Thus, we have

$$\text{var}(T_{R,c}) \approx (1 - e^{-pc})^2 \text{var}(T_R). \quad (\text{Eq. 6.9})$$

5

An approximate formula for $\text{var}(T_R)$ was derived in Jewett et al (43). For two related individuals with relationship R , we model the total IBD as a Gaussian random variable with mean $E[T_{R,c}]$ and variance $\text{var}(T_{R,c})$.

S6.4: The distributions of $N_{i,j}$ and $T_{i,j}$ for unrelated individuals

10 When individuals i and j are unrelated, we assume that the observed segments between them arise entirely from false positive segments due to imputation or other sources. In Section S6.5, we demonstrate that the expected number of false positive segments when one individual is high coverage and the other individual has low coverage c can be modeled as

$$15 \quad E[N_{i,j}] \approx \gamma_1/c \quad (\text{Eq. 6.10})$$

for some constant γ_1 , and we show that $\text{var}[N_{i,j}] \approx \gamma_1/c$ for the same constant γ_1 , suggesting that $N_{i,j}$ is reasonably modeled by a Poisson distribution. Thus, for two unrelated individuals i and j , we model $N_{i,j}$ as a Poisson random variable with parameter γ_1/c .

20

In Section S6.5, we also demonstrate that the expected total false positive IBD between two unrelated individuals has mean

$$E[T_{i,j}] \approx \gamma_2/c \quad (\text{Eq. 6.11})$$

and that the variance is approximately

$$\text{var}(T_{i,j}) \approx \gamma_3/c \quad (\text{Eq. 6.12})$$

5

for constants γ_2 and γ_3 . Thus, for two unrelated individuals, we model the total IBD $T_{i,j}$ as a Gaussian random variable with mean γ_2/c and variance γ_3/c .

Section S6.5: False positive and false negative rates of IBD

Using the same data set described in Supplementary Text S3, we computed true-positive, false-positive, 10 true-negative, and false-negative rates as a function of coverage, as well as the relationship between the true and observed segment lengths.

In Equation (Eq. 6.6), we used a simple and integrable expression for the per-segment true positive rate 15 $Pr(O | c, l)$ as a function of the true segment length and coverage. The form of this equation comes from the empirical true-positive rate as a function of coverage (Fig. S6.2). By minimizing the mean squared error

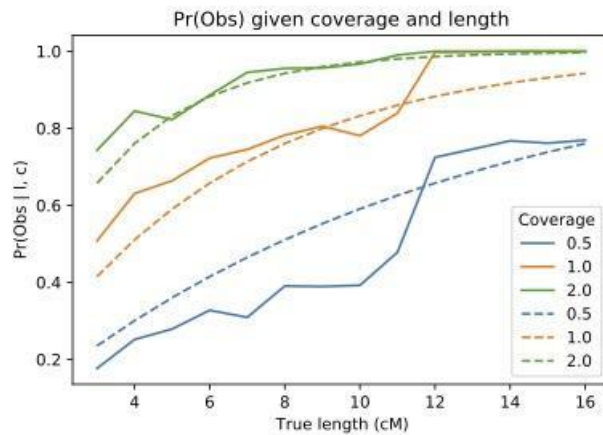


Fig S6.2: True-positive rate of observing an IBD segment of a given length for several different coverages. Solid curves show empirical values. Dashed curves show fitted values using Equation (SE6.3).

between the empirical and fitted values in Equation (Eq. 6.3), we found that a value of $q = 0.179$ provided a good fit to the empirical data.

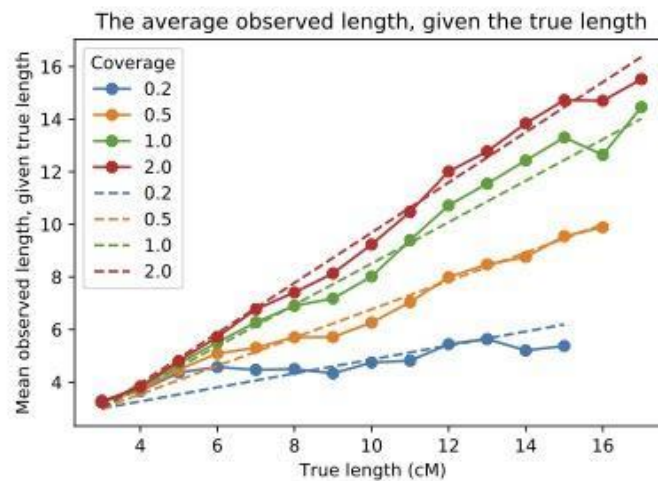


Fig S6.3: Empirically-observed mean segment lengths as a function of the true segment length. Shown by coverage. Solid curves correspond to the empirical data. Dashed curves are the fitted values.

The form of Equation (Eq. 6.4) also comes from the empirical data. We observed that the mean observed length was approximately linear in the true length, with a constant that depended on the coverage. We found that the relationship in Equation (Eq. 6.4) captured the empirical relationship. By minimizing the mean squared error between the predicted and empirical mean observed lengths using Equation (Eq. 6.4), we
5 found that a value of $p = 1.79$ provided a good fit for the data (Fig. S6.3).

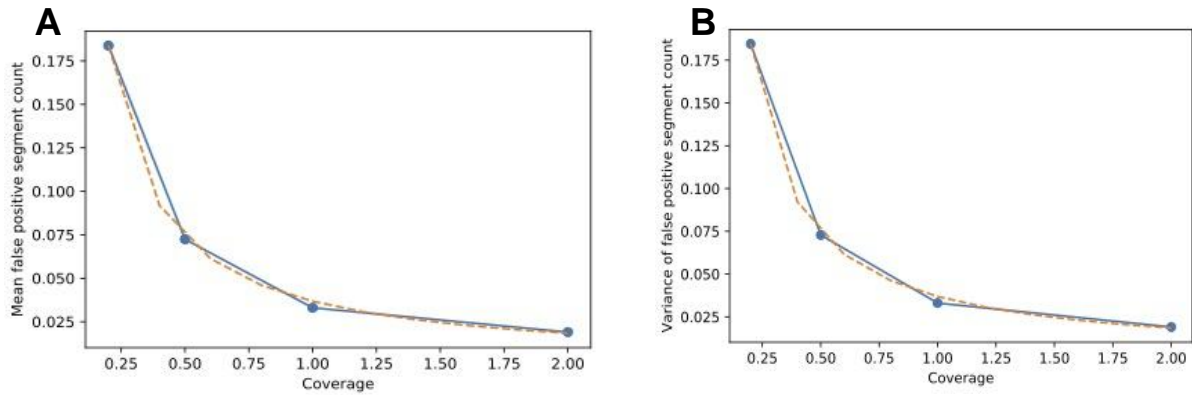


Figure S6.4: Mean (A) and variance (B) in the number of false-positive segments observed between a pair of individuals as a function of the coverage of one of the individuals. Solid curves show empirical values, dashed curves minimize the mean squared error between empirical and fitted values. Both fitted curves are $0.036/c$.

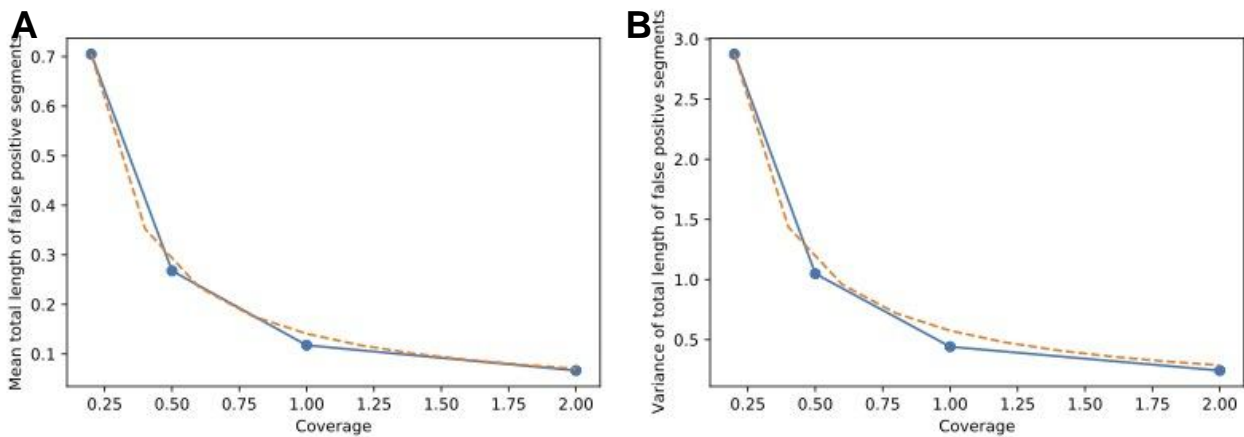


Figure S6.5: Mean (A) and variance (B) in the total observed length of false-positive IBD between a pair of individuals, one of whom has coverage c . Solid curves indicate empirical values and dashed curves indicate fitted values.

We found that the number of observed false-positive segments as a function of coverage is well modeled by Equation (Eq. 6.10). Furthermore, from Figs. S6.4A and S6.4B, it can be seen that both the mean and variance are well approximated by γ_1/c , for the same value of $\gamma_1 = 0.036$. Thus, the expected number of false-positive segments can be modeled by a Poisson random variable with parameter γ_1/c .

Finally, the expected total length of false-positive IBD is well approximated by Equation (Eq. 6.11) and its variance is well approximated by Equation (Eq. 6.12), as can be seen in Figs S6.5A and S6.5B. By minimizing the mean squared error between the empirical and predicted values, we found that values of $\gamma_2 = 0.141$ and $\gamma_3 = 0.575$ provided a good fit.

5 ***S6.6: Pedigree inference***

Present-day pedigrees were inferred among individuals sharing at least a threshold amount of IBD with a historical individual in a given Catocin family. The threshold was the one chosen to minimize false positive IBD sharing, given in Section S3.2 in Supplementary Text S3. Present-day family sets were first created by grouping individuals who shared at least 200 cM of IBD with at least one other person in the group. The individual in each group with the highest average sharing to all other group members was chosen as the focal individual and the pedigree of the group was inferred using Bonsai (43). We then identified the common ancestor of the present-day pedigree and exhaustively considered all positions to which the lineage extending from the common ancestor could attach in the historical family's pedigree (Fig. S6.1). Positions were either lineages extending up from an unsampled individual or down from any individual and the possible partners of the individual. Lineages extending directly down from individuals in Fig. S6.1 are short-hand for lineages extending down from the individual and a partner.

For each position in the historical family, we considered lineages extending from the most recent common ancestor of the present-day pedigree to the position on the historical pedigree. We considered degrees ranging from 0 to 15 degrees, where 0 degrees indicated that the common ancestor of the present-day pedigree was an individual in the historical pedigree. The likelihood of the attachment point and degree was computed using Equation (Eq. 6.1).

The probability that a present-day pedigree attached to a given position on the historical pedigree was computed by assuming that the prior probability of attachment to any point on the historical family's

pedigree was uniform across all attachment points. Let D denote the data (IBD segments and ages) and let A denote the arrangement (degree of relationship and point of connection on the historical pedigree). Then we have

$$5 \quad Pr(A | D) = \frac{Pr(D|A)Pr(A)}{Pr(D)} \propto Pr(D|A) = L_A \quad (\text{Eq. 6.13})$$

where L_A is given in Equation (Eq. 6.1). Thus $Pr(A | D)$ can be computed by normalizing the values of L_A . When computing Equation (Eq. 6.1), we took the age of each historical individual to be their estimated age at burial, plus the time difference between the present year and their date of burial (Table S1).

10 The probability of any pedigree connecting through a given arrangement A is then

$$Pr(A) = \sum_{ped} Pr(A|D_{ped})Pr(ped) = \frac{1}{P} \sum_{ped} Pr(A | D_{ped}), \quad (\text{Eq. 6.14})$$

15 where ped indicates a particular present-day pedigree, D_{ped} denotes the data for the pedigree, and P is the number of present-day pedigrees. The probabilities $Pr(A)$ are the values shown in Fig. 6 in the main text.

S6.7: Ancestries of pedigrees

The ancestry of each present-day individual connected to a historical family was computed using the Ancestry Composition local ancestry inference method (42) and global ancestry proportions were aggregated with a confidence threshold of 51%. We computed the admixture fraction f_p^A for population p on lineage A as

$$f_p^A = \sum_{i=1}^{N_A} Pr(p | i) Pr(i) = \frac{1}{N_A} \sum_{i=1}^{N_A} Pr(p | i), \quad (\text{Eq. 6.15})$$

where N_A is the number of individuals whose most likely connection is through arrangement A and $Pr(p|i)$ is the admixture fraction for population p of individual i . These are the values in the pie charts shown in Fig. 6.

5 ***S6.8: Resampling test of present-day pedigrees with American ancestry related to Catoctin Family A***

The ancestries of pedigrees attached through different lineages is informative about the accuracy of the method for connecting present-day and historical pedigrees through different arrangements. Ancestry information was not used when computing the probabilities of arrangements and can therefore be used as a
10 check. In particular, for Family A, we know that individual f must have had a significant amount Indigenous American ancestry because their children, 1 and 2, have Indigenous American ancestry that is not observed in their parent, 3 (Fig. 2). We do not observe high proportions of Indigenous American ancestry in individual 24 in Catoctin Family A.

15 This high Indigenous American ancestry in individual f allows us to test whether connections of present-day pedigrees to Family A through individual f are consistent with their known recent Indigenous American ancestry. In particular, we expect that individual f has collateral relatives shared through their Indigenous American ancestors. We expect that such relatives would be enriched among the set of pedigrees related to Catoctin Family A that have particularly high Indigenous American ancestry.

20 We considered present-day pedigrees whose sampled individuals had at least twice as much inferred Indigenous American ancestry as African ancestry. Of 149 present-day pedigrees that satisfied this criterion, all but one pedigree had a most likely connection through individual f . To evaluate whether this result was statistically significant, we considered the mean of the 149 log likelihoods of connecting through
25 individual f . We repeatedly sampled 149 pedigrees from among the set of pedigrees with

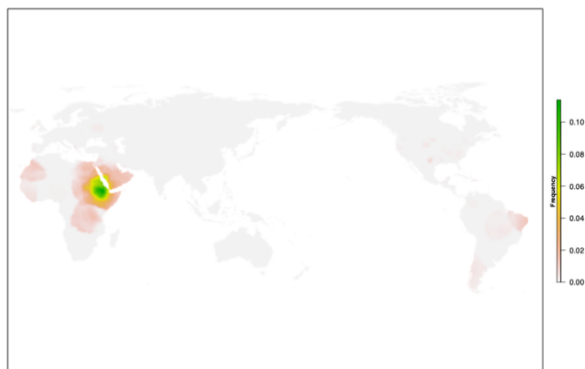
This is the author's version of the work. It is posted here by permission of the AAAS for personal use, not for redistribution. The definitive version was published in Science on August 4th, 2023, DOI: [10.1126/science.ade4995](https://doi.org/10.1126/science.ade4995).

$f_{American}/f_{African} < 2$ and computed the mean log likelihood of attaching through individual f . Out of 1,000,000 samples of 149 such pedigrees, we found that no sample had a mean log likelihood as high as the mean log likelihood in the high American ancestry pedigrees. This yields a p-value for the resampling test of $p < 10^{-6}$.

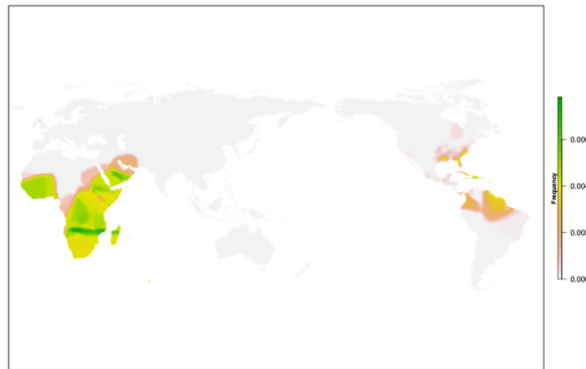
Supplementary Figs

Y-Haplogroup Distribution

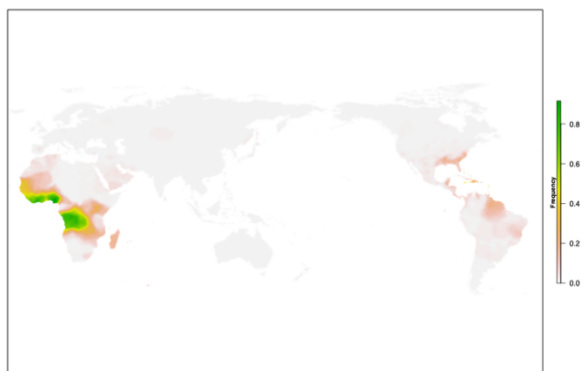
Haplogroup A1b1
Burial 4



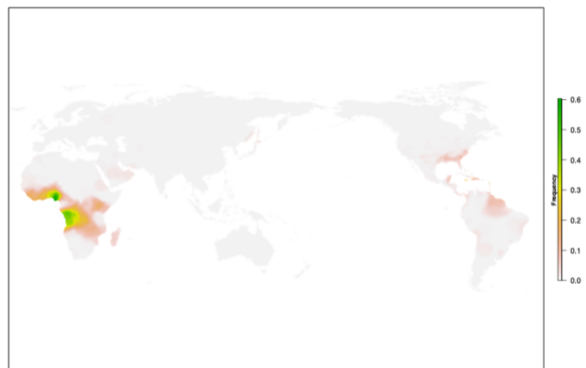
Haplogroup E1b1a1a1a
Burial 8 (E1b1a1a1a) & Burial 15 (E1b1a1a1a2a1a)



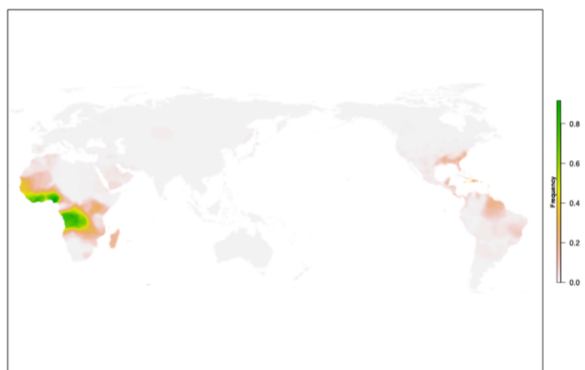
Haplogroup E1b1a1
Burial 26 (E1b1a1~)



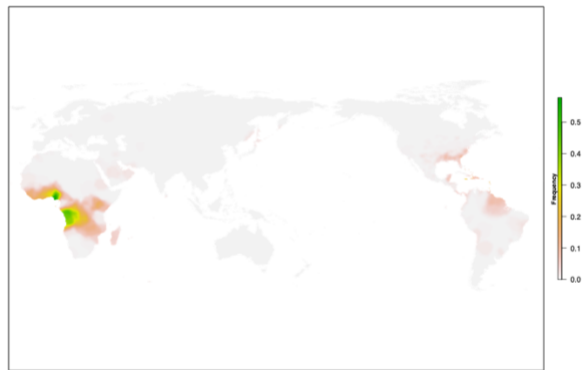
Haplogroup E1b1a1a1c1a
Burials 17 & 24 (Both E1b1a1a1c1a1)



Haplogroup E1b1a1a1 (E-M180)
Burial 5

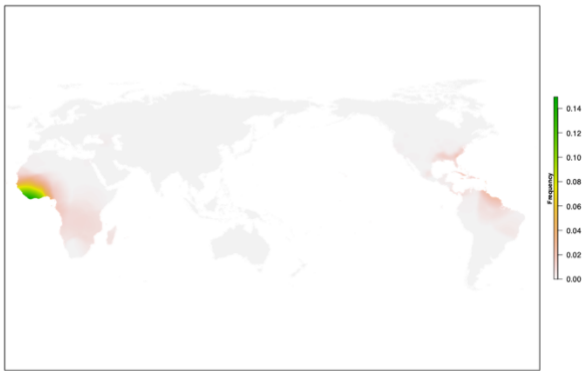


Haplogroup E1b1a1a1c1a1
Burial 22 (E1b1a1a1c1a1a3a1d1)



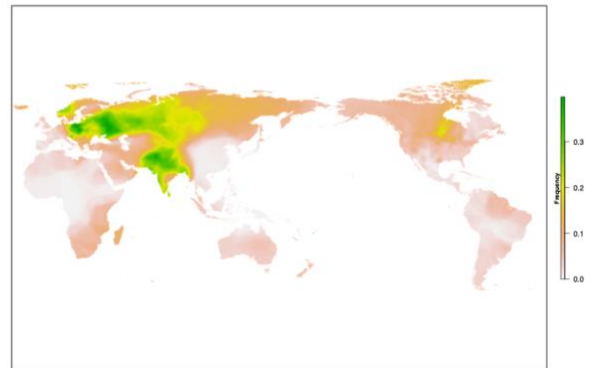
Haplogroup E1b1a1a1c1b

Burials 1, 2 (E1b1a1a1a1c1b1) & 6 (E1b1a1a1a1c1b2a)



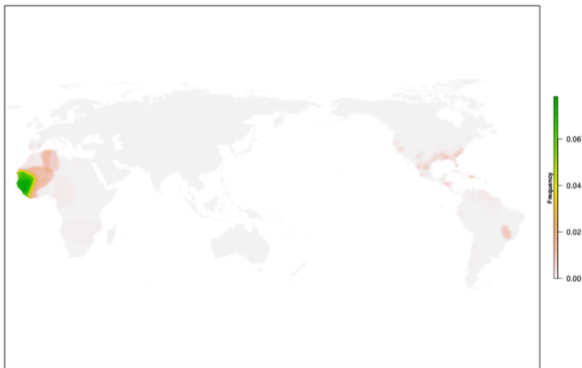
Haplogroup R1a1a1

Burial 32



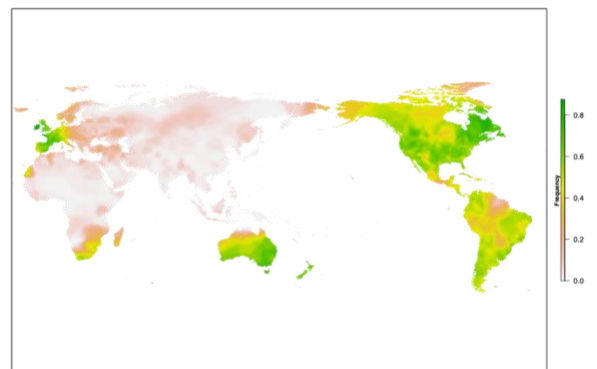
Haplogroup E1b1a1a1c2c

Burial 33



Haplogroup R1b1a

Burials 10 (R1b1a1b1a1a2c1a1h2a~) & 34 (R1b1a1a2a1a2c1)



Haplogroup E2b

Burial 13

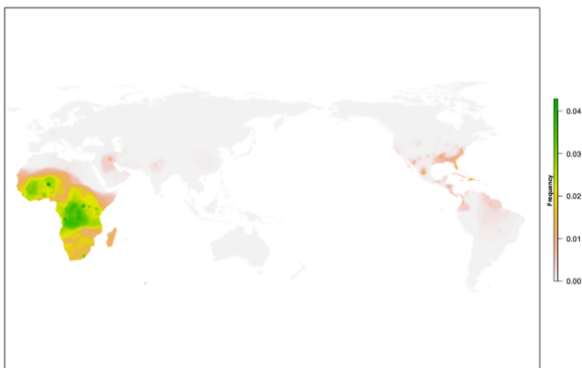
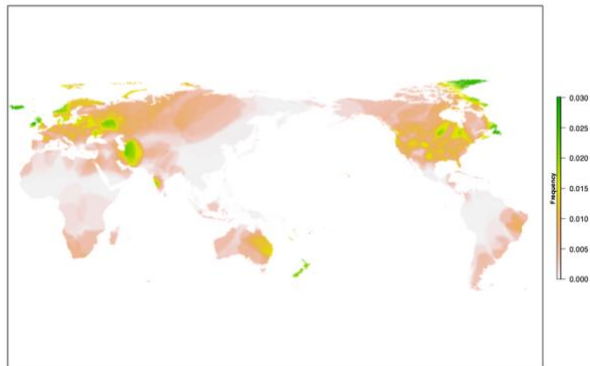


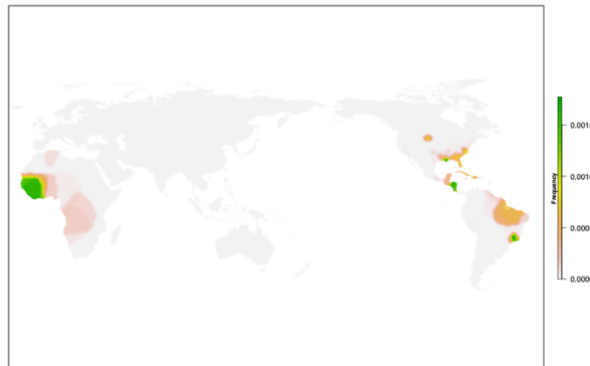
Fig. S1. Geographic distribution of the observed Y haplogroup frequencies in the 23andMe database using Kriging interpolation. For each haplogroup, the Catoctin individuals who have been assigned that haplogroup are indicated. In cases where the Catoctin individuals have been assigned a haplogroup that is a subclade of the displayed haplogroup, the full assigned haplogroup is reported in parentheses.

mt-Haplogroup Distributions

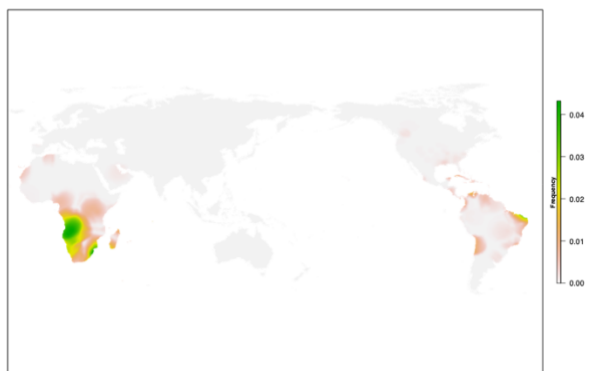
Haplogroup J1b1a
Burial 32 (J1b1a1a)



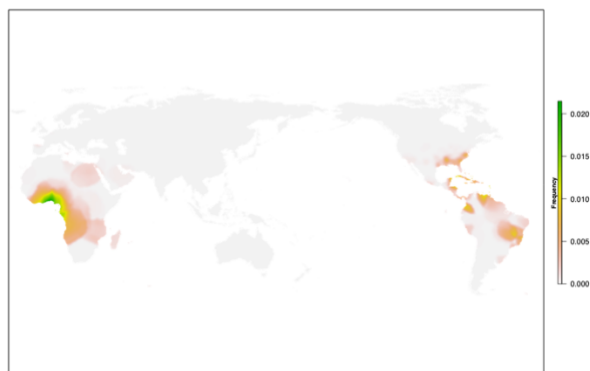
Haplogroup L2a1a1
Burial 6



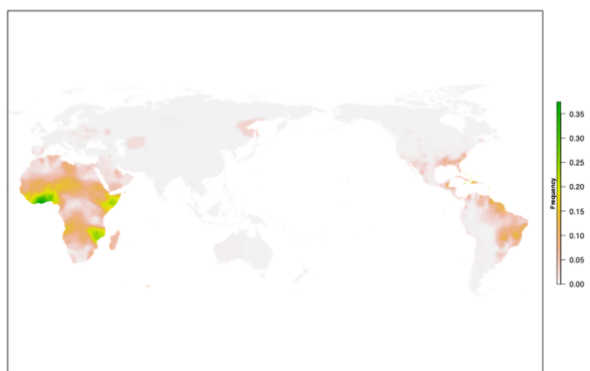
Haplogroup L0a1b1a
Burial 4



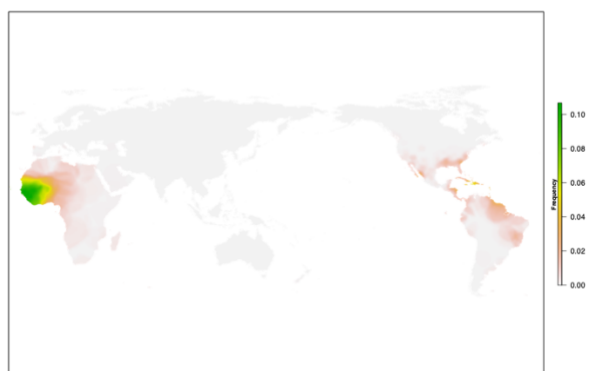
Haplogroup L2b1a3
Burials 11, 12, 13, & 28



Haplogroup L2a1
Burials 15, 18, 23 (all L2a1+143+16189 (16192)+@16309) &
33 (L2a1+143+@16309)

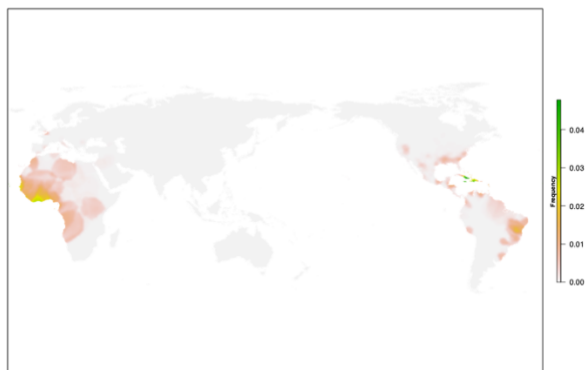


Haplogroup L2c
Burial 26



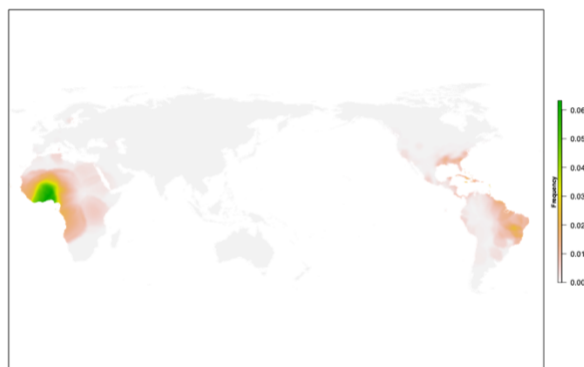
Haplogroup L3d1b3

Burial 22



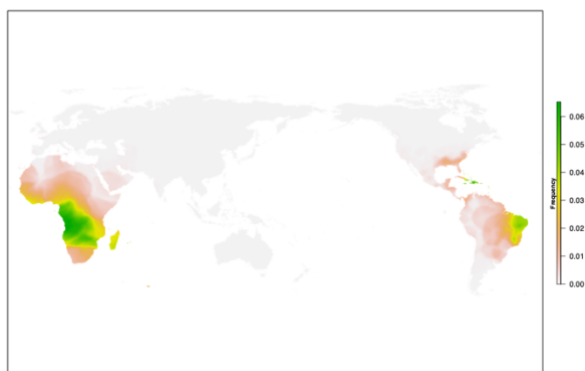
Haplogroup L3e2

Burials 17 & 19



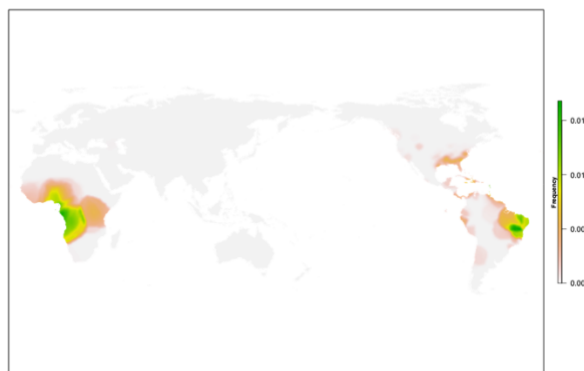
Haplogroup L3e1

Burials 5, 34, and 35



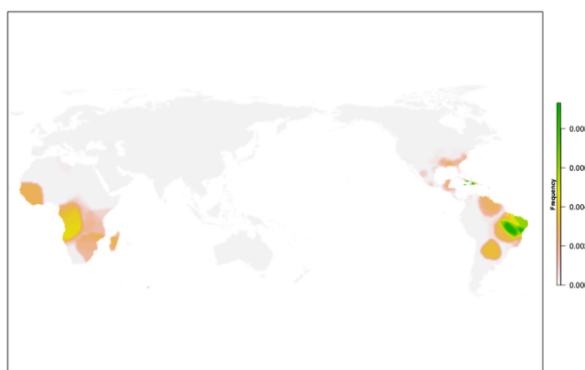
Haplogroup L3e2a1b1

Burials 1, 2, 3, 8 and 24



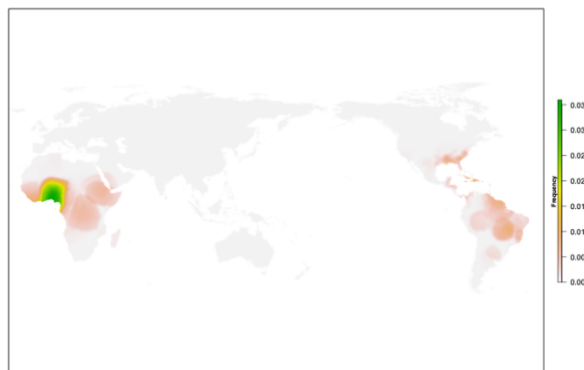
Haplogroup L3e1a1a

Burial 7



Haplogroup L3f1b1

Burial 9 (L3f1b1a)



Haplogroup L3f1b3
Burial 10



Haplogroup L4b2b1
Burial 14

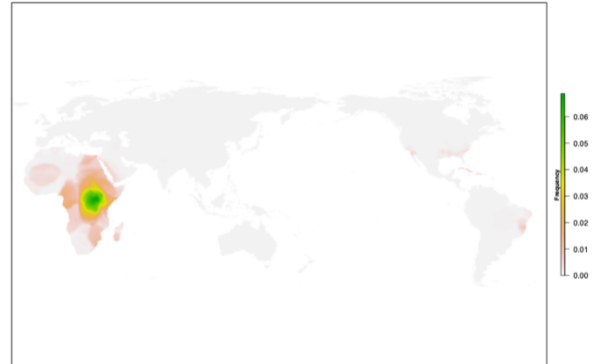


Fig. S2. Geographic distribution of the observed mt haplogroup frequencies in the 23andMe database using Kriging interpolation. For each haplogroup, the Catoctin individuals who have been assigned that haplogroup are indicated. In cases where the Catoctin individuals have been assigned a haplogroup that is a subclade of the displayed haplogroup, the full assigned haplogroup is reported in parentheses.

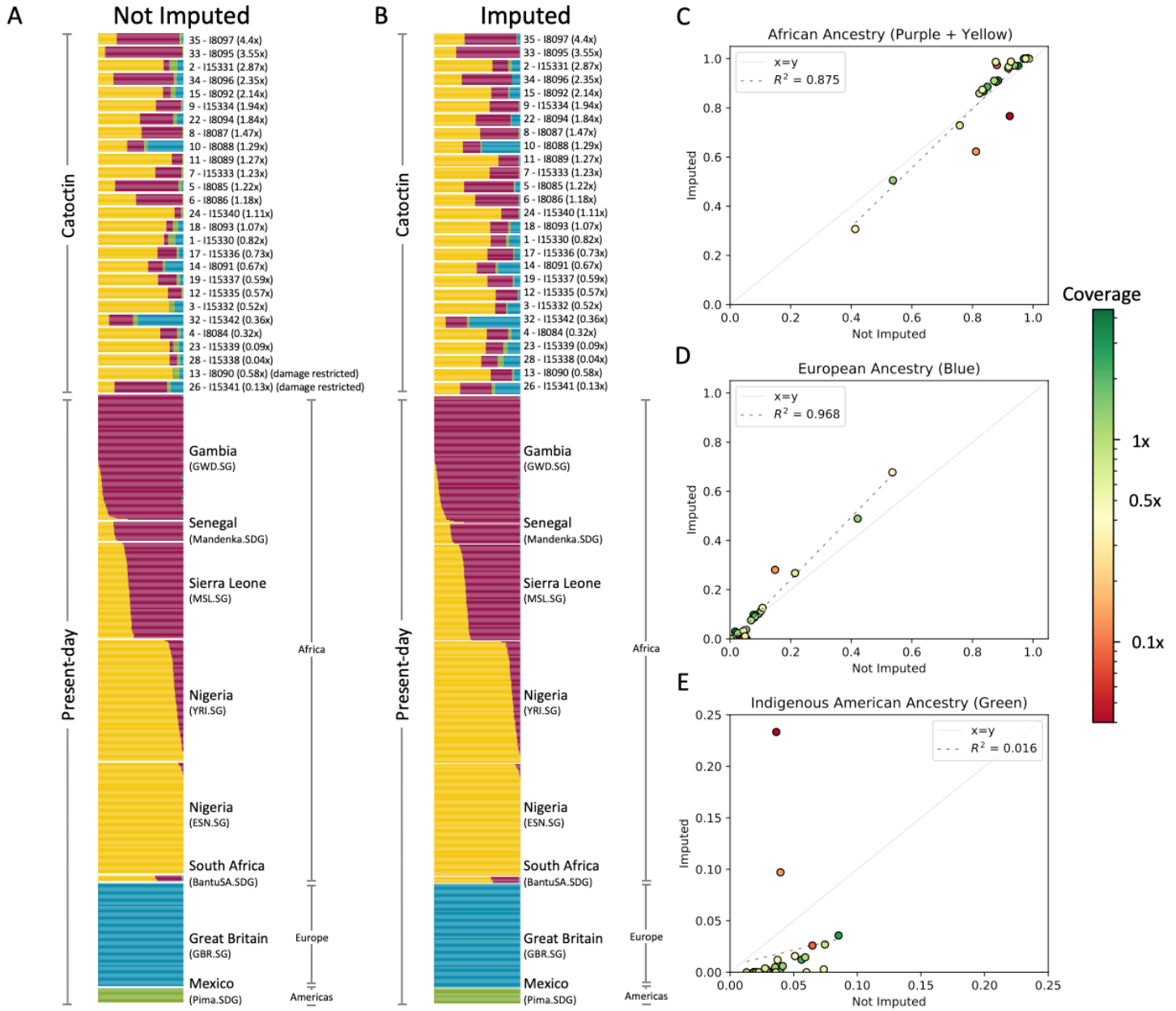


Fig. S3. ADMIXTURE analysis of 531 present-day individuals drawn from the public dataset from Africa (GWD.SG, Mandenka.SDG, MSL.SG, YRI.SG, ESN.SG and BantuSA.SDG), Europe (GBR.SD) and the Americas (Pima.SDG) and not imputed (a) or imputed (b) versions of the 27 Catocotin individuals with $K = 4$ ancestral components. The Catocotin individuals are ordered from highest to lowest coverage, placing the two individuals who are damage restricted in the non-imputed dataset last. Scatterplots demonstrate the difference in the amount of ancestry assigned to African (c), European (d) and Indigenous American (e) sources when calculated using the not imputed versus imputed datasets. The biggest deviations from a 1:1 ratio ($x=y$) occur among the lowest coverage individuals (shown in red) for all cases, particularly those with $<0.5x$ coverage.

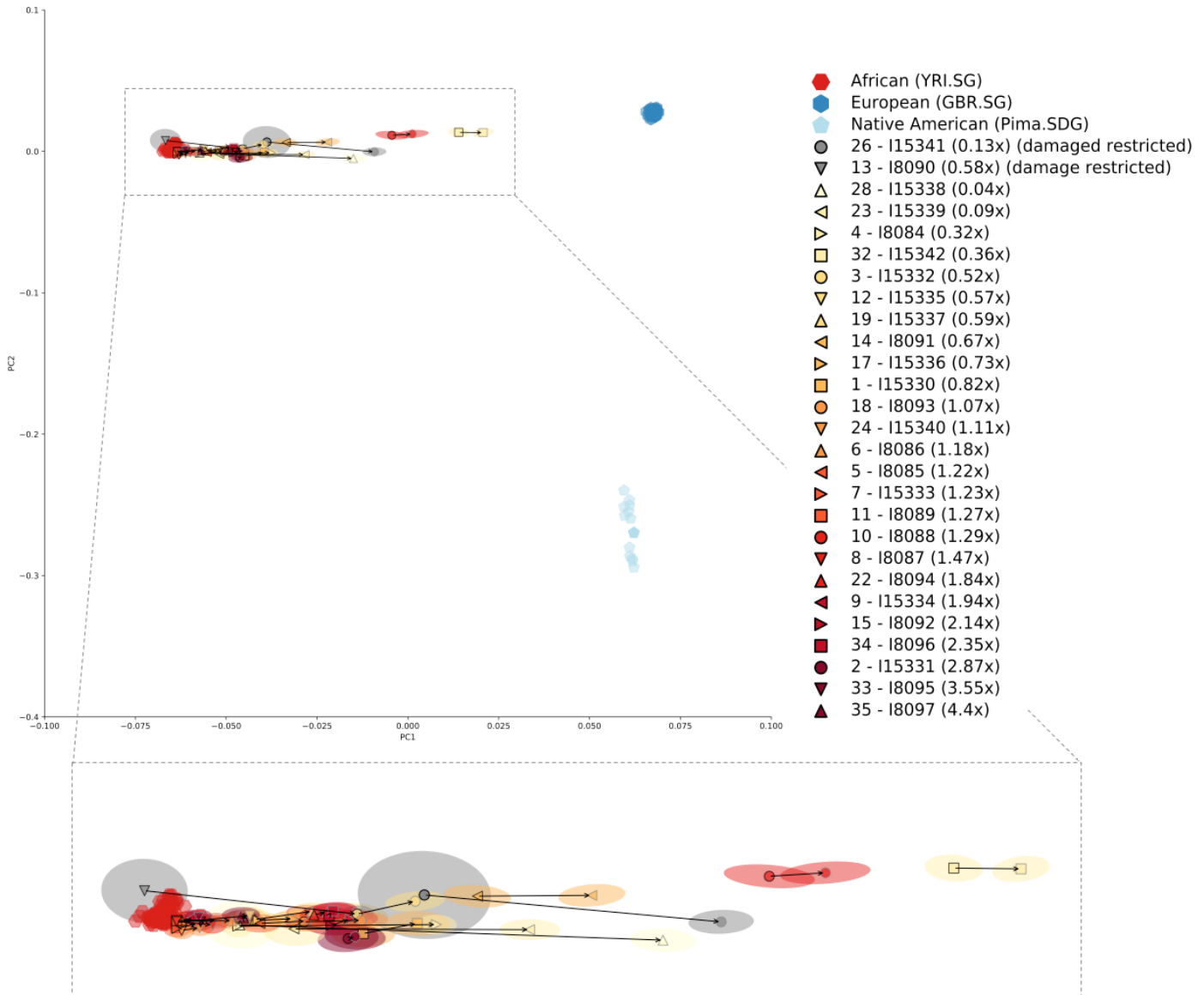


Fig. S4. African American Ancestry PCA. A principal component analysis of 213 present-day individuals from representative European (GBR.SG), African (YRI.SG) and Indigenous American (Pima.SDG) populations drawn from the public dataset. We projected the 27 Catocitin individuals onto the resulting PCA plot using non-imputed (black outline) and imputed (gray outline) versions of the Catocitin datasets. For each individual, a black arrow shows the change in position between the non-imputed and imputed versions of the data (pointing from the non-imputed data point towards the imputed data point). Ovals around each marker show the 95% confidence interval for the position of the marker. A zoomed-in view of the portion of the figure indicated with dotted lines is shown at the bottom of the figure. The position of the lowest

coverage and/or damage restricted Catoctin individuals changed the most dramatically between the non-imputed and imputed datasets.

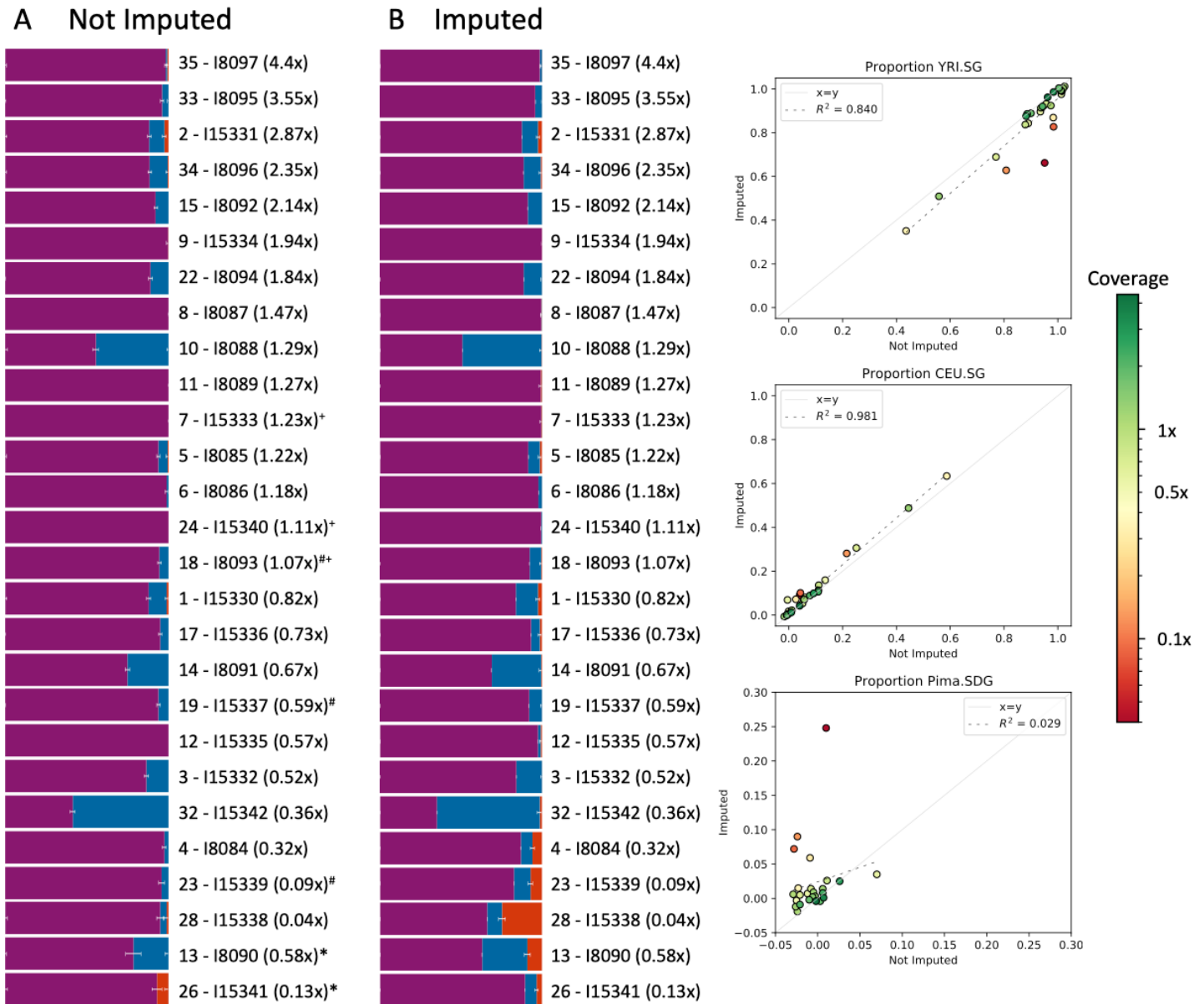


Fig. S5. qpADM estimates of African, European and Indigenous American Ancestry Proportions. The proportion of ancestry assigned to each Catoctin individual from representative African (YRI.SG), European (GBR.SG) and Indigenous American (Pima.SDG) populations drawn from the public dataset by the tool qpAdm using the not imputed (a) and imputed (b) datasets. Error bars indicate 1 standard error. Hash symbols (#) indicate models with p-values < 0.01 and plus signs (+) indicate models with ancestry proportion estimates that fall more than 3 standard errors outside the range of 0-1. Asterisks (*) indicate damage restricted data. In panels c-e, scatterplots demonstrate the difference in the amount of ancestry assigned to YRI.SG (c), CEU.SG (d) and Pima.SDG (e) sources when calculated using the not imputed versus imputed datasets. The biggest deviations from a 1:1 ratio ($x=y$) occur among the lowest coverage individuals (shown in red) for all cases, particularly those with < 0.5x coverage.

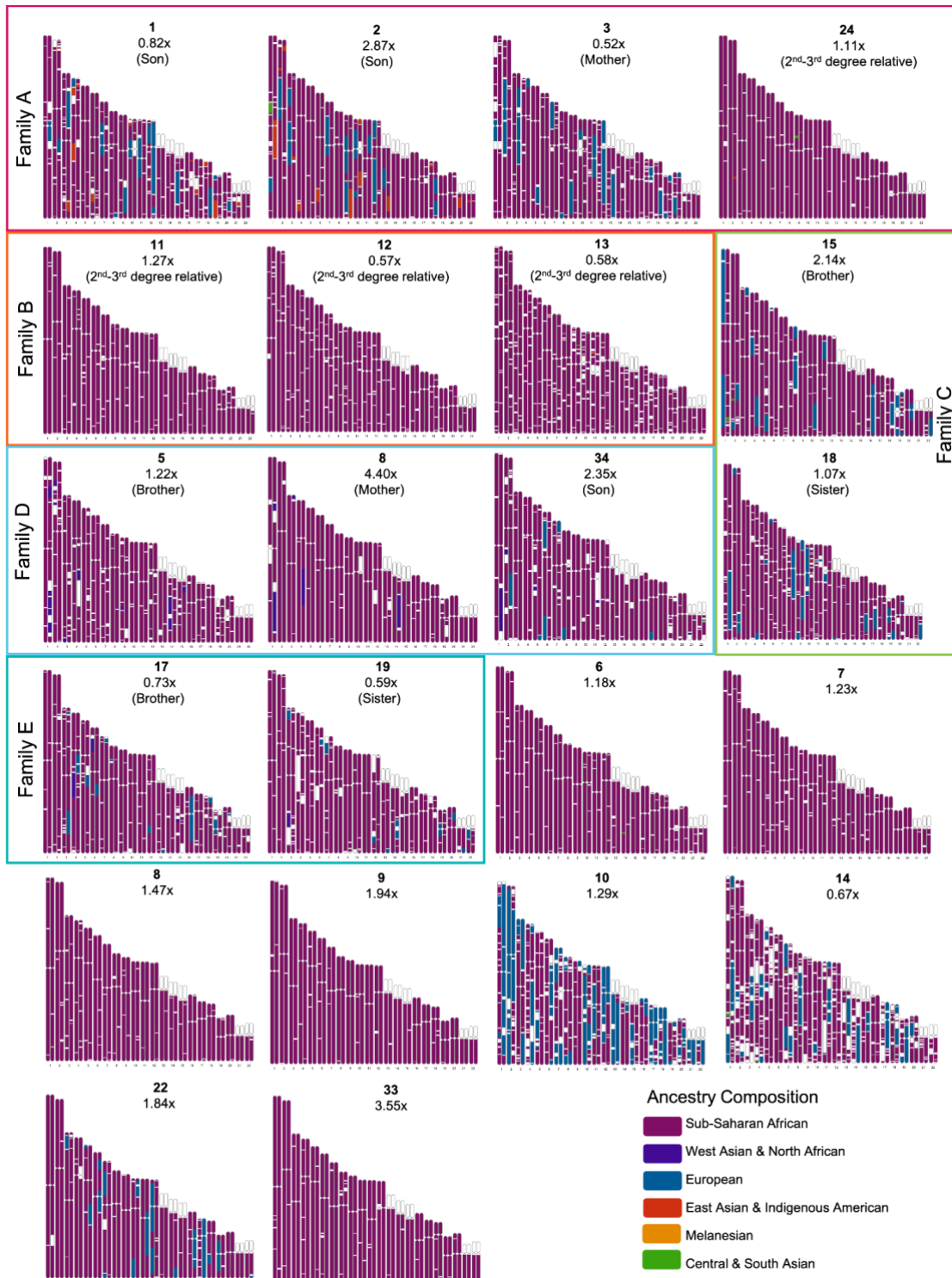


Fig. S6. Chromosome paintings showing the ancestry assigned to portions of the autosomal chromosomes for the 22 Catocytin individuals with >0.5x coverage. Catocytin individuals are grouped together into their assigned genetic families when possible. Across the genome, ancestry is assigned to one of six ancestry components defined using 23andMe reference populations: Sub-Saharan African (purple), West Asian & North African (dark blue), European (dark teal), East Asian & Indigenous American (red), Melanesian (orange), and Central & South Asian (green). Portions of the genome that could not be assigned to any of these components are shown in white.

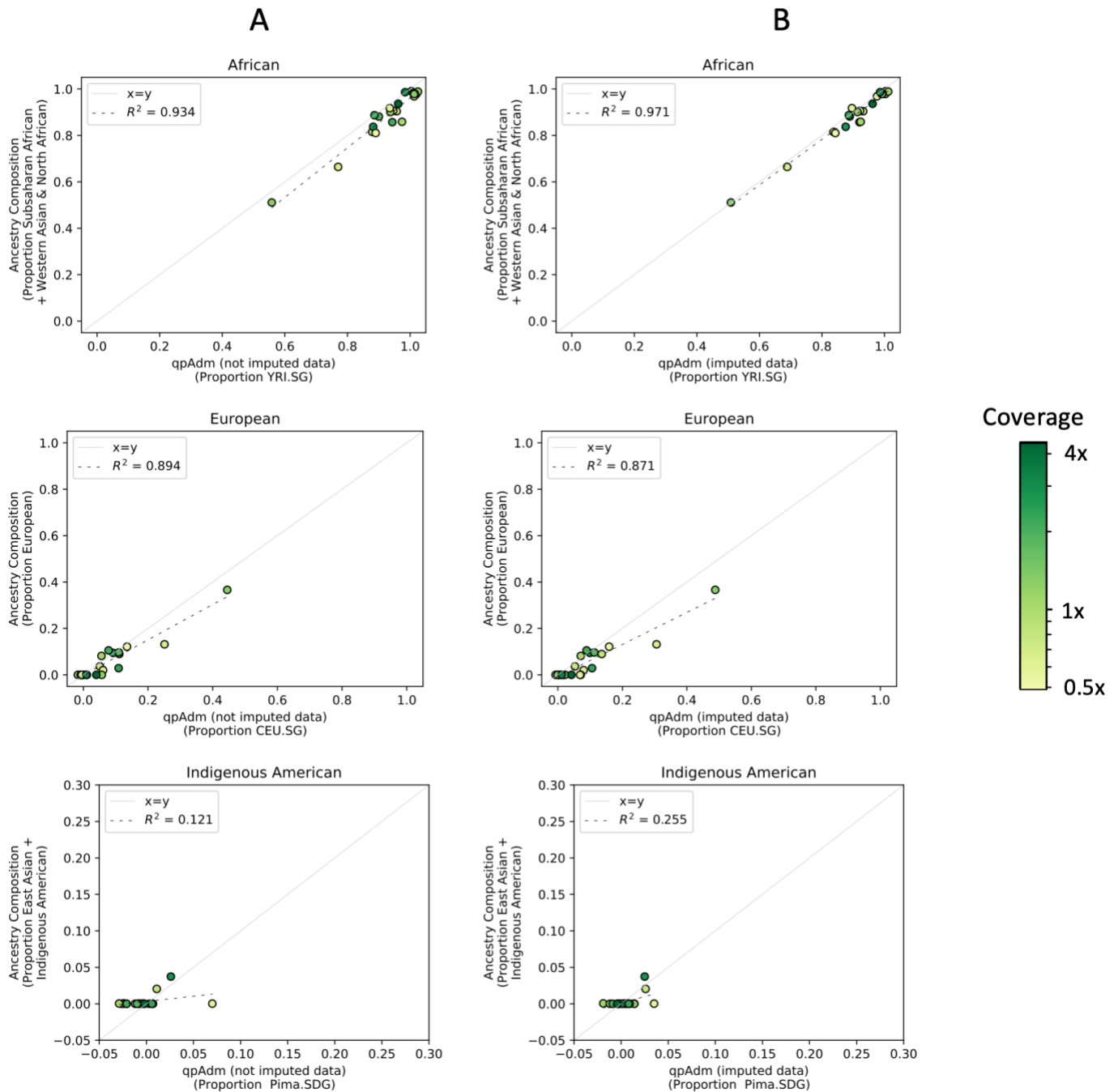


Fig. S7. Correlation between Ancestry Composition and qpAdm assignments. Plots showing the proportion of ancestry assigned to African (top), European (middle) and Indigenous American (bottom) sources by qpAdm (using the public dataset) and Ancestry Composition (using 23andMe reference populations) for each Catoclin individual (blue dots) with $>0.5x$ coverage when calculated using the not imputed (a) and imputed (b) datasets.

Distribution of Total IBD Detected

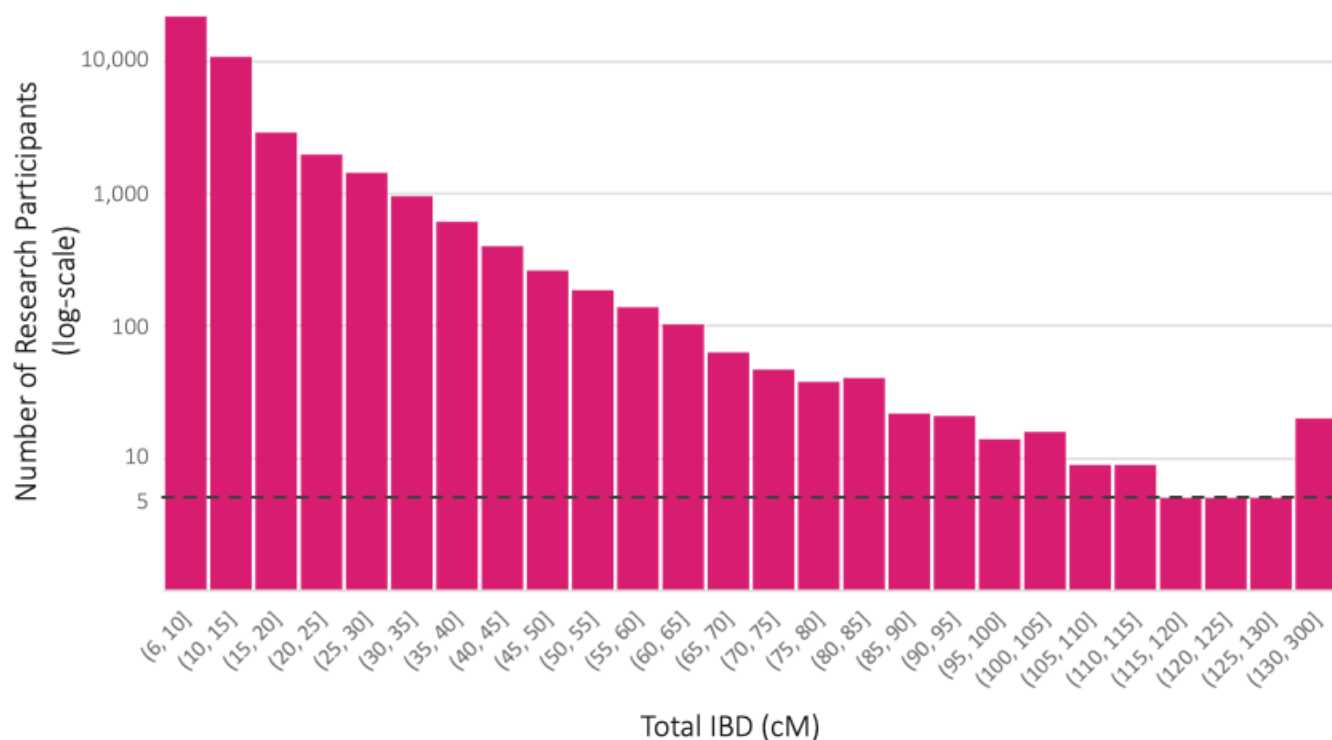
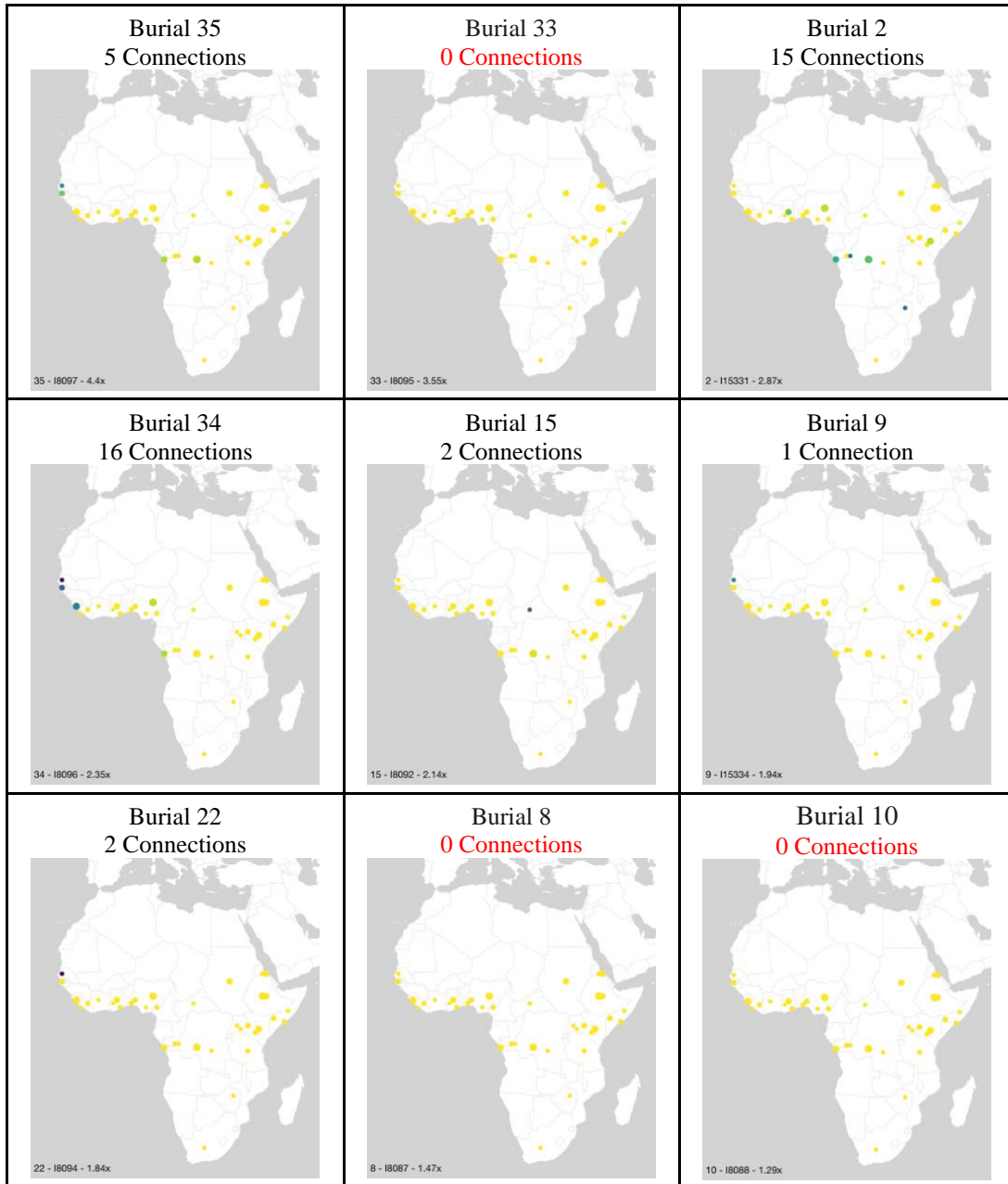
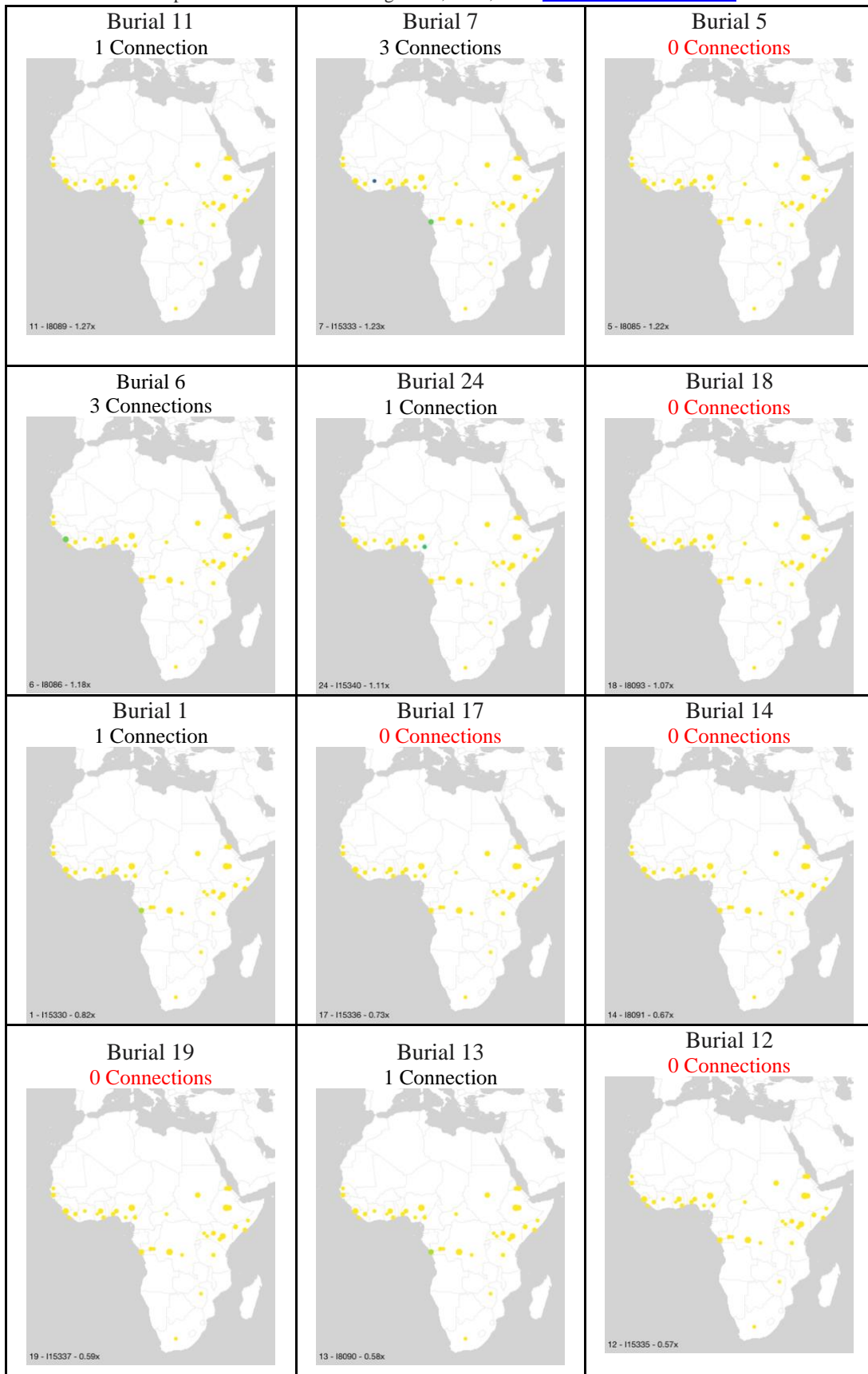


Fig. S8. Histogram of total IBD detected among 23andMe research participants who share IBD with one or more Catoctin individuals. For research participants who share IBD with multiple Catoctin individuals, the larger amount of total IBD is reported. Bin sizes were selected to include a minimum of 5 research participants.



Fig. S9. Histogram of total IBD shared with each Catoctin individual. Bins with ≤ 5 associated 23andMe research participants are reported as 5, indicated by the black, dotted horizontal line. A minimum segment length threshold was applied based on coverage using the following thresholds: $\geq 2x$: 6cM, $1-2x$: 9 cM, $0.5-1x$: 10 cM. Catoctin individuals with $< 1x$ coverage are labeled in red to indicate that these results should be interpreted with caution. The total number of connections shared with each Catoctin individual is indicated above each plot, using the same masking approach for bins with ≥ 5 connections.





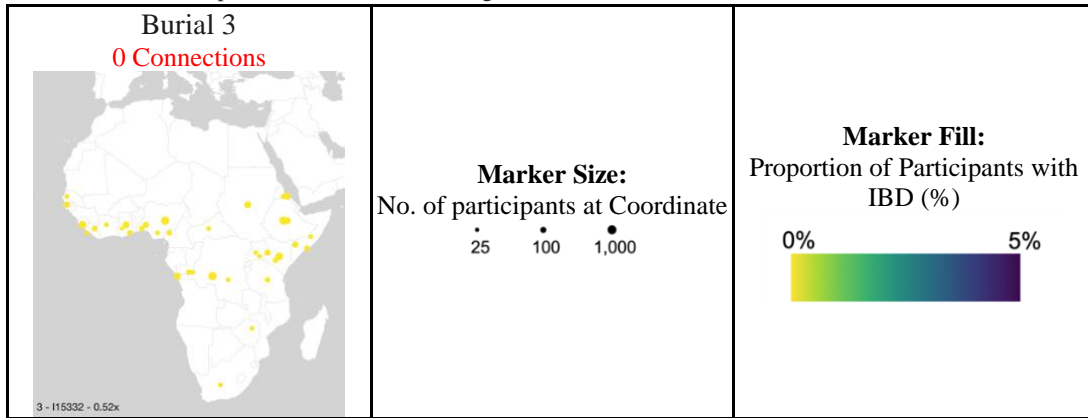
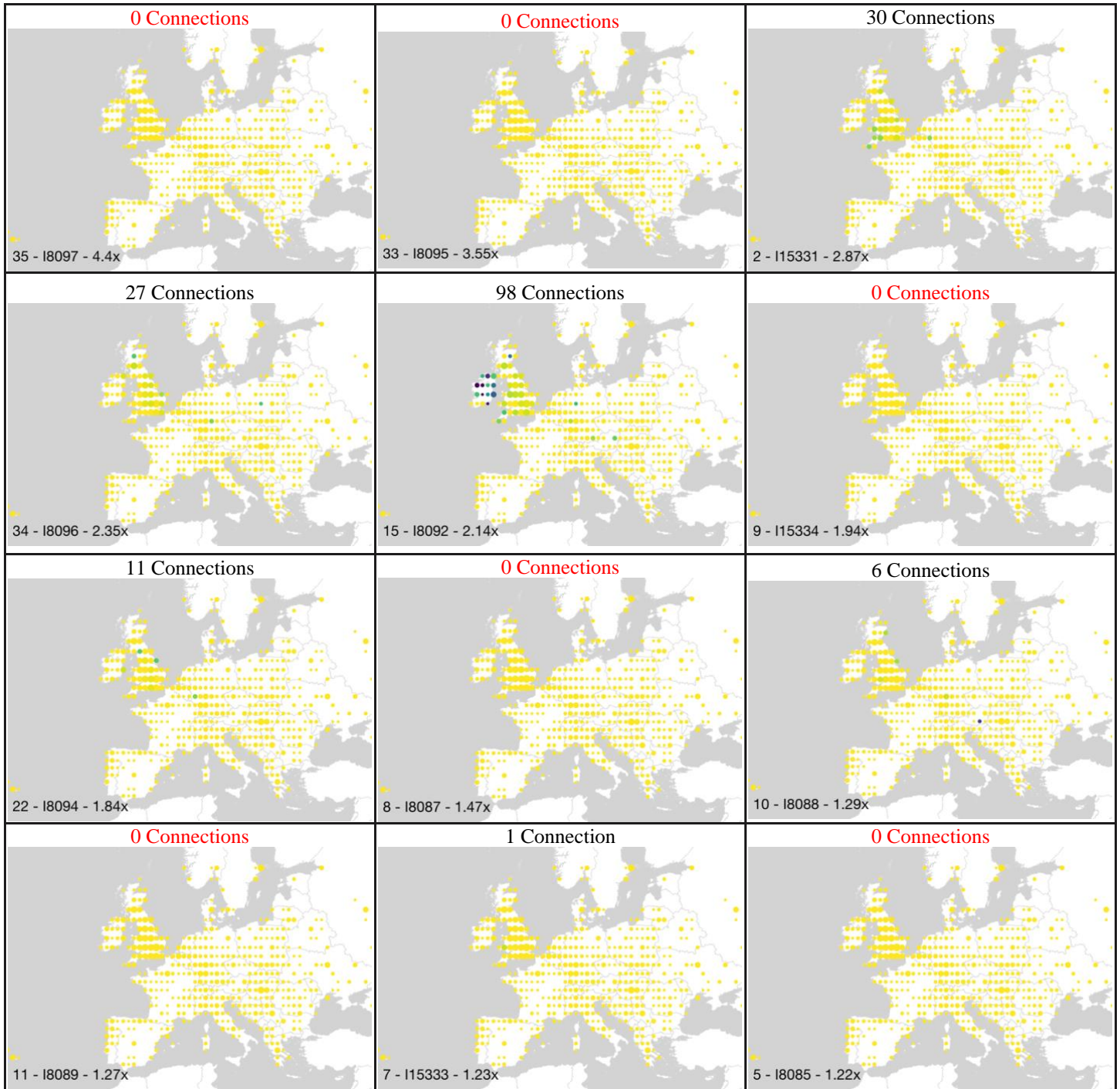


Fig. S10. Genetic connections to each of the Catoctin individuals among African participants. The proportion of 23andMe participants with $\geq 95\%$ Sub-Saharan African ancestry in Africa who share IBD with each Catoctin individual with $>0.5x$ coverage. Geographic coordinates are rounded to the nearest integer, and only coordinates that have at least 25 associated participants are shown. To further protect participant privacy, we randomly downsample to include results for only 80% of participants. The size of the marker corresponds to the number of participants associated with each site, while the color indicates the proportion of participants who share IBD with the Catoctin individuals. No participants share ≥ 30 cM of IBD with one or more Catoctin individuals, so no marker outlines are shown. The total number of IBD connections observed is reported above each image, when 0 connections are observed, this number is reported in red.



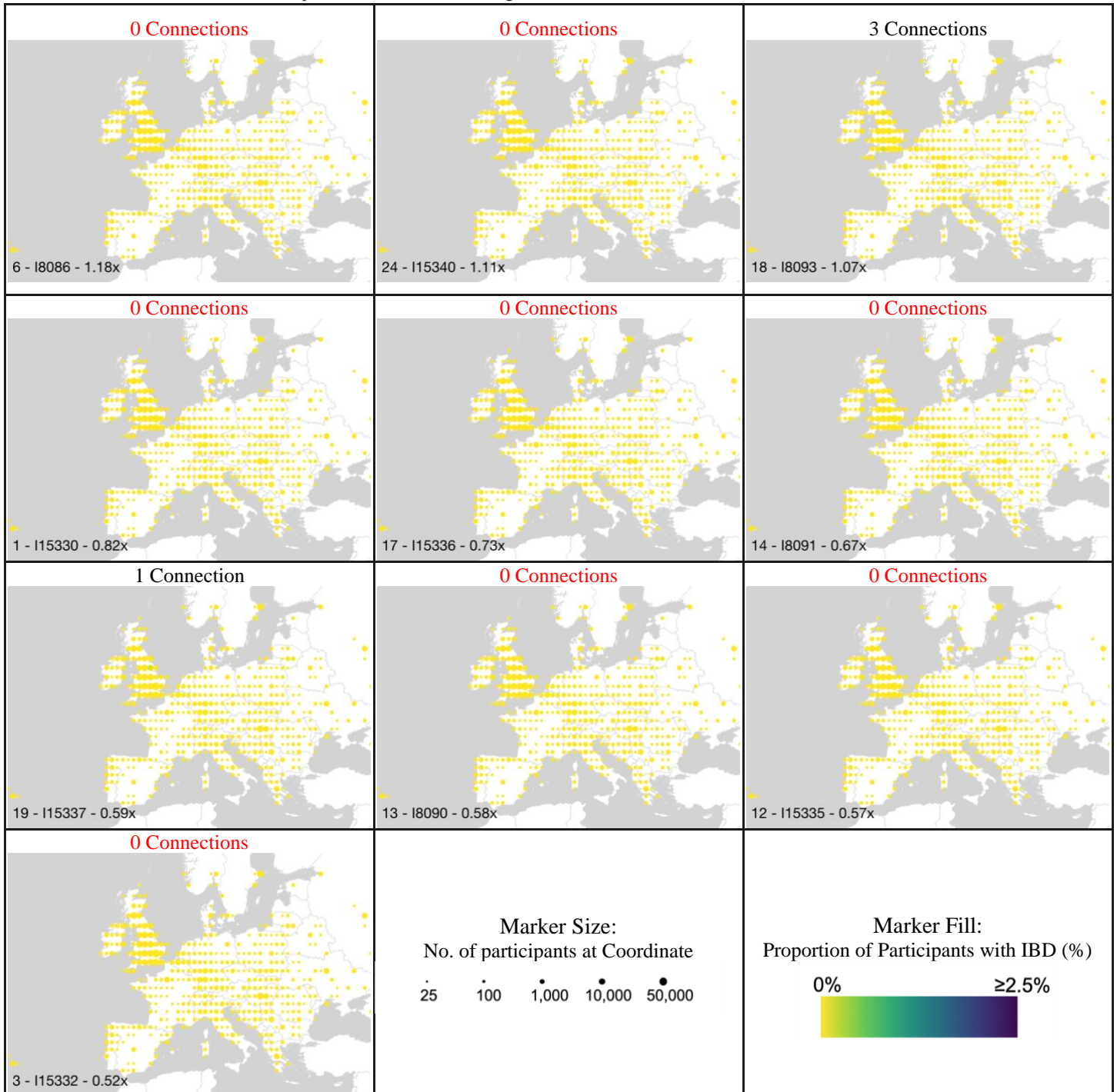
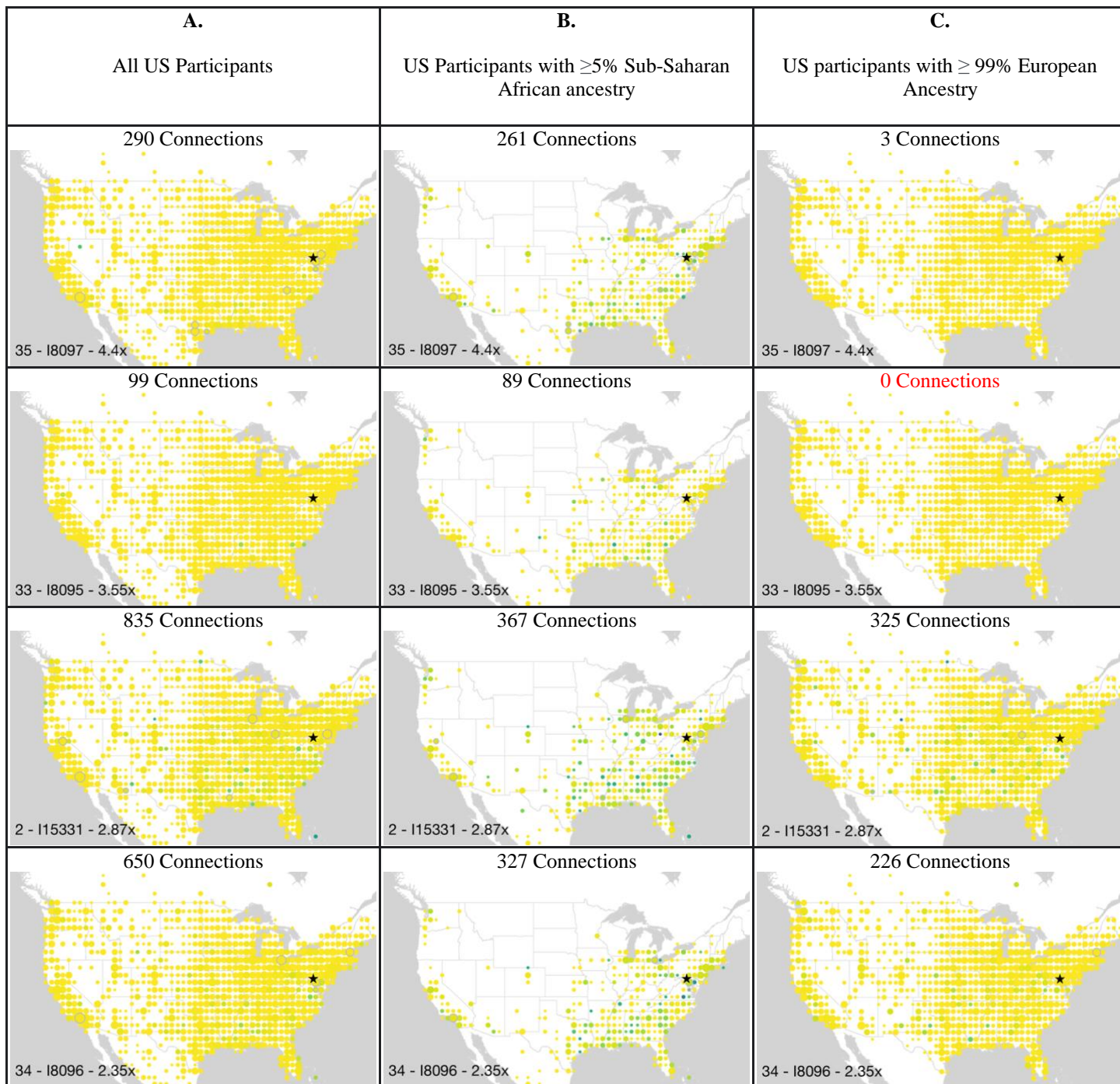
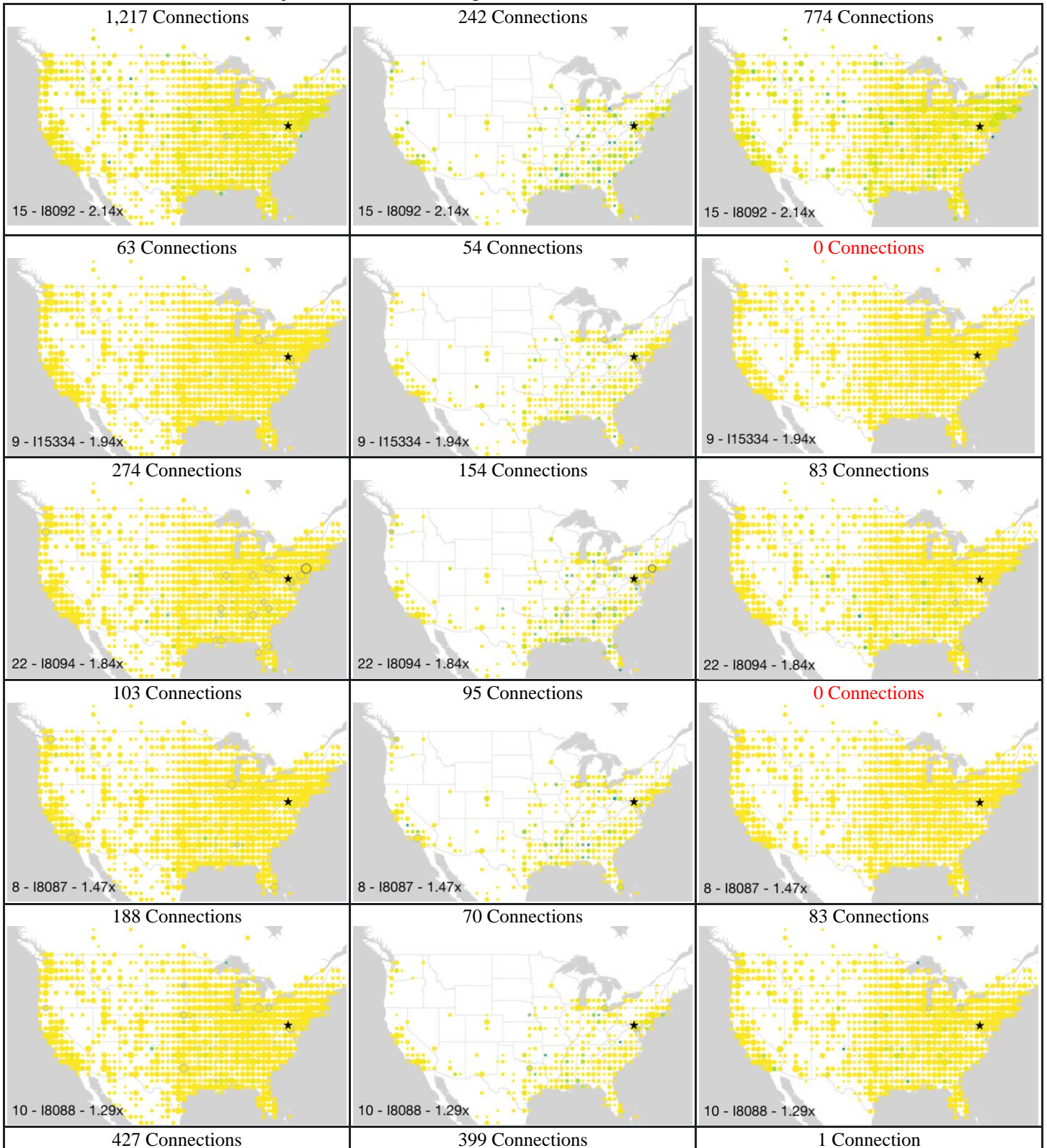
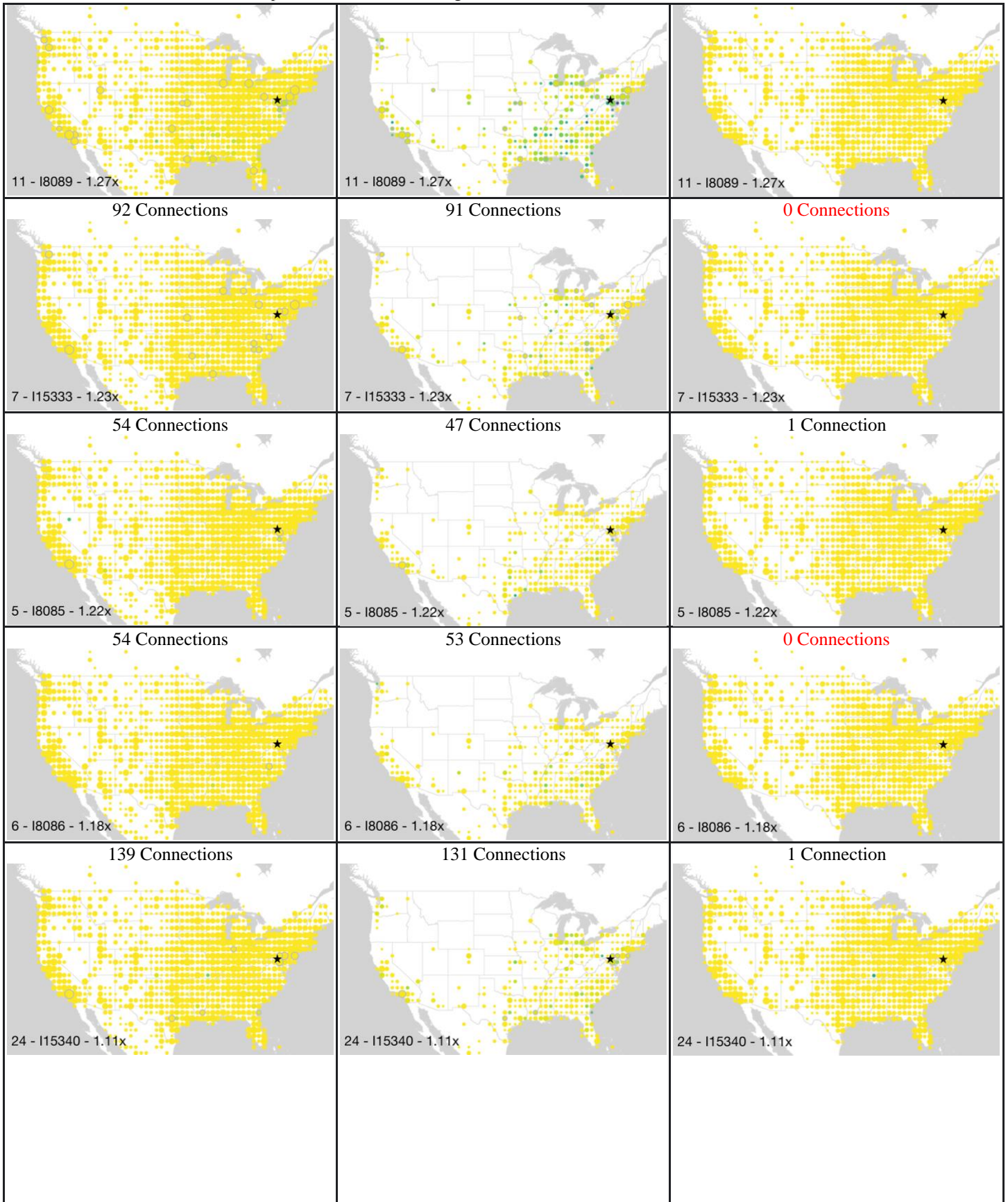
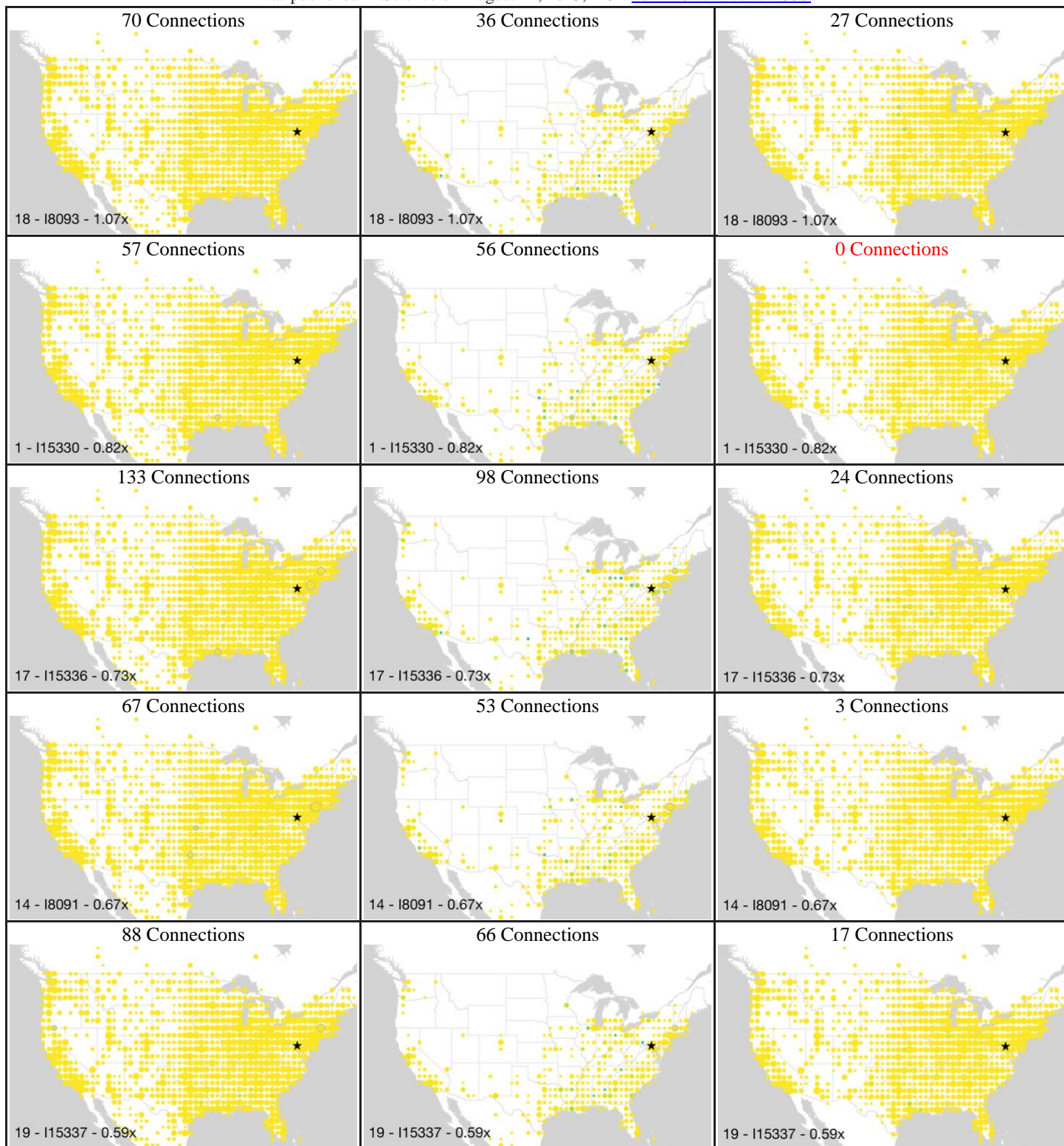


Fig. S11. Genetic connections to each of the Catoctin individuals among European participants. The proportion of 23andMe participants with $\geq 99\%$ European ancestry in western and central Europe who share IBD with each Catoctin individual with $>0.5x$ coverage. Geographic coordinates are rounded to the nearest integer, and only coordinates that have at least 25 associated participants are shown. To further protect participant privacy, we randomly downsample to include results for only 80% of participants. The size of the marker corresponds to the number of participants associated with each site, while the color indicates the proportion of participants who share IBD with the Catoctin individuals. No participants share ≥ 30 cM of IBD with one or more Catoctin individuals, so no marker outlines are shown. The total number of IBD connections observed is reported above each image, when 0 connections are observed, this number is reported in red.









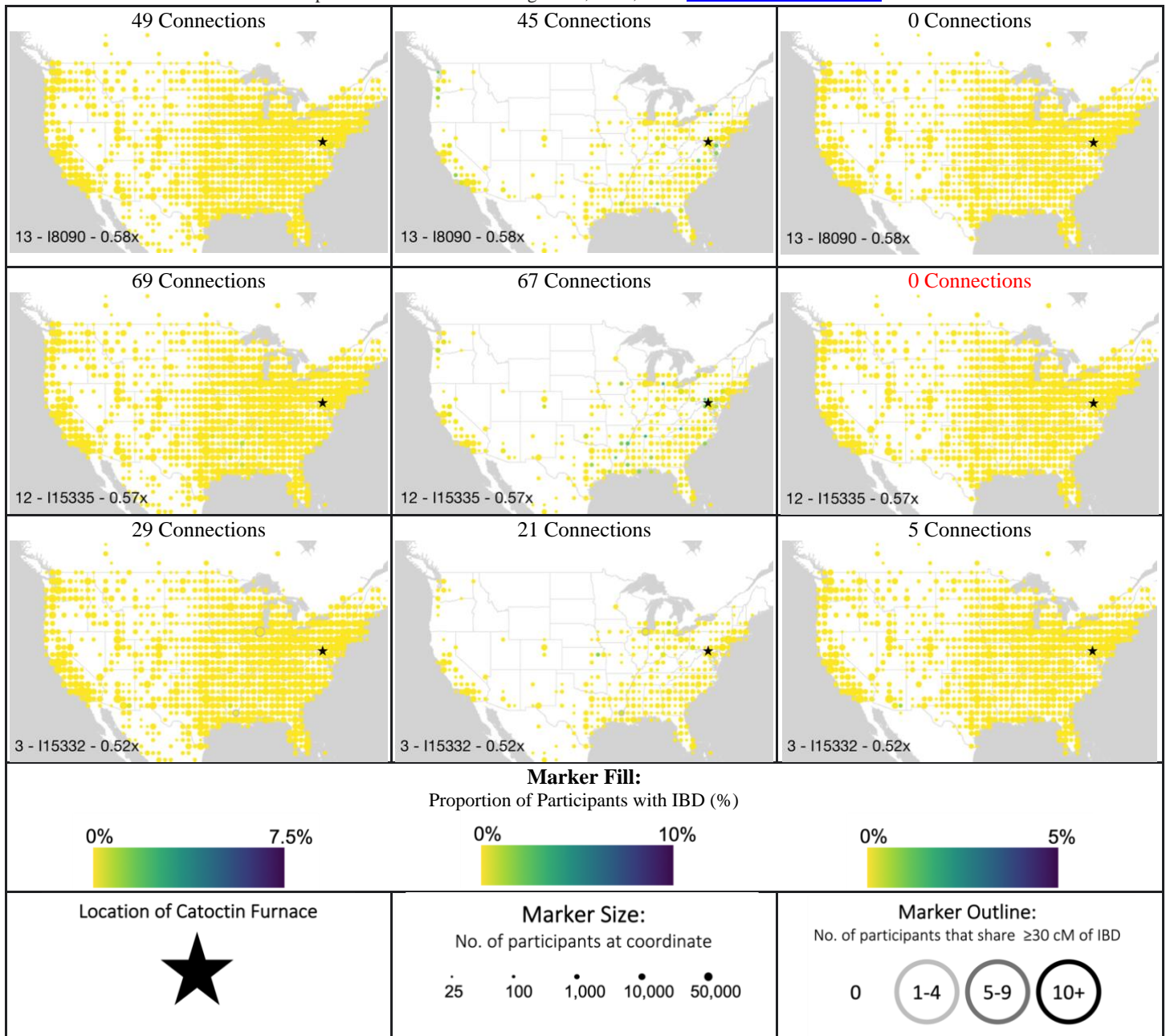


Fig. S12. Geographic distribution of distant and close relatives of each of the Catoctin individuals in the United States. The proportion of 23andMe participants at given geographic coordinates in the contiguous United States who share IBD with each of the 22 Catoctin individuals (one individual per row). Geographic coordinates are rounded to the nearest integer, and only coordinates that have at least 25 associated participants are shown. To further protect participant privacy, we randomly downsample to include results for only 80% of participants. The size of the marker corresponds to the number of participants associated with each site, while the color indicates the proportion of participants who share IBD with the Catoctin individuals. Marker outlines indicate the number of participants at each coordinate who share ≥ 30 cM of IBD with the specified Catoctin individual. Column A (left) reports results for all participants, column B (middle) shows participants with $\geq 5\%$ Sub-Saharan African ancestry and column C (right) $\geq 99\%$ European ancestry. The total number of IBD connections observed is reported above each image, when 0 connections are observed, this number is reported in red.

5

10

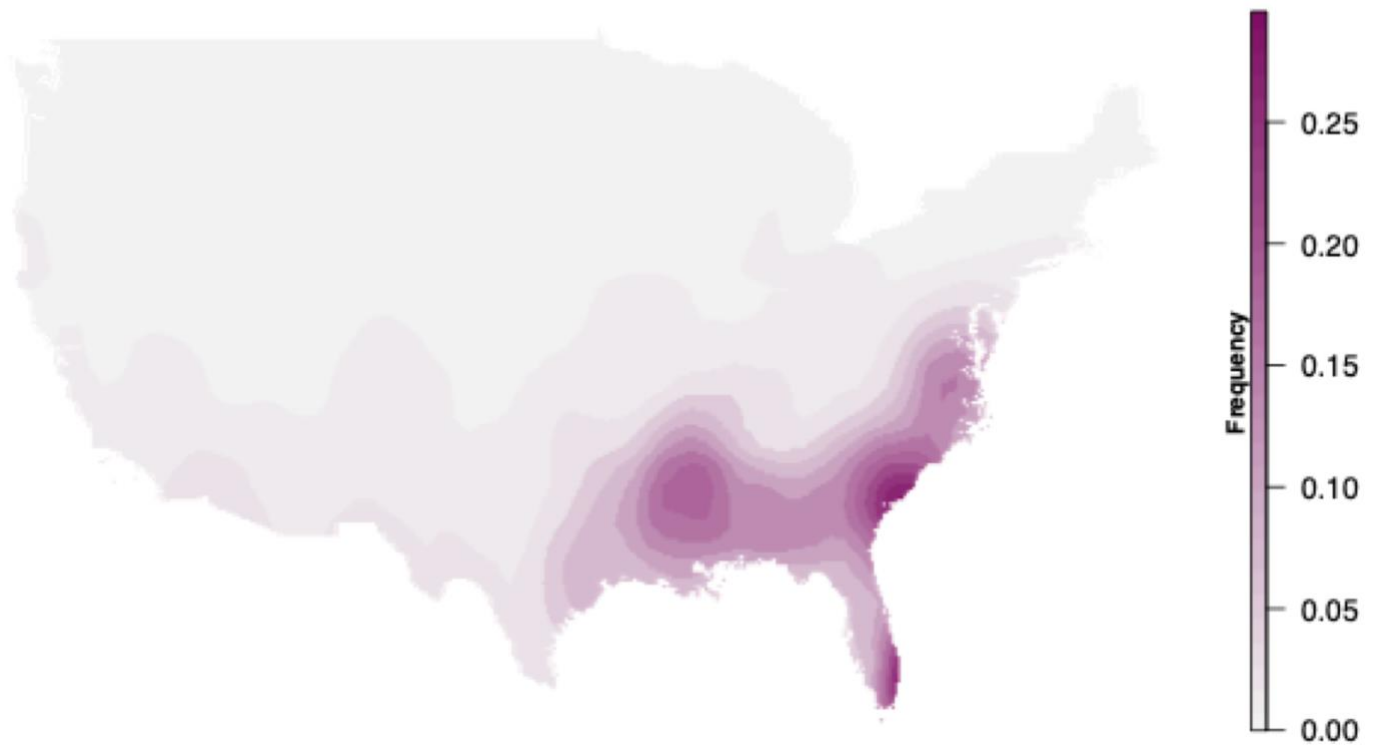


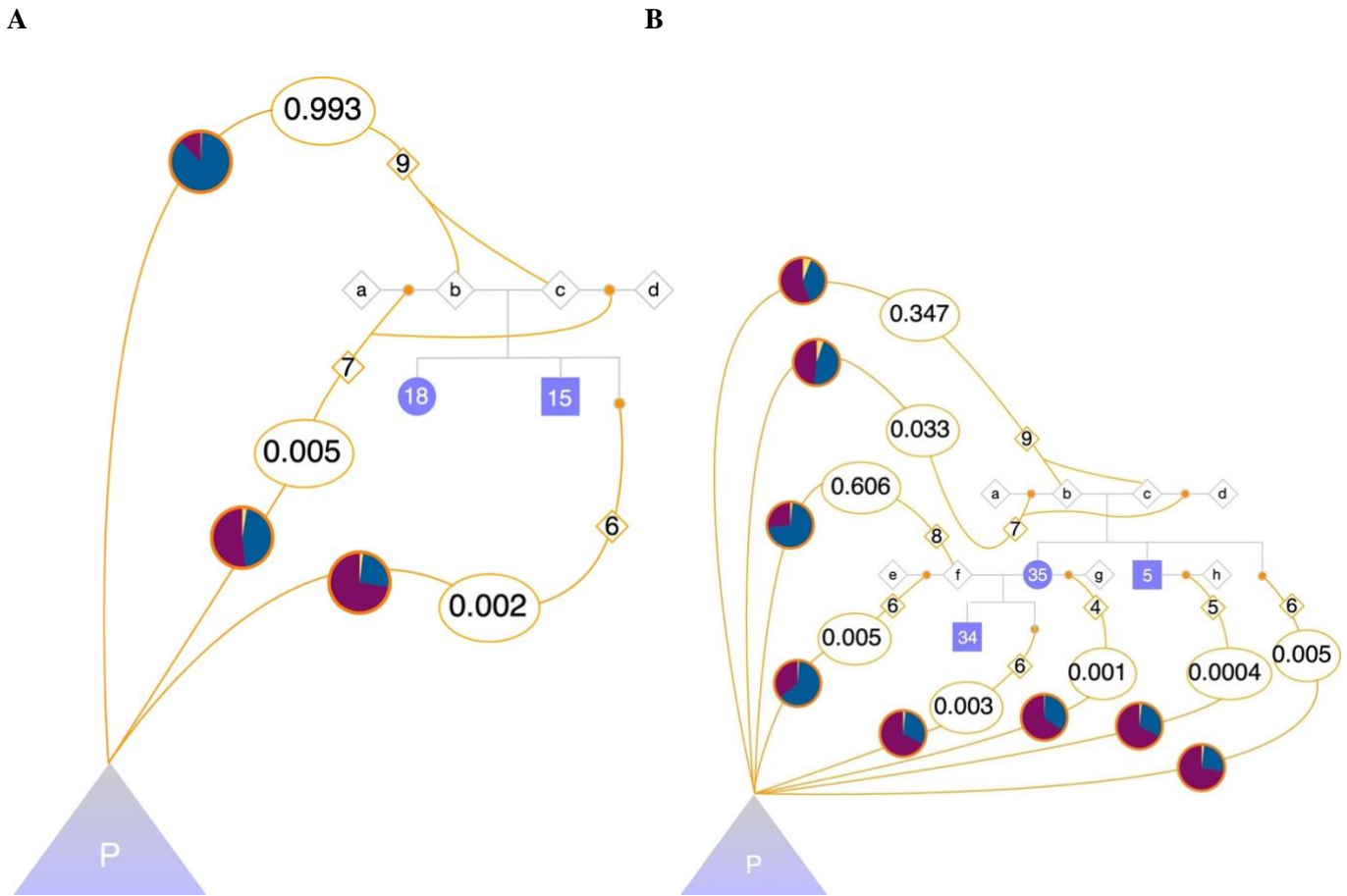
Fig. S13. Geographic distribution of 23andMe research participants with Sub-Saharan African ancestry in the contiguous United States. Predicted African ancestry proportions in the US using participants' grandparent birth locations. Prediction surfaces were generated using Kriging interpolation on the mean proportion of African ancestry at each unique geographic coordinate.

15

20

25

5

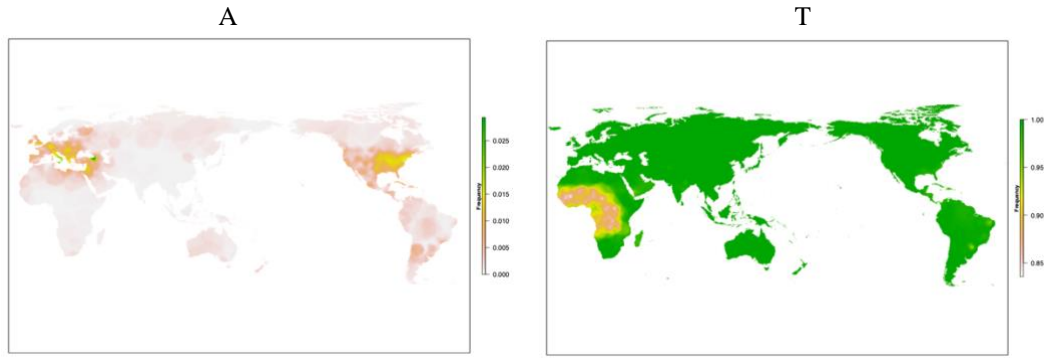


10

Fig. S14. Connections between Catoctin Family C and D and present-day pedigrees. The pedigree for Catoctin Family C (panel A) and Family D (panel B) is shown with blue-shaded individuals connected by grey lines. Open gray diamonds indicate un-genotyped individuals in each Catoctin family. The large purple triangle represents all present-day pedigrees composed of 23andMe research participants, and the probability distribution of how these pedigrees connect to the historical pedigree is inferred. Orange lines represent lineages connecting a present-day pedigree to the historical pedigree. Numbers in ovals give the probability that a present-day pedigree attached to a given point on the historical pedigree, scaled to a percentage. Numbers in diamonds indicate the average degree of a lineage connecting to a particular point. Pie charts show the average European (blue), African (red), and Indigenous American (yellow) admixture proportions of individuals in pedigrees whose most likely point of connection was through the lineage.

20

Sickle Cell Anemia/Trait (*rs334* or *i3003137*)



increased Risk of G6PD Deficiency (*rs1050828*)

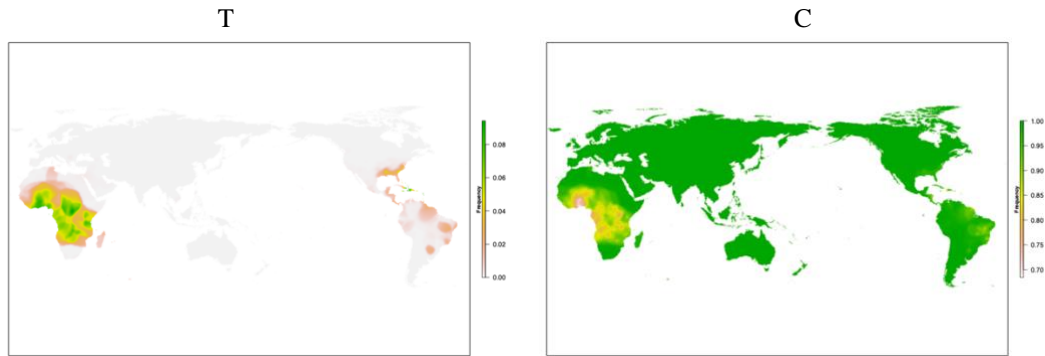


Fig. S15. Geographic distribution of biologically significant alleles. Heatmaps showing the geographic distribution of biologically significant alleles among 23andMe research participants using Kriging interpolation. For each phenotypically important SNP, the effect allele is shown in the left panel.

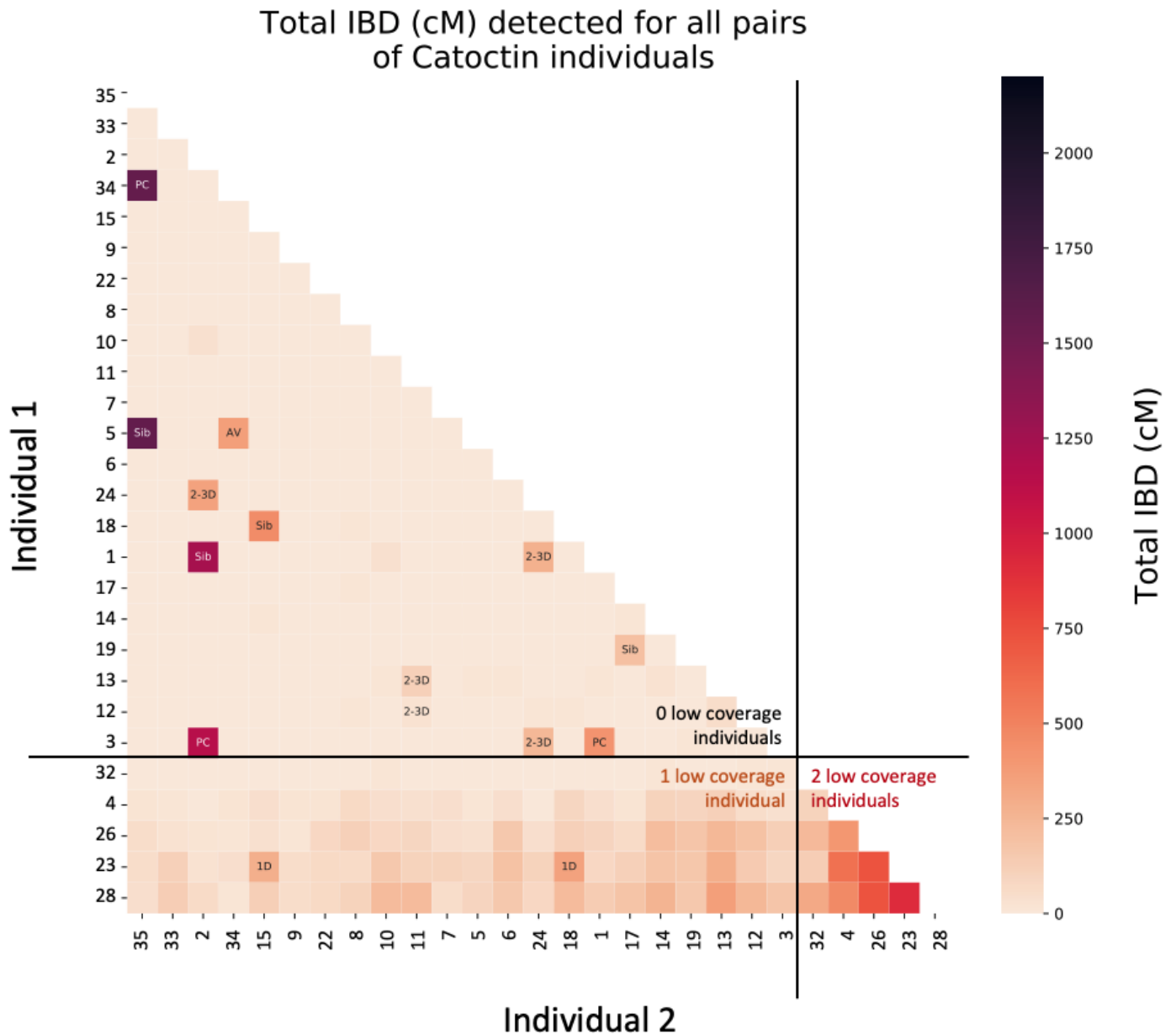


Fig. S16. Heatmap of total IBD measured between all pairs of Catoctin individuals. Individuals sorted from highest (top) to lowest (bottom) coverage. Comparisons between individuals with $<0.5x$ coverage are likely to have high rates of false positive IBD, therefore black lines are used to separate individuals with $>0.5x$ coverage from those with $<0.5x$ coverage. Comparisons in the upper left quadrant contain the least false positive IBD as they involve no low coverage individuals, while comparisons in the lower right quadrant are expected to have very high rates of false positive IBD as they involve 2 low coverage individuals. Genetic relatives that were independently identified using an alternative method not based on imputation and IBD analysis (80) are annotated as follows: PC: Parent-Child; Sib: Sibling; AV: avuncular; 1D: 1st degree relative ; 2-3D: 2nd to 3rd degree relative. We do not observe high amounts of IBD among any pairs of individuals that were not already identified as genetic relatives using the allele frequency-based method, which can detect relatives as distant as the 3rd degree, suggesting that while close genetic relationships are common among the Catoctin individuals, more distant relationships are less common.

References 74 - 124

74. R. Pinhasi, D. M. Fernandes, K. Sirak, O. Cheronet, Isolating the human cochlea to generate bone powder for ancient DNA analysis. *Nature Protocols*. **14**, 1194–1205 (2019).
- 5 75. R. Pinhasi, D. Fernandes, K. Sirak, M. Novak, S. Connell, S. Alpaslan-Roodenberg, F. Gerritsen, V. Moiseyev, A. Gromov, P. Raczky, A. Anders, M. Pietrusewsky, G. Rollefson, M. Jovanovic, H. Trinhhoang, G. Bar-Oz, M. Oxenham, H. Matsumura, M. Hofreiter, Optimal Ancient DNA Yields from the Inner Ear Part of the Human Petrous Bone. *PLOS ONE*. **10**, e0129102 (2015).
- 10 76. I. Mathieson, S. Alpaslan-Roodenberg, C. Posth, A. Szécsényi-Nagy, N. Rohland, S. Mallick, I. Olalde, N. Broomandkhoshbacht, F. Candilio, O. Cheronet, D. Fernandes, M. Ferry, B. Gamarra, G. G. Fortes, W. Haak, E. Harney, E. Jones, D. Keating, B. Krause-Kyora, I. Kucukkalipci, M. Michel, A. Mittnik, K. Nägele, M. Novak, J. Oppenheimer, N. Patterson, S. Pfrengle, K. Sirak, K. Stewardson, S. Vai, S. Alexandrov, K. W. Alt, R. Andreescu, D. Antonović, A. Ash, N. Atanassova, K. Bacvarov, M. B. Gusztáv, H. Bocherens, M. Bolus, A. Boroneanț, Y. Boyadzhiev, A. Budnik, J. Burmaz, S. Chohadzhiev, N. J. Conard, R. Cottiaux, M. Čuka, C. Cupillard, D. G.
- 15 Drucker, N. Elenski, M. Francken, B. Galabova, G. Ganetsovski, B. Gély, T. Hajdu, V. Handzhyska, K. Harvati, T. Higham, S. Iliev, I. Janković, I. Karavanić, D. J. Kennett, D. Komšo, A. Kozak, D. Labuda, M. Lari, C. Lazar, M. Leppek, K. Leshtakov, D. L. Vetro, D. Los, I. Lozanov, M. Malina, F. Martini, K. McSweeney, H. Meller, M. Mendušić, P. Mirea, V. Moiseyev, V. Petrova, T. D. Price, A. Simalcsik, L. Sineo, M. Šlaus, V. Slavchev, P. Stanev, A. Starović, T. Szeniczey, S. Talamo, M. Teschler-Nicola, C. Thevenet, I. Valchev, F. Valentin, S. Vasilyev, F.
- 20 Veljanovska, S. Venelinova, E. Veselovskaya, B. Viola, C. Virag, J. Zaninović, S. Zäuner, P. W. Stockhammer, G. Catalano, R. Krauß, D. Caramelli, G. Zariņa, B. Gaydarska, M. Lillie, A. G. Nikitin, I. Potekhina, A. Papatthanasidou, D. Borić, C. Bonsall, J. Krause, R. Pinhasi, D. Reich, The genomic history of southeastern Europe. *Nature*. **555**, 197–203 (2018).
- 25 77. D. M. Behar, M. Van Oven, S. Rosset, M. Metspalu, E.-L. Loogväli, N. M. Silva, T. Kivisild, A. Torroni, R. Villems, A “Copernican” reassessment of the human mitochondrial DNA tree from its root. *The American Journal of Human Genetics*. **90**, 675–684 (2012).
78. H. Li, R. Durbin, Fast and accurate long-read alignment with Burrows–Wheeler transform. *Bioinformatics*. **26**, 589–595 (2010).
79. P. Skoglund, B. H. Northoff, M. V. Shunkov, A. P. Derevianko, S. Pääbo, J. Krause, M. Jakobsson, Separating endogenous ancient DNA from modern day contamination in a Siberian Neandertal. *Proceedings of the National Academy of Sciences*. **111**, 2229–2234 (2014).
- 30 80. I. Olalde, S. Mallick, N. Patterson, N. Rohland, V. Villalba-Mouco, M. Silva, K. Dulias, C. J. Edwards, F. Gandini, M. Pala, P. Soares, M. Ferrando-Bernal, N. Adamski, N. Broomandkhoshbacht, O. Cheronet, B. J. Culleton, D. Fernandes, A. M. Lawson, M. Mah, J. Oppenheimer, K. Stewardson, Z. Zhang, J. M. J. Arenas, I. J. T. Moyano, D.
- 35 C. Salazar-García, P. Castanyer, M. Santos, J. Tremoleda, M. Lozano, P. G. Borja, J. Fernández-Eraso, J. A. Mujika-Alustiza, C. Barroso, F. J. Bermúdez, E. V. Mínguez, J. Burch, N. Coromina, D. Vivó, A. Cebrià, J. M. Fullola, O. García-Puchol, J. I. Morales, F. X. Oms, T. Majó, J. M. Vergès, A. Díaz-Carvajal, I. Ollich-Castanyer, F. J. López-Cachero, A. M. Silva, C. Alonso-Fernández, G. D. de Castro, J. J. Echevarría, A. Moreno-Márquez, G. P. Berlanga, P. Ramos-García, J. Ramos-Muñoz, E. V. Vila, G. A. Arzo, Á. E. Arroyo, K. T. Lillios, J. Mack, J.
- 40 Velasco-Vázquez, A. Waterman, L. B. de L. Enrich, M. B. Sánchez, B. Agustí, F. Codina, G. de Prado, A. Estalrich, Á. F. Flores, C. Finlayson, G. Finlayson, S. Finlayson, F. Giles-Guzmán, A. Rosas, V. B. González, G. G. Atiénzar, M. S. H. Pérez, A. Llanos, Y. C. Marco, I. C. Beneyto, D. López-Serrano, M. S. Tormo, A. C. Valera, C. Blasco, C. Liesau, P. Ríos, J. Daura, M. J. de P. Michó, A. A. Diez-Castillo, R. F. Fernández, J. F. Farré, R. Garrido-Pena, V. S. Gonçalves, E. Guerra-Doce, A. M. Herrero-Corral, J. Juan-Cabanilles, D. López-Reyes, S. B.
- 45 McClure, M. M. Pérez, A. O. Foix, M. S. Borràs, A. C. Sousa, J. M. V. Encinas, D. J. Kennett, M. B. Richards, K. W. Alt, W. Haak, R. Pinhasi, C. Lalueza-Fox, D. Reich, The genomic history of the Iberian Peninsula over the past 8000 years. *Science*. **363**, 1230–1234 (2019).
81. É. Harney, N. Patterson, D. Reich, J. Wakeley, Assessing the performance of qpAdm: a statistical tool for studying population admixture. *Genetics*. **217** (2021), doi:10.1093/genetics/iyaa045.

82. D. H. Alexander, J. Novembre, K. Lange, Fast model-based estimation of ancestry in unrelated individuals. *Genome Res.* **19**, 1655–1664 (2009).
83. N. Patterson, A. L. Price, D. Reich, Population Structure and Eigenanalysis. *PLOS Genetics.* **2**, e190 (2006).
84. V. M. Narasimhan, N. Patterson, P. Moorjani, N. Rohland, R. Bernardos, S. Mallick, I. Lazaridis, N. Nakatsuka, I. Olalde, M. Lipson, A. M. Kim, L. M. Olivieri, A. Coppa, M. Vidale, J. Mallory, V. Moiseyev, E. Kitov, J. Monge, N. Adamski, N. Alex, N. Broomandkhoshbacht, F. Candilio, K. Callan, O. Cheronet, B. J. Culleton, M. Ferry, D. Fernandes, S. Freilich, B. Gamarra, D. Gaudio, M. Hajdinjak, É. Harney, T. K. Harper, D. Keating, A. M. Lawson, M. Mah, K. Mandl, M. Michel, M. Novak, J. Oppenheimer, N. Rai, K. Sirak, V. Slon, K. Stewardson, F. Zalzalá, Z. Zhang, G. Akhatov, A. N. Bagashev, A. Bagnera, B. Baitanayev, J. Bendezu-Sarmiento, A. A. Bissembaev, G. L. Bonora, T. T. Charginov, T. Chikisheva, P. K. Dashkovskiy, A. Derevianko, M. Dobeš, K. Douka, N. Dubova, M. N. Duisengali, D. Enshin, A. Epimakhov, A. V. Fribus, D. Fuller, A. Goryachev, A. Gromov, S. P. Grushin, B. Hanks, M. Judd, E. Kazizov, A. Khokhlov, A. P. Krygin, E. Kupriyanova, P. Kuznetsov, D. Luiselli, F. Maksudov, A. M. Mamedov, T. B. Mamirov, C. Meiklejohn, D. C. Merrett, R. Micheli, O. Mochalov, S. Mustafokulov, A. Nayak, D. Pettener, R. Potts, D. Razhev, M. Rykun, S. Sarno, T. M. Savenkova, K. Sikhymbaeva, S. M. Slepchenko, O. A. Soltobaev, N. Stepanova, S. Svyatko, K. Tabaldiev, M. Teschler-Nicola, A. A. Tishkin, V. V. Tkachev, S. Vasilyev, P. Velemínský, D. Voyakin, A. Yermolayeva, M. Zahir, V. S. Zubkov, A. Zubova, V. S. Shinde, C. Lalueza-Fox, M. Meyer, D. Anthony, N. Boivin, K. Thangaraj, D. J. Kennett, M. Frachetti, R. Pinhasi, D. Reich, The formation of human populations in South and Central Asia. *Science.* **365** (2019), doi:10.1126/science.aat7487.
85. L. Van Dorp, S. Lowes, J. L. Weigel, N. Ansari-Pour, S. López, J. Mendoza-Revilla, J. A. Robinson, J. Henrich, M. G. Thomas, N. Nunn, Genetic legacy of state centralization in the Kuba Kingdom of the Democratic Republic of the Congo. *Proceedings of the National Academy of Sciences.* **116**, 593–598 (2019).
86. B. A. Jackson, J. L. Wilson, S. Kirbah, S. S. Sidney, J. Rosenberger, L. Bassie, J. A. Alie, D. C. McLean, W. T. Garvey, B. Ely, Mitochondrial DNA genetic diversity among four ethnic groups in Sierra Leone. *American journal of physical anthropology.* **128**, 156–163 (2005).
87. B. M. Henn, C. R. Gignoux, M. Jobin, J. M. Granka, J. Macpherson, J. M. Kidd, L. Rodríguez-Botigué, S. Ramachandran, L. Hon, A. Brisbin, Hunter-gatherer genomic diversity suggests a southern African origin for modern humans. *Proceedings of the National Academy of Sciences.* **108**, 5154–5162 (2011).
88. V. D. Blondel, J.-L. Guillaume, R. Lambiotte, E. Lefebvre, Fast unfolding of communities in large networks. *Journal of statistical mechanics: theory and experiment.* **2008**, P10008 (2008).
89. M. Bastian, S. Heymann, M. Jacomy, "Gephi: an open source software for exploring and manipulating networks" in (2009).
90. Enslaved faces from African American cemetery in Catoctin, Maryland recreated - The Washington Post, (available at <https://www.washingtonpost.com/history/2021/07/09/african-american-cemetery-catoctin-enslaved-faces/>).
91. A. Roberts, Historical Society unveils facial reconstructions of African-Americans once enslaved in Thurmont. *The Frederick News-Post*, (available at https://www.fredericknewspost.com/news/economy_and_business/tourism/historical-society-unveils-facial-reconstructions-of-african-americans-once-enslaved-in-thurmont/article_57a8171b-f3e2-52c8-bb8d-a6fc6d189ef2.html).
92. S. M. Fullerton, S. S.-J. Lee, Secondary uses and the governance of de-identified data: Lessons from the human genome diversity panel. *BMC Medical Ethics.* **12**, 16 (2011).
93. D. B. Resnik, The Human Genome Diversity Project: Ethical Problems and Solutions. *Politics and the Life Sciences.* **18**, 15–23 (1999).
94. J. O'Connell, T. Yun, M. Moreno, H. Li, N. Litterman, A. Kolesnikov, E. Noblin, P.-C. Chang, A. Shastri, E. H. Dorfman, S. Shringarpure, A. Auton, A. Carroll, C. Y. McLean, A population-specific reference panel for improved genotype imputation in African Americans. *Commun Biol.* **4**, 1–9 (2021).
95. E. R. Ebel, F. Reis, D. A. Petrov, S. Beleza, Historical trends and new surveillance of Plasmodium falciparum drug resistance markers in Angola. *Malaria Journal.* **20**, 175 (2021).
96. L. Sweeney, k-ANONYMITY: A MODEL FOR PROTECTING PRIVACY. *Int. J. Unc. Fuzz. Knowl. Based Syst.* **10**, 557–570 (2002).
97. E. Birney, M. Inouye, J. Raff, A. Rutherford, A. Scally, The language of race, ethnicity, and ancestry in human

genetic research (2021), , doi:10.48550/arXiv.2106.10041.

98. J. K. Wagner, J.-H. Yu, J. O. Ifekwunigwe, T. M. Harrell, M. J. Bamshad, C. D. Royal, Anthropologists' views on race, ancestry, and genetics. *American Journal of Physical Anthropology*. **162**, 318–327 (2017).
99. I. Mathieson, A. Scally, What is ancestry? *PLOS Genetics*. **16**, e1008624 (2020).
- 5 100. C. Agyemang, R. Bhopal, M. Bruijnzeels, Negro, Black, Black African, African Caribbean, African American or what? Labelling African origin populations in the health arena in the 21st century. *Journal of Epidemiology & Community Health*. **59**, 1014–1018 (2005).
101. AP says it will capitalize Black but not white | AP News, (available at <https://apnews.com/article/entertainment-cultures-race-and-ethnicity-us-news-ap-top-news-7e36c00c5af0436abc09e051261fff1f>).
- 10 102. G. Coop, Genetic similarity versus genetic ancestry groups as sample descriptors in human genetics (2023), , doi:10.48550/arXiv.2207.11595.
103. A. C. F. Lewis, S. J. Molina, P. S. Appelbaum, B. Dauda, A. Di Rienzo, A. Fuentes, S. M. Fullerton, N. A. Garrison, N. Ghosh, E. M. Hammonds, D. S. Jones, E. E. Kenny, P. Kraft, S. S.-J. Lee, M. Mauro, J. Novembre, A. Panofsky, M. Sohail, B. M. Neale, D. S. Allen, Getting genetic ancestry right for science and society. *Science*. **376**, 250–252 (2022).
- 15 104. M. Miyagi, E. M. Guthman, S. D.-K. Sun, Transgender rights rely on inclusive language. *Science*. **374**, 1568–1569 (2021).
105. J. Brück, Ancient DNA, kinship and relational identities in Bronze Age Britain. *Antiquity*. **95**, 228–237 (2021).
106. S. S. Ebenesersdóttir, M. Sandoval-Velasco, E. D. Gunnarsdóttir, A. Jagadeesan, V. B. Guðmundsdóttir, E. L. Thordardóttir, M. S. Einarsdóttir, K. H. S. Moore, Á. Sigurðsson, D. N. Magnúsdóttir, H. Jónsson, S. Snorraddóttir, E. Hovig, P. Møller, I. Kockum, T. Olsson, L. Alfredsson, T. F. Hansen, T. Werge, G. L. Cavalleri, E. Gilbert, C. Lalueza-Fox, J. W. Walser, S. Kristjánsdóttir, S. Gopalakrishnan, L. Árnadóttir, Ó. Þ. Magnússon, M. T. P. Gilbert, K. Stefánsson, A. Helgason, Ancient genomes from Iceland reveal the making of a human population. *Science*. **360**, 1028–1032 (2018).
- 25 107. I. Olalde, S. Brace, M. E. Allentoft, I. Armit, K. Kristiansen, T. Booth, N. Rohland, S. Mallick, A. Szécsényi-Nagy, A. Mittnik, E. Altena, M. Lipson, I. Lazaridis, T. K. Harper, N. Patterson, N. Broomandkoshbacht, Y. Diekmann, Z. Faltyskova, D. Fernandes, M. Ferry, E. Harney, P. de Knijff, M. Michel, J. Oppenheimer, K. Stewardson, A. Barclay, K. W. Alt, C. Liesau, P. Ríos, C. Blasco, J. V. Miguel, R. M. García, A. A. Fernández, E. Bánffy, M. Bernabò-Brea, D. Billoin, C. Bonsall, L. Bonsall, T. Allen, L. Büster, S. Carver, L. C. Navarro, O. E. Craig, G. T. Cook, B. Cunliffe, A. Denaire, K. E. Dinwiddy, N. Dodwell, M. Ernée, C. Evans, M. Kuchařík, J. F. Farré, C. Fowler, M. Gazenbeek, R. G. Pena, M. Haber-Urriarte, E. Haduch, G. Hey, N. Jowett, T. Knowles, K. Massy, S. Pfrengle, P. Lefranc, O. Lemerrier, A. Lefebvre, C. H. Martínez, V. G. Olmo, A. B. Ramírez, J. L. Maurandi, T. Majó, J. I. McKinley, K. McSweeney, B. G. Mende, A. Modi, G. Kulcsár, V. Kiss, A. Czene, R. Patay, A. Endrődi, K. Köhler, T. Hajdu, T. Szeniczey, J. Dani, Z. Bernert, M. Hoole, O. Cheronet, D. Keating, P. Velemínský, M. Dobeš, F. Candilio, F. Brown, R. F. Fernández, A.-M. Herrero-Corral, S. Tusa, E. Carnieri, L. Lentini, A. Valenti, A. Zanini, C. Waddington, G. Delibes, E. Guerra-Doce, B. Neil, M. Brittain, M. Luke, R. Mortimer, J. Desideri, M. Besse, G. Brücken, M. Furmanek, A. Hałaszkó, M. Mackiewicz, A. Rapiński, S. Leach, I. Soriano, K. T. Lillios, J. L. Cardoso, M. P. Pearson, P. Włodarczak, T. D. Price, P. Prieto, P.-J. Rey, R. Risch, M. A. Rojo Guerra, A. Schmitt, J. Serrallongue, A. M. Silva, V. Smrčka, L. Vergnaud, J. Zilhão, D. Caramelli, T. Higham, M. G. Thomas, D. J. Kennett, H. Fokkens, V. Heyd, A. Sheridan, K.-G. Sjögren, P. W. Stockhammer, J. Krause, R. Pinhasi, W. Haak, I. Barnes, C. Lalueza-Fox, D. Reich, The Beaker phenomenon and the genomic transformation of northwest Europe. *Nature*. **555**, 190–196 (2018).
108. “Allen Ancient Genome Diversity Project / John Templeton Ancient DNA Atlas.”
- 45 109. I. Lazaridis, D. Nadel, G. Rollefson, D. C. Merrett, N. Rohland, S. Mallick, D. Fernandes, M. Novak, B. Gamarra, K. Sirak, S. Connell, K. Stewardson, E. Harney, Q. Fu, G. Gonzalez-Fortes, E. R. Jones, S. A. Roodenberg, G. Lengyel, F. Bocquentin, B. Gasparian, J. M. Monge, M. Gregg, V. Eshed, A.-S. Mizrahi, C. Meiklejohn, F. Gerritsen, L. Bejbaru, M. Blüher, A. Campbell, G. Cavalleri, D. Comas, P. Froguel, E. Gilbert, S. M. Kerr, P. Kovacs, J. Krause, D. McGettigan, M. Merrigan, D. A. Merriwether, S. O'Reilly, M. B. Richards, O. Semino, M. Shamoon-Pour, G. Stefanescu, M. Stumvoll, A. Tönjes, A. Torroni, J. F. Wilson, L. Yengo, N. A. Hovhannisyan, N. Patterson, R. Pinhasi, D. Reich, Genomic insights into the origin of farming in the ancient Near East. *Nature*. **536**, 419–424 (2016).
- 50

110. M. G. Llorente, E. R. Jones, A. Eriksson, V. Siska, K. W. Arthur, J. W. Arthur, M. C. Curtis, J. T. Stock, M. Coltorti, P. Pieruccini, S. Stretton, F. Brock, T. Higham, Y. Park, M. Hofreiter, D. G. Bradley, J. Bhak, R. Pinhasi, A. Manica, Ancient Ethiopian genome reveals extensive Eurasian admixture in Eastern Africa. *Science* (2015), doi:10.1126/science.aad2879.
- 5 111. P. de B. Damgaard, R. Martiniano, J. Kamm, J. V. Moreno-Mayar, G. Kroonen, M. Peyrot, G. Barjamovic, S. Rasmussen, C. Zacho, N. Baimukhanov, V. Zaibert, V. Merz, A. Biddanda, I. Merz, V. Loman, V. Evdokimov, E. Usmanova, B. Hemphill, A. Seguin-Orlando, F. E. Yediay, I. Ullah, K.-G. Sjögren, K. H. Iversen, J. Choin, C. de la Fuente, M. Ilardo, H. Schroeder, V. Moiseyev, A. Gromov, A. Polyakov, S. Omura, S. Y. Senyurt, H. Ahmad, C. McKenzie, A. Margaryan, A. Hameed, A. Samad, N. Gul, M. H. Khokhar, O. I. Goriunova, V. I. Bazaliiskii, J. Novembre, A. W. Weber, L. Orlando, M. E. Allentoft, R. Nielsen, K. Kristiansen, M. Sikora, A. K. Outram, R. Durbin, E. Willerslev, The first horse herders and the impact of early Bronze Age steppe expansions into Asia. *Science* (2018), doi:10.1126/science.aar7711.
- 15 112. C. Gamba, E. R. Jones, M. D. Teasdale, R. L. McLaughlin, G. Gonzalez-Fortes, V. Mattiangeli, L. Domboróczki, I. Kővári, I. Pap, A. Anders, A. Whittle, J. Dani, P. Raczky, T. F. G. Higham, M. Hofreiter, D. G. Bradley, R. Pinhasi, Genome flux and stasis in a five millennium transect of European prehistory. *Nat Commun.* **5**, 5257 (2014).
113. D. Gokhman, E. Lavi, K. Prüfer, M. F. Fraga, J. A. Riancho, J. Kelso, S. Pääbo, E. Meshorer, L. Carmel, Reconstructing the DNA Methylation Maps of the Neandertal and the Denisovan. *Science*. **344**, 523–527 (2014).
114. T. Günther, H. Malmström, E. M. Svensson, A. Omrak, F. Sánchez-Quinto, G. M. Kılınc, M. Krzewińska, G. Eriksson, M. Fraser, H. Edlund, A. R. Munters, A. Coutinho, L. G. Simões, M. Vicente, A. Sjölander, B. J. Sellevold, R. Jørgensen, P. Claes, M. D. Shriver, C. Valdiosera, M. G. Netea, J. Apel, K. Lidén, B. Skar, J. Storå, A. Götherström, M. Jakobsson, Population genomics of Mesolithic Scandinavia: Investigating early postglacial migration routes and high-latitude adaptation. *PLOS Biology*. **16**, e2003703 (2018).
- 20 115. M. Ferrando-Bernal, C. Morcillo-Suarez, T. de-Dios, P. Gelabert, S. Civit, A. Díaz-Carvajal, I. Ollich-Castanyer, M. E. Allentoft, S. Valverde, C. Lalueza-Fox, Mapping co-ancestry connections between the genome of a Medieval individual and modern Europeans. *Scientific Reports*. **10**, 6843 (2020).
- 25 116. A. Margaryan, D. J. Lawson, M. Sikora, F. Racimo, S. Rasmussen, I. Moltke, L. M. Cassidy, E. Jørsboe, A. Ingason, M. W. Pedersen, T. Korneliusson, H. Wilhelmson, M. M. Buś, P. de Barros Damgaard, R. Martiniano, G. Renaud, C. Bhérer, J. V. Moreno-Mayar, A. K. Fotakis, M. Allen, R. Allmäe, M. Molak, E. Cappellini, G. Scorrano, H. McColl, A. Buzhilova, A. Fox, A. Albrechtsen, B. Schütz, B. Skar, C. Arcini, C. Falys, C. H. Jonson, D. Błaszczuk, D. Pezhemsky, G. Turner-Walker, H. Gestsdóttir, I. Lundstrøm, I. Gustin, I. Mainland, I. Potekhina, I. M. Muntoni, J. Cheng, J. Stenderup, J. Ma, J. Gibson, J. Peets, J. Gustafsson, K. H. Iversen, L. Simpson, L. Strand, L. Loe, M. Sikora, M. Florek, M. Vretemark, M. Redknap, M. Bajka, T. Pushkina, M. Søvsvø, N. Grigoreva, T. Christensen, O. Kastholm, O. Uldum, P. Favia, P. Holck, S. Sten, S. V. Arge, S. Ellingvåg, V. Moiseyev, W. Bogdanowicz, Y. Magnusson, L. Orlando, P. Pentz, M. D. Jessen, A. Pedersen, M. Collard, D. G. Bradley, M. L. Jørkov, J. Arneborg, N. Lynnerup, N. Price, M. T. P. Gilbert, M. E. Allentoft, J. Bill, S. M. Sindbæk, L. Hedeager, K. Kristiansen, R. Nielsen, T. Werge, E. Willerslev, Population genomics of the Viking world. *Nature*. **585**, 390–396 (2020).
- 30 117. M. Sikora, V. V. Pitulko, V. C. Sousa, M. E. Allentoft, L. Vinner, S. Rasmussen, A. Margaryan, P. de Barros Damgaard, C. de la Fuente, G. Renaud, M. A. Yang, Q. Fu, I. Dupanloup, K. Giampoudakis, D. Nogués-Bravo, C. Rahbek, G. Kroonen, M. Peyrot, H. McColl, S. V. Vasilyev, E. Veselovskaya, M. Gerasimova, E. Y. Pavlova, V. G. Chasnyk, P. A. Nikolskiy, A. V. Gromov, V. I. Khartanovich, V. Moiseyev, P. S. Grebenyuk, A. Y. Fedorchenko, A. I. Lebedintsev, S. B. Slobodin, B. A. Malyarchuk, R. Martiniano, M. Meldgaard, L. Arppe, J. U. Palo, T. Sundell, K. Mannermaa, M. Putkonen, V. Alexandersen, C. Primeau, N. Baimukhanov, R. S. Malhi, K.-G. Sjögren, K. Kristiansen, A. Wessman, A. Sajantila, M. M. Lahr, R. Durbin, R. Nielsen, D. J. Meltzer, L. Excoffier, E. Willerslev, The population history of northeastern Siberia since the Pleistocene. *Nature*. **570**, 182–188 (2019).
- 40 118. T. Kivisild, L. Saag, R. Hui, S. A. Biagini, V. Pankratov, E. D'Atanasio, L. Pagani, L. Saag, S. Rootsi, R. Mägi, E. Metspalu, H. Valk, M. Malve, K. Irtdt, T. Reisberg, A. Solnik, C. L. Scheib, D. N. Seidman, A. L. Williams, K. Tambets, M. Metspalu, Patterns of genetic connectedness between modern and medieval Estonian genomes reveal the origins of a major ancestry component of the Finnish population. *The American Journal of Human Genetics*. **108**, 1792–1806 (2021).
- 50 119. C. D. Huff, D. J. Witherspoon, T. S. Simonson, J. Xing, W. S. Watkins, Y. Zhang, T. M. Tuohy, D. W. Neklason, R.

W. Burt, S. L. Guthery, S. R. Woodward, L. B. Jorde, Maximum-likelihood estimation of recent shared ancestry (ERSA). *Genome Res.* **21**, 768–774 (2011).

120. A. THOMAS, M. H. SKOLNICK, C. M. LEWIS, Genomic mismatch scanning in pedigrees. *Mathematical Medicine and Biology: A Journal of the IMA.* **11**, 1–16 (1994).

5 121. A. W. Wohns, Y. Wong, B. Jeffery, A. Akbari, S. Mallick, R. Pinhasi, N. Patterson, D. Reich, J. Kelleher, G. McVean, A unified genealogy of modern and ancient genomes (2021), p. 2021.02.16.431497, , doi:10.1101/2021.02.16.431497.

10 122. M. H. Gouveia, V. Borda, T. P. Leal, R. G. Moreira, A. W. Bergen, F. S. G. Kehdy, I. Alvim, M. M. Aquino, G. S. Araujo, N. M. Araujo, V. Furlan, R. Liboredo, M. Machado, W. C. S. Magalhaes, L. A. Michelin, M. R. Rodrigues, F. Rodrigues-Soares, H. P. Sant Anna, M. L. Santolalla, M. O. Scliar, G. Soares-Souza, R. Zamudio, C. Zolini, M. C. Bortolini, M. Dean, R. H. Gilman, H. Guio, J. Rocha, A. C. Pereira, M. L. Barreto, B. L. Horta, M. F. Lima-Costa, S. M. Mbulaiteye, S. J. Chanock, S. A. Tishkoff, M. Yeager, E. Tarazona-Santos, Origins, Admixture Dynamics, and Homogenization of the African Gene Pool in the Americas. *Molecular Biology and Evolution.* **37**, 1647–1656 (2020).

15 123. F. L. C. Jackson, So many Nigerians: why is Nigeria overrepresented as the ancestral genetic homeland of Legacy African North Americans? *The American Journal of Human Genetics.* **108**, 202–208 (2021).

124. A. Ko, R. Nielsen, Composite likelihood method for inferring local pedigrees. *PLOS Genetics.* **13**, e1006963 (2017).